

University of Groningen

Peeking behind the horizon

Brijan, Jan-Willem

DOI:
[10.33612/diss.98240363](https://doi.org/10.33612/diss.98240363)

IMPORTANT NOTE: You are advised to consult the publisher's version (publisher's PDF) if you wish to cite from it. Please check the document version below.

Document Version
Publisher's PDF, also known as Version of record

Publication date:
2019

[Link to publication in University of Groningen/UMCG research database](#)

Citation for published version (APA):
Brijan, J-W. (2019). *Peeking behind the horizon: a study of black holes in the AdS/CFT correspondence*. [Thesis fully internal (DIV), University of Groningen]. University of Groningen.
<https://doi.org/10.33612/diss.98240363>

Copyright

Other than for strictly personal use, it is not permitted to download or to forward/distribute the text or part of it without the consent of the author(s) and/or copyright holder(s), unless the work is under an open content license (like Creative Commons).

The publication may also be distributed here under the terms of Article 25fa of the Dutch Copyright Act, indicated by the "Taverne" license. More information can be found on the University of Groningen website: <https://www.rug.nl/library/open-access/self-archiving-pure/taverne-amendment>.

Take-down policy

If you believe that this document breaches copyright please contact us providing details, and we will remove access to the work immediately and investigate your claim.

Downloaded from the University of Groningen/UMCG research database (Pure): <http://www.rug.nl/research/portal>. For technical reasons the number of authors shown on this cover page is limited to 10 maximum.



university of
 groningen

Peeking behind the horizon

A study of black holes
in the AdS/CFT correspondence

PhD thesis

to obtain the degree of PhD at the
University of Groningen
on the authority of the
Rector Magnificus Prof. C. Wijmenga
and in accordance with
the decision by the College of Deans.

This thesis will be defended in public on

Friday 18 October 2019 at 16:15 hours

by

Johan Willem Alexander Brijan

born on 26 December 1989
in Emmen, the Netherlands

Supervisor

Prof. E.A. Bergshoeff

Co-supervisor

Dr. K. Papadodimas

Assessment committee

Prof. C.F.F. van den Broeck

Prof. R.G.E Timmermans

Prof. S. Vandoren

Van Swinderen Institute PhD series 2019

ISBN: 978-94-034-1952-7 (printed version)

ISBN: 978-94-034-1951-0 (electronic version)

The work described in this thesis was performed at the Van Swinderen Institute for Particle Physics and Gravity of the University of Groningen.

Printed by Gildeprint

Copyright © 2019 Jan-Willem Brijan

Contents

1	Introduction	9
2	The black hole information paradox	19
2.1	Hawking radiation	19
2.2	Complementarity	28
2.3	Strong subadditivity, small corrections and firewalls	32
2.3.1	Entanglement and the theorem of strong subadditivity . .	32
2.4	A new tool: the AdS/CFT correspondence	34
2.4.1	Flux tubes and the large N limit	34
2.4.2	String theory and the AdS/CFT correspondence	37
2.5	Complementarity revised using AdS/CFT	43
2.5.1	Rindler space as an example	44
2.5.2	Rindler space and the eternal black hole	49
3	A toy model for black holes	55
3.1	Introduction	55
3.2	The setup	59
3.3	Operator algebras in time bands	62
3.3.1	Explicit construction of arbitrary states using operators in the band	71
3.4	Interior operators and precursors	72
3.5	Conclusion and discussion	77

4	Black hole formation	81
4.1	Introduction	81
4.2	A lightning review of the uniformization problem	87
4.2.1	Basic set up	88
4.2.2	The vacuum block and semiclassical correlation functions	90
4.2.3	The defining equation for the uniformizing coordinates . .	94
4.3	Lorentzian time-evolution on the radial plane	95
4.3.1	Late-time behavior of the correlators	98
4.3.2	Monodromy preserving diffeomorphisms and their bulk interpretation as boundary gravitons	101
4.4	Chern-Simons interpretation of the monodromy	107
4.4.1	Wilson loops in Chern-Simons theory	108
4.4.2	The nothingness trick	109
4.5	An example and numerical black holes with soft gravitational hair	113
4.5.1	The continuous limit as an example	113
4.5.2	Numerical results including soft gravitational hair	115
4.6	Conclusion and discussion	119
5	Conclusions	123
5.1	Outlook	125
6	Gluren achter de horizon	127
7	Acknowledgments	133
	Appendices	135
A	Euclidean black hole temperature	137
B	The holographic bound	139

C	A black hole formed by collapse	141
C.1	Introduction	141
C.1.1	Scalar field in AdS_3	143
C.1.2	Scalar field in BTZ	144
C.1.3	Defining various modes	145
C.1.4	Mode expansions in various regions	146
C.1.5	Matching conditions	150
D	Curriculum vitae	153
D.1	Working experience	153
D.2	Education	153

1

Introduction

General relativity might be one of the most famous and successful theories published in over 100 years. It describes the gravitational interaction between massive bodies, generalizing special relativity and the Newtonian theory of gravity into a geometric theory. The Einstein field equations describe the curvature of space and time due to energy and momentum of matter and radiation. On the other hand we have quantum field theory, underlying the standard model of particle physics. It is successful in describing three of the four known fundamental forces; the electromagnetic, weak and strong interactions. An unanswered question to date is how to unify the classical theory describing gravity with quantum field theory, which would lead to a theory of quantum gravity. One possible way of approaching the problem is studying gravity in a regime where it is strong, for instance in the neighborhood of black holes.

The first discovered non-trivial exact solution of the Einstein field equations is the Schwarzschild metric

$$ds^2 = - \left(1 - \frac{2GM}{r}\right) dt^2 + \left(1 - \frac{2GM}{r}\right)^{-1} dr^2 + r^2 (d\theta^2 + \sin^2 \theta d\phi^2),$$

which describes the geometry outside a spherical mass. The solution has two singularities, where some of the metric components blow up; one at zero radius, and one at the Schwarzschild radius $r_S = 2GM$. The latter is a coordinate singularity that can be transformed away. For objects larger than their Schwarzschild radius one can use the solution without worrying about the singularity at the origin. The Schwarzschild radius is small for most objects, roughly nine millimeter for the earth, so corrections to flat space are small on the surface (that is, on earth the deviation from a flat metric are of the order of 10^{-9}). Of course one has to be careful to call this small, because it is large

enough to make an apple fall. For neutron stars the corrections become significant ($O(10^{-1})$), because the surface of the star is close to the Schwarzschild radius.

When all mass of a body is concentrated within its Schwarzschild radius, the metric describes a black hole whose size is given by its Schwarzschild radius. The Schwarzschild black hole, which is static and has no charge, is characterized by one quantum number; its mass. This in turn determines its temperature as computed by Hawking [1], and the size of the horizon which is located at the Schwarzschild radius. The horizon is not a physical surface, it is merely the collection of points from which it becomes impossible to escape from the gravitational pull of the mass, as seen from the outside. Even light cannot escape its gravitational pull. The horizon divides the solution in two separate patches, the interior and the exterior.

Due to gravitational redshift it appears to an observer far away that an object will never cross the event horizon. However, by performing a coordinate transformation to, for instance, the Kruskal extension one can see that objects cross the horizon in finite proper time. An observer crossing the event horizon of a sufficiently large black hole will not notice anything unusual according to classical GR. For a small black hole the curvature at the horizon is large and one starts to feel the effect of tidal forces.

In 1973 Bekenstein proposed that the area of a black hole is related to the entropy of a black hole and its surface gravity corresponds to its temperature [2]. In 1974 Hawking showed that black holes, having a temperature, actually radiate with an energy spectrum as if it were a perfect black body. Due to the geometry of the spacetime in between an observer at infinity and the black hole horizon, the spectrum can deviate; some frequencies may be enhanced whereas others are suppressed, in the literature this is termed a gray body spectrum. The entropy of the black hole was found to be given by

$$S = \frac{A}{4G},$$

where A denotes the surface area of the black hole and G is Newtons constant. For a solar mass black hole the entropy is of $O(10^{77})$, and the number of microstates is the exponential of that, which seems incompatible with only one number characterizing a black hole in GR. In the special case of super symmetric black holes the entropy was explained by Strominger and Vafa by counting the microstates of a BPS black hole, using string theory arguments [3].

Having a temperature and entropy means that black holes will radiate. A natural objection would be that one does not expect a body to radiate energy if not even light can escape its gravitational pull. The process of radiation can be visualized as follows; at the horizon virtual pairs of particles are created, where the energy of each pair adds up to zero. The particle with negative energy disappears behind the horizon and extracts (positive) energy from the black hole, while the particle with positive energy flies away to infinity. In this way energy is carried away from the black hole.

A bigger puzzle however is the thermality of the radiation. The quantum mechanical state describing the object that forms a black hole, whether it is a star, dust or any other object, could be pure. It is impossible for a pure state to evolve under unitary time evolution into a mixed state.

Another way of understanding why this is a problematic result, is that regardless of the state that formed the black hole, the final state will always be a thermal density matrix. It is characterized only by the temperature of the black hole. This leads to information loss, which is inconsistent with quantum mechanics. This was an important problem in the theoretical physics community for many years. In the literature this is known as the black hole information paradox.

Hawking assumed that *information* was simply *lost*. However other solutions were proposed as well. A particular solution was proposed [4], namely that black holes do not evaporate completely, but a massive *remnant* remains which carries information about the formation. With today's knowledge this idea seems not viable anymore, as we will discuss later. Another idea is that the radiation appears to be thermal, but actually has *small corrections*. When one captures a large fraction of the quanta emitted the small corrections combine to disclose the purity of the radiation. As an analogy one could think about burning a piece of paper, the photons that are emitted will look thermal, however if all radiation and ash would be collected, it is in principle possible to reconstruct exactly what was burnt. The difference between this example and black hole evaporation is that the latter has a horizon, and excitations behind it cannot influence what is outside according to general relativity.

In this thesis we will focus on the latter option, where small corrections will purify the radiation. It was shown by Page [5] that when one considers the black hole and its radiation as two subsystems that together form a random pure state, tracing over the black hole subsystem results into a mixed state. As the

radiation subsystem becomes as large as the black hole subsystem, its entropy starts to decrease until eventually a pure state remains. This is consistent with quantum mechanics, and today we believe that this is a plausible explanation of the situation.

With the conjecture of the gauge/gravity duality, also called the Anti de Sitter / conformal field theory (AdS/CFT) correspondence [6–8], the discussion of whether or not information is lost appeared to be settled. Because the field theory side is unitary, its dual in gravity must also be unitary and hence information is not lost. The question of what mechanism allows information to be carried away by seemingly thermal radiation is not answered by the duality, however it does offer new tools to study the problem.

The information problem described above only focused on the perception of an observer that stays outside the black hole. When the interior is included the information paradox becomes more subtle. The interior can be included in the following way: one can study Cauchy slices with certain properties [9], these slices are called ‘nice slices’. They are smooth and do not cut through regions with high spacetime curvature and cover the collapsing matter as well as the early radiation. They do so in such a way that the particles on the slice have low energy in the local frame.

Now there is a new conflict with quantum mechanics, the black hole seems to work like a quantum cloning device! At late time the radiation could be deciphered, giving a quantum description of the initial state that formed the black hole, however this information is already present at the other side of the same slice. By dividing the slice in two parts separated by the horizon the Hilbert space of states seems to be factorized into a tensor product. This is due to the niceness conditions, since low energy local operators commute with spacelike separated operators. When the infalling state is stored in the Hilbert space of the interior, then at most a negligible part can be found in the Hilbert space of the exterior, which is an argument loss of locality.

However when we consider a theory of quantum gravity there is no such thing as exact locality. Due to the non-local nature of gravity the Hilbert space cannot be factorized, and the argument of quantum cloning breaks down. The non-local nature of quantum gravity can be understood from the commutator of seemingly spacelike separated fields. Because the theory is invariant under diffeomorphisms there are no local invariants and the commutator of local fields cannot be fixed.

An idea proposed by 't Hooft [10] and refined by Susskind and others [11] is called *complementarity*. It is based on the idea that an observer far away sees a hot membrane a Planck length outside the horizon, also called the stretched horizon, which emits thermal radiation. However for a freely falling observer this membrane disappears, hence she sees no thermal radiation and therefore she does not see any information loss. These two descriptions are not inconsistent, since the infalling observer cannot communicate its findings about the disappearing membrane to the outside observer. Since these properties cannot be measured at the same time, they fit the complementarity principle of Bohr [12], one example of complementarity is the particle- wave duality.

Alongside the idea of complementarity, another idea of what a black hole looks like was proposed by Mathur [13]. It is called the *Fuzzball* proposal, we would like to mention it here for the sake of completeness. The black hole is replaced by a more general solution of supergravity or string theory; it does not have a horizon, but it looks like a black hole from far away while the “interior” is filled with “quantum fuzz”. The entropy is simply that of statistical origin. Due to the absence of a horizon, there is no information loss; matter coming from the asymptotic past will get trapped by the bound state for a long time, before it escapes to the asymptotic future [14]. Inside the horizon there is no empty space, it is filled with bound states of branes, that should grow in size when more are put together. Fluctuations of these branes extend to macroscopic scales. This resolves how information that is expected to be stored in the singularity at $r = 0$ can be carried a Schwarzschild radius distance away from it, before it is carried away to infinity. However when an observer dives into a fuzzball, she will encounter quantum fuzz, whereas general relativity predicts that nothing special occurs when crossing the horizon.

Later, the information paradox was refined in two different ways that challenged the ideas of complementarity.

First Mathur proved an argument in [15] suggesting that small corrections that were expected to restore the pure state to leading order in the Hawking computation are not enough.

Secondly AMPS(S), the authors of [16, 17], considered an observer that can extract information from the early radiation and consequently dives into the black hole. To obtain a pure state once the black hole has evaporated, early radiation has to be entangled with late radiation. However to ensure a smooth crossing of the horizon the modes across the horizon have to be maximally entangled. This violates the monogamy of entanglement. It was suggested that

the information in the late radiation is simply embedded in the Hilbert space of the early radiation. They argue however that this is in conflict with quantum mechanics, since an infalling observer could perform a measurement on the early radiation to find the early radiated bit it is entangled with, then dive into the black hole and encounter the same bit of information there, seemingly cloning the bit. So after crossing the horizon, carrying the data of the bit that was deciphered the original bit that was thrown into the black hole can be encountered, so that the observer actually has two copies of the same bit! This is one way to phrase the information paradox. One option to resolve the paradox is that the entanglement across the horizon is not there, which makes the crossing of the horizon an unpleasant experience [17]. The infalling observer would see a wall of highly energetic particles: a *firewall*.

As we mentioned above, the gauge/gravity duality can offer new tools to study gravity problems from the field theory perspective. The CFT machinery was used by Papadodimas and Raju [18] to construct a mathematical framework for the theory of complementarity in the context of AdS/CFT. In the CFT we can classify operators as ‘complicated’ or ‘simple’. Observers that only have access to simple operators can only perform simple measurements, they will see a firewall at the horizon. However observers that have access to complicated operators see that the firewall disappears, and will conclude that one can smoothly cross the horizon. In this thesis we will focus on this possible resolution of the black hole information paradox.

As a warm-up for black holes we will study Rindler space. The analogy between Rindler space and black holes becomes clear when we look at the Penrose diagram of the eternal black hole in a thermofield doubled (TFD) state [19] and compare it to the diagram of Rindler space in figure 2.8. The eternal black hole has a spacetime region outside the horizon, a black hole region, an identical copy of the exterior region on the other side of the black hole region and a ‘white hole’ region. Rindler space has four wedges, two can be seen as a future and past wedge, which are separated by a Rindler horizon from the left and right wedge. When an observer in the right (or left) wedge only has access to operators from that wedge, the Rindler horizon cannot be crossed smoothly to the future wedge. Only when modes from the other wedge are taken into account the horizon can be crossed smoothly. This is very similar to the eternal black hole case; when operators from one CFT that is dual to one universe are considered, the black hole horizon cannot be smoothly crossed. However when a particular combination of operators of *both* CFTs is considered,

the black hole horizon can be smoothly crossed, as in Rindler space. This is treated more elaborately in section 2.5.

When we look at a one sided black hole in AdS, only one boundary is present. However it is still possible to construct operators that have the same properties as the operators living in the second CFT. For reasons that will become clear later we shall call them *mirror operators*. These operators are extremely complicated, unlike the simple, single trace operators describing the exterior of the black hole. The division of operators in simple and complicated provides a mathematical rigorous description of the idea of black hole complementarity; an infalling observer that can do low energy, simple experiments will see a firewall just outside the horizon, however when one has access to the full theory the crossing is smooth. Therefore one possible way to avoid the necessity of a firewall is to distinguish between coarse- and fine graining of information in the Hilbert space, which was already used in the ‘old’ description of complementarity. The added feature is that the mirror operators have to depend on the black hole state to ensure that an infalling observer does not measure highly energetic particles near the horizon, and that Hawking radiation can be ‘purified’ using small corrections [20].

The black hole in the AdS/CFT correspondence is a challenging object to study technically, therefore we want to investigate questions regarding locality, causality, and mirror operators in a simpler setting in chapter 3. We describe, in the context of the AdS/CFT correspondence, how loss of locality can even be seen in empty AdS. We consider a large N CFT with an AdS bulk dual. From the CFT perspective we consider a set of operators that live in a time band, which is shorter than the light crossing time of AdS. This naturally divides the bulk spacetime into two regions, an annular region that is causally connected to the boundary CFT and a causal diamond in the center, that is causally disconnected from the boundary. We argue that this divides the operators on the boundary in two classes as well; namely simple operators and small products thereof (small in the order of N) and complicated operators. The complicated operators can be constructed from a large product of simple operators. We shall argue that the simple operators describe physics in the annular region, whereas the complicated operators describe physics in the diamond.

We show that we can probe regions in the bulk with complicated operators in the time band that are causally disconnected from this region. Since locality only has to hold up to a certain energy threshold, we can have significant viola-

tions of locality when we consider complicated operators as they are identified with complicated, high energy experiments. These complicated operators in the time band that can describe physics behind a causal horizon have similar properties as the mirror operators describing physics behind a black hole horizon, which are essential for black hole complementarity.

Before we described physics behind a causal horizon, and a static black hole horizon. The next step after peeking behind a causal horizon, and that of a static black hole, is to go beyond the horizon of a black hole formed by collapse, which is a challenging task due to the time dependent nature of the setup. New features can be studied, such as the trans-Planckian problem. It arises when one traces a Hawking particle that has escaped to infinity back to the horizon. The wavelength of the photons will be stretched due to the gravitational redshift, hence tracing it back makes it small; in fact, Hawking showed the frequency diverges at the horizon.

To understand the problems above from the CFT side, we first have to investigate black hole formation in greater detail. Black hole formation in AdS could be interpreted as thermalization of the boundary CFT. We will study this in a two dimensional CFT that is dual to three dimensional anti de Sitter space. In two dimensions the CFT computations become easier because then we can exploit the Virasoro algebra. The black hole shares most of its qualitative features with higher dimensional AdS black holes, therefore the insights that we get are useful to understand higher dimensional black hole problems conceptually.

In the framework of the $\text{AdS}_3/\text{CFT}_2$ correspondence a black hole in the bulk corresponds to a thermal state in the dual CFT, which is characterized by the Hawking temperature. In the CFT we start by constructing a heavy state by inserting primary operators with high scaling dimension, namely scaling with the central charge c in the limit $c \rightarrow \infty$. We then consider a two point function of probe operators on top of this state in late Lorentzian time to obtain the temperature. For a large number of heavy operators it naively looks like the perturbative expansion in $\frac{1}{c}$ breaks down and it becomes hard to extract even the leading order semi-classical behavior of the correlators. It was proposed that there exists a conformal transformation to absorb the heaviness of the operators in the background [21, 22], so that it is still possible to write down a power series expansion in $1/c$. This is known as the “uniformization problem”, which becomes more difficult as the number of heavy operator insertions increases.

In the bulk this corresponds to a energy being injected from the boundary. When a certain threshold is reached this will collapse into a black hole. Depending on the distribution this can result in a static black hole or an oscillating black hole, i.e. a black hole dressed by boundary gravitons. We will show numerically that there can be a large difference between the initial energy injected to the system and the energy of a black hole final state estimated using thermodynamics of the black hole. The difference in energy is interpreted to be stored in boundary gravitons.

2

The black hole information paradox

In this chapter we shall provide a short overview of the revived black hole information paradox. In this work we will focus on complementarity [11] as a resolution. In [18] a way that complementarity could be implemented was proposed that we will further investigate. In this chapter we shall give some heuristic arguments on the origin of Hawking radiation. After that we will discuss the implications it had, to introduce the later chapters of this thesis.

2.1 Hawking radiation

Quantum field theory in curved space has certain features that we do not see in flat space. Time dependence and regions of high curvature cause particles to be created [23]. Hawking radiation arises in the vicinity of a black hole. The process of black hole evaporation was first described in [1] and reviewed extensively in for instance [15, 24, 25], where in this section we will follow the latter. Black hole radiation itself was first predicted by Zel'dovich [26], for rotating black holes. It was based on the idea that the rotation amplifies some waves, assuming a similar quantum effect of spontaneous emission of energy and angular momentum [24].

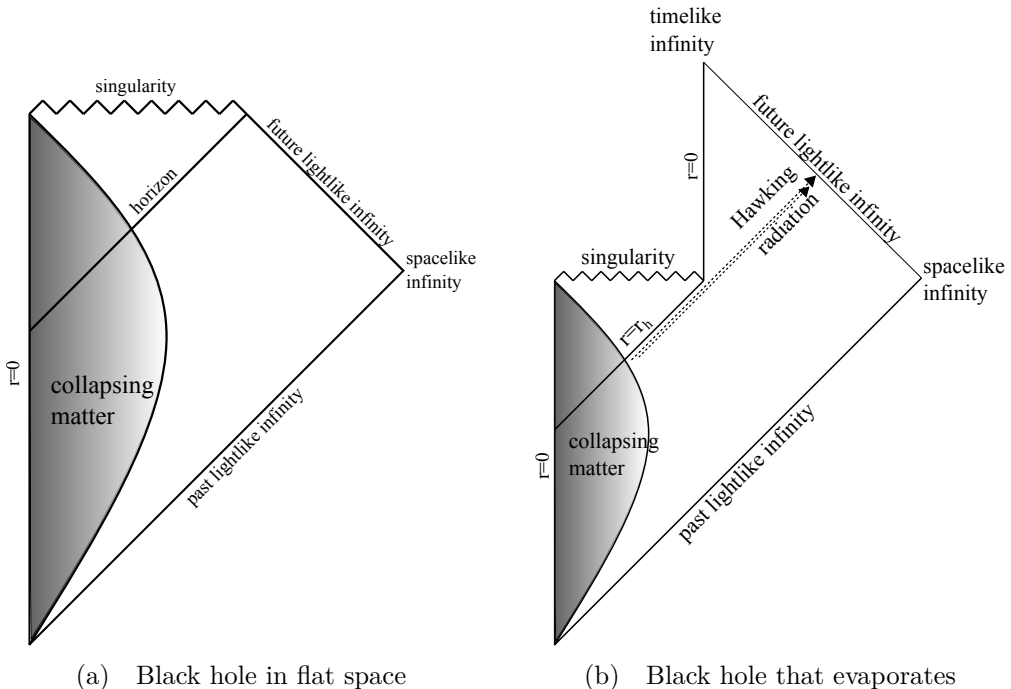


Figure 2.1: Penrose diagram of a black hole in flat space 2.1a and the conjectured diagram of a black hole that evaporates through Hawking radiation 2.1b.

To understand the origin of the radiation we will study the Kruskal extension of the Schwarzschild metric. We start with the latter,

$$ds^2 = - \left(1 - \frac{2GM}{r} \right) dt^2 + \left(1 - \frac{2GM}{r} \right)^{-1} dr^2 + r^2 (d\theta^2 + \sin^2 \theta d\phi^2), \quad (2.1)$$

where the horizon is located at the Schwarzschild radius $r_h = 2GM$. We now introduce the tortoise coordinate

$$r_* = \int f(r)^{-1} dr = \int \left(1 - \frac{r_h}{r} \right)^{-1} dr = r + r_h \ln(r - r_h), \quad (2.2)$$

so that the metric becomes conformally flat

$$ds^2 = \left(1 - \frac{r_h}{r} \right) (-dt^2 + dr_*^2) + r^2 (d\theta^2 + \sin^2 \theta d\phi^2). \quad (2.3)$$

We now define the ingoing and outgoing Eddington-Finkelstein coordinates

$$u = t + r_* \quad \text{and} \quad v = t - r_*, \quad (2.4)$$

respectively. The metric then becomes

$$ds^2 = - \left(1 - \frac{r_h}{r}\right) dudv + r^2 (d\theta^2 + \sin^2 \theta d\phi^2). \quad (2.5)$$

To bring the horizon to a finite distance, we change coordinates again to $U = -e^{-u/2r_h}$ and $V = e^{v/2r_h}$. Then the metric takes the form

$$ds^2 = -\frac{4r_h^3}{r} e^{-r/r_h} dU dV + r^2 (d\theta^2 + \sin^2 \theta d\phi^2). \quad (2.6)$$

As a final step we move back from null coordinates to spacelike and timelike coordinates by taking $U = T - X$ and $V = T + X$ to find the metric

$$ds^2 = \frac{4r_h^3}{r} e^{-r/r_h} (-dT^2 + dX^2) + r^2 (d\theta^2 + \sin^2 \theta d\phi^2). \quad (2.7)$$

The coordinate transformation going from the original coordinates to the ones above is given by

$$\begin{aligned} X &= \left(\frac{r}{r_h} - 1\right)^{\frac{1}{2}} e^{r/2r_h} \cosh(t/2r_h) & T &= \left(\frac{r}{r_h} - 1\right)^{\frac{1}{2}} e^{r/2r_h} \sinh(t/2r_h), \quad (r > r_h) \\ X &= \left(1 - \frac{r}{r_h}\right)^{\frac{1}{2}} e^{r/2r_h} \sinh(t/2r_h) & T &= \left(1 - \frac{r}{r_h}\right)^{\frac{1}{2}} e^{r/2r_h} \cosh(t/2r_h), \quad (r < r_h) \end{aligned} \quad (2.8)$$

with the constraint $r > 0$ and $T^2 - X^2 < 1$. The Schwarzschild coordinates t, r cover the black hole exterior $x > |T|$, which is region *I* in the diagram. Maximally extending the geometry by analytic continuation we obtain the other three regions.

Spacetime regions of the Kruskal extension

Region I	$U < 0, V > 0$	Schwarzschild
Region II	$U > 0, V > 0$	black hole interior
Region III	$U > 0, V < 0$	mirrored exterior
Region IV	$U < 0, V < 0$	white hole interior

Table 2.1: Regions of the maximally extended Schwarzschild solution

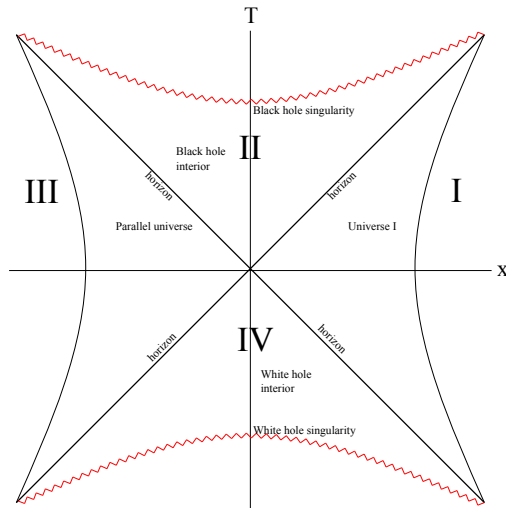


Figure 2.2: The Kruskal extension of the Schwarzschild black hole.

The singularity is located in the future and past interior at $r = 0$, the two exterior universes are joined with a non traversable Einstein-Rosen bridge.

An infalling observer in these coordinates takes a finite proper time τ to fall through the horizon, whereas an outside observer will note an infinite time t . In the Kruskal coordinates the falling in occurs along lines of almost constant V , since the observer will be accelerated all the way from infinity the speed will become constant and close to the speed of light. While U goes through zero implies that the proper time goes as

$$d\tau \propto e^{-t/r_h} dt, \quad (2.9)$$

where τ crosses the horizon smoothly at $U = 0$, and $V = \text{cst.}$ The outside observer only has access to region I, for this person spacetime stops at the horizon. We can perform a Bogoliubov transformation between the basis of the infalling observer and the outside observer to obtain Hawking's result. The field of the infalling observer is expanded in his eigentime τ with dual frequency ν and that of the outside observer in time t and dual frequency ω . The coordinates (u, v) are lightcone coordinates only valid in region I and II. The massless scalar field in Eddington-Finkelstein coordinates (2.5) obeys, ignoring the angular part,

$$\partial_u \partial_v \phi = 0, \quad (2.10)$$

and in Kruskal-Szekeres coordinates (2.6) we have

$$\partial_U \partial_V \phi = 0. \quad (2.11)$$

Expanding the field in the outgoing (right moving) modes in both coordinate systems we get

$$\phi_R = \int_0^\infty \frac{d\omega}{2\pi\sqrt{2\omega}} \left(b_\omega e^{-i\omega u} + b_\omega^\dagger e^{i\omega u} \right) = \int_0^\infty \frac{d\nu}{2\pi\sqrt{2\nu}} \left(a_\nu e^{-i\nu U} + a_\nu^\dagger e^{i\nu U} \right). \quad (2.12)$$

The usual commutation relations are given by

$$\left[a_\nu, a_{\nu'}^\dagger \right] = 2\pi\delta(\nu - \nu'), \text{ and } \left[b_\omega, b_{\omega'}^\dagger \right] = 2\pi\delta(\omega - \omega'). \quad (2.13)$$

Since the Kruskal coordinates (U,V) are smooth across the horizon these will be used by the infalling observer, whereas the outside observer uses the other expansion which has a well defined frequency. The relation between the modes is given by

$$b_\omega = \int_0^\infty \frac{d\nu}{2\pi} \left(\alpha_{\omega\nu} a_\nu + \beta_{\omega\nu} a_\nu^\dagger \right). \quad (2.14)$$

The Bogoliubov coefficients are obtained by taking the modes in (2.12) and performing the coordinate transformation to the other frame and taking the Fourier transform

$$\begin{aligned} \alpha_{\omega\nu} &= 2r_h \sqrt{\omega/\nu} (2r_h\nu)^{2ir_h\omega} e^{\pi r_h\omega} \Gamma(-2ir_h\omega), \text{ and} \\ \beta_{\omega\nu} &= 2r_h \sqrt{\omega/\nu} (2r_h\nu)^{2ir_h\omega} e^{-\pi r_h\omega} \Gamma(-2ir_h\omega). \end{aligned} \quad (2.15)$$

When the coefficient $\beta_{\omega\nu}$ is nonzero the vacuum of one observer will not look like the vacuum for the other observer. Using the operators of the infalling observer acting on the black hole vacuum state gives $a_\nu |0\rangle_{BH} = 0$, whilst with the operators of the asymptotic the result will be different. The number of particles the asymptotic observer sees is given by $N = |\beta_{\omega\nu}|^2$, that is, the outside observer sees

$$\langle 0_{BH} | b_\omega^\dagger b_{\omega'} | 0_{BH} \rangle = \frac{2\pi\delta(\omega - \omega')}{e^{4\pi r_h\omega} - 1}, \quad (2.16)$$

which is the spectrum of a perfect black body with inverse temperature $\beta = 4\pi r_h = 8\pi GM$. An observer far away could see a different spectrum due to a

gray body factor, which is caused by the metric stretching some wavelengths and shortening others.

The divergence in the expression (2.16) comes from the plane wave approximation, in fact we should have considered a wave packet, then the divergent part goes away [1]. This approximation however does yield the correct result. Another possible objection is that we used the Schwarzschild solution, which is actually static. The evaporation is so slow ($t_{\text{evap}} \approx 10^{67}$ y for a solar mass black hole) that the static solution is a reasonable approximation.

The black body spectrum entails that the only information the radiation carries is the temperature of the black hole. No information about the formation of the black hole can be extracted from the radiation. With every quantum that is emitted the black hole will lose some of its energy, until it has evaporated completely. This means that when only the radiation remains, all information about the formation and whatever fell into the black hole is gone. This is in contradiction with quantum mechanics, where time evolution is *unitary* and thus in principle it is reversible. This contradiction is called the *black hole information paradox*. With the discovery of the AdS/CFT correspondence the discussion whether or not information is destroyed by a black hole was settled; since the bulk theory with gravity and evaporating black holes is dual to a conformal field theory that is manifestly unitary the evaporation process has to be unitary as well. This argument convinced Hawking [27]. The correspondence however does not answer the question of how information is actually carried out. In the next section we will study this question in detail.

Thermal radiation, the Page curve and a spin chain example

According to Hawking's computation a black hole emits thermal radiation, which can be described with a density matrix. The initial state, which could be a pure state, that collapsed into a black hole that consequently evaporates thermally, is in contradiction with quantum mechanics. A proposal for the resolution of the information paradox is that the photons only *appear* to be thermal. That is, there are *small corrections* on top of the thermal state that, when many photons are taken together, combine to disclose a pure state.

When we consider the black hole as seen from infinity we expect from Hawking's computation that the Von Neumann entropy of the radiation goes up with every quantum that is emitted, because every single one appears to be thermal.

From unitarity of quantum mechanics however we expect that the entropy in the end should be zero because all information of the initial pure state is captured in the radiation, leaving no ambiguity about the final state. In this section we shall give some examples and show how the entropy of the radiation, in what is called the Page curve, is constructed from basic quantum mechanics. The problem of seemingly thermal radiation we treat by considering a spin chain example which has all the properties we require. First we show that a pure state can never evolve into a mixed state. The density matrix of a pure state has the property that

$$\rho_{pure}^2 = \rho_{pure} \quad (2.17)$$

Now let us consider time evolution with a Unitary operator so that

$$\rho(t) = U\rho(t=t_0)U^\dagger \quad (2.18)$$

when we square this we see that it satisfies (2.17)

$$\begin{aligned} \rho(t)^2 &= U\rho(t=t_0)U^\dagger U\rho(t=t_0)U^\dagger \\ &= U\rho(t=t_0)U^\dagger = \rho(t) \end{aligned} \quad (2.19)$$

And therefore a pure state can not evolve under unitary time evolution to a mixed state. Using this result and the fact that the entropy of our initial state was zero we know that after the entropy in the end must be zero. In between we do not know what the Von Neumann entropy

$$S = -\text{Tr} [\rho \ln(\rho)] , \quad (2.20)$$

does. The entropy of the subsystem is given by

$$S_A = -\text{tr} \rho_A \ln \rho_A, \quad (2.21)$$

where the reduced density matrix of one subsystem is given by tracing out the other subsystem

$$\rho_A = -\text{tr}_B \rho_{AB}, \quad (2.22)$$

where ρ_{AB} denotes the density matrix of the systems A and B taken together. The entropies of the subsystems and the entropy of the total system obey the triangle inequality

$$S_A + S_B \geq S_{AB} = 0. \quad (2.23)$$

Where we used the fact that the entropy of a pure state, which we started out with, is zero. Hence the entropy of the subsystem and its complement is the

same. Therefore we know that the entropy of the radiation as a function of captured quanta is monotonically increasing, up to the point where half the initial entropy of the black hole has been radiated away. This moment in time is called the Page time t_{Page} [28].

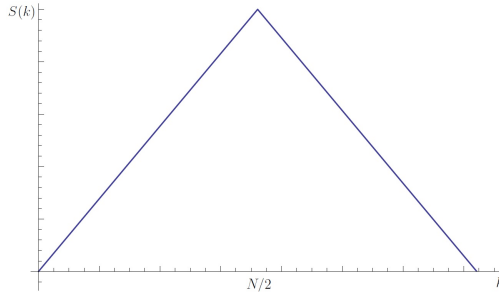


Figure 2.3: Entanglement entropy of a subsystem of size k . The total system consists of N bits.

The Von Neumann entropy of the system can go down because we are looking at the micro states of the system (fine grained). This is not the macroscopic (coarse grained) entropy of a system considered in thermodynamics, which can only grow over time. The spin chain serves as a toy model for black hole evaporation showing how the entanglement entropy of the radiation can go up and down. However knowing the exact form of the Page curve for black holes would be similar to actually solving the information problem in some theories [29].

The remainder that needs explanation is the apparent contradiction of thermal radiation as was derived by Hawking and the pure state which has zero entropy that we just found. In order to explain this phenomenon we turn a chain of N spin- $\frac{1}{2}$ particles as an example. $|\Phi\rangle_i = |\uparrow\uparrow\downarrow \dots \uparrow\rangle$ denotes an orthonormal basis of the spin chain, where the spins have a definite value

$$|\Psi\rangle = \sum_i \frac{c_i}{\sqrt{2^N}} |\Phi\rangle_i. \quad (2.24)$$

To simplify the calculation we assume that the coefficients c_i have unit norm. The computation could be done with random coefficients as well. When we extract a single spin from the chain and label it A and the remaining spin

system we call B we can decompose $|\Psi\rangle$, after properly normalizing, as follows

$$|\Psi\rangle = \frac{1}{\sqrt{2^N}} \sum_{i=1}^{2^{N-1}} p_i |\uparrow, i\rangle + q_i |\downarrow, i\rangle, \quad (2.25)$$

where the coefficients take the form $p_j = e^{i\theta_j}$, $q_i = e^{i\theta_i}$, with θ a random phase. The sum now runs from $i = 1$ to 2^{N-1} because we explicitly split of the first spin while the rest of the spins can be in any possible configuration. The density matrix is given by

$$\rho^{AB} = |\Psi\rangle \langle \Psi| = \frac{1}{2^N} \sum_{i,j}^{2^{N-1}} \begin{pmatrix} p_i p_j^* & p_i q_j^* \\ q_i p_j^* & q_i q_j^* \end{pmatrix}. \quad (2.26)$$

The reduced density matrix of the extracted spin is given by (2.22) so that after tracing out B, which gives a δ_{ij} we find

$$\rho_A = \frac{1}{2^N} \sum_i^{2^{N-1}} \begin{pmatrix} p_i p_i^* & p_i q_i^* \\ q_i p_i^* & q_i q_i^* \end{pmatrix}. \quad (2.27)$$

The diagonal elements are $\frac{1}{2}$ with zero variance, since the spread in the absolute value squared is zero. For the off diagonal terms we find

$$\frac{1}{2^N} \langle \sum_i^{2^{N-1}} p_i q_i^* \rangle = \frac{1}{2^N} \sum_i^{2^{N-1}} \langle p_i \rangle \langle q_i^* \rangle = 0, \quad (2.28)$$

because the numbers are random, uncorrelated phases. The variance is given by

$$\begin{aligned} \text{Var}(p_i q_i^*) &= \langle \left(\frac{1}{2^N} \sum_i^{2^{N-1}} p_i q_i \right)^2 \rangle - \langle \frac{1}{2^N} \sum_i^{2^{N-1}} p_i q_i^* \rangle^2 \\ &= \langle \left(\frac{1}{2^{2N}} \sum_i^{2^{N-1}} |p_i|^2 |q_i|^2 \right) \rangle - \frac{1}{2^{2N}} \langle \sum_{i \neq j}^{2^{N-1}} p_i p_j^* q_i^* q_j \rangle \\ &= \frac{2^{N-1}}{2^{2N}} + \frac{1}{2^{2N}} \sum_{i \neq j}^{2^{N-1}} \langle p_i \rangle \langle p_j^* \rangle \langle q_i^* \rangle \langle q_j \rangle \\ &= O(2^{-N}), \end{aligned} \quad (2.29)$$

where in the last step we used that the expectation value of the independent random numbers is zero. Hence we find that the off diagonal terms are exponentially small with the number of spins [18]. The Von Neumann entropy of A is given by $S_A = \ln(2)$, when neglecting the off diagonal terms, which is the maximum entropy of a state with Hilbert space dimension two. Extracting k spins gives an entropy $S_A^{k\text{spins}} = k \ln(2)$, up to the point where we extracted $\frac{N}{2}$ spins. The diagonal elements become smaller since they go as 2^{-k} and the off-diagonal terms have a typical size of 2^{-N} so as k approaches $N/2$ these values approach each other and the form of a thermal density matrix breaks down [18, 28]. At this point the entropy of both subsystems is maximal, after extracting more bits the entropy has to go down since the entropy of the subsystems is the same. After the half-way point of evaporation it has been suggested that information can be recovered at the same rate as it fell in. It seems like the black hole behaves like a mirror [30].

The spin-chain is an example of a pure state that appears to be thermal, analogous to the emission of seemingly thermal evaporation of a black hole. Page realized that following the above reasoning and, considering that the star from which the black hole has collapsed could have been in a pure state, the entropy of black hole radiation is maximal when half of the initial degrees of freedom are remaining in the black hole state and the other half is in the radiation, and that after this point the entropy should go down [28].

2.2 Complementarity

The previous analysis of Page suggests that the information paradox could be resolved by taking the exponentially small corrections to Hawking’s calculation into account. However the situation changes when we include the interior of the black hole as well. Let us take a look at the Penrose diagram of the evaporating black hole in figure 2.4, where we have drawn two “nice slices” in red. They are spacelike hypersurfaces that intersect the collapsing matter as well as the radiation. Because the gravitational collapse as well as the evaporation can be described with low energetic particles and the evaporation of the black hole is slow, the adiabatic theorem tells us that we do not have to take high energetic modes into account. Therefore the whole process can be described by low energy effective field theory.

On the same spacelike slice the collapsing matter as well as a large part

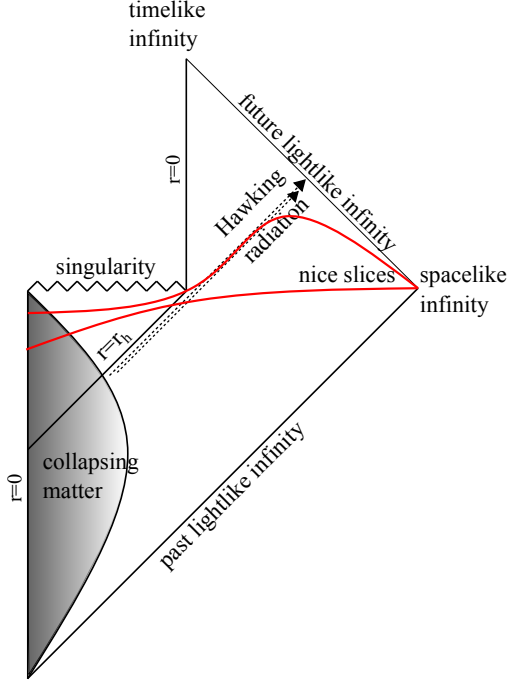


Figure 2.4: Black hole that evaporates, including nice slices (red).

of the radiation is present. Because the evaporation is unitary, no information about the quantum state of the collapsing matter is lost. However it appears it is present at two different locations on the same slice! This is quantum cloning, which is not allowed by linearity of quantum mechanics. When we assume quantum cloning is possible we run into a contradiction; let us construct a unitary operator that duplicates a state onto an empty state

$$U |\psi\rangle |e\rangle = |\psi\rangle \otimes |\psi\rangle . \quad (2.30)$$

When we take the state to be $|\psi\rangle = c_1 |\uparrow\rangle + c_2 |\downarrow\rangle$, with the c_i some coefficients, the cloning operation will give

$$U |\psi\rangle |e\rangle = c_1^2 |\uparrow\uparrow\rangle + c_1 c_2 |\uparrow\downarrow\rangle + c_2 c_1 |\downarrow\uparrow\rangle + c_2^2 |\downarrow\downarrow\rangle , \quad (2.31)$$

whereas linear superposition predicts

$$U (c_1 |\uparrow\rangle + c_2 |\downarrow\rangle) |e\rangle = c_1 |\uparrow\uparrow\rangle + c_2 |\downarrow\downarrow\rangle . \quad (2.32)$$

Hence when we allow for quantum cloning we run into a contradiction.

A possible resolution was proposed in [10, 11], which was named *complementarity*. Here a “stretched horizon” is proposed, a hot membrane one Planck length outside the actual horizon. To an outside observer it seems that information thrown into the black hole is scrambled in the degrees of freedom on the membrane and then re-emitted in Hawking radiation. However for a bit of information, or an observer, falling into the black hole the membrane would disappear. The information would cross the horizon as predicted by general relativity, and eventually fall into the singularity. This seems to resolve the information paradox at first sight; there are two descriptions of the same event, however the observer falling in cannot communicate its findings to the outside observer. Hence there are two different descriptions of the same event, this is why it is called black hole *complementarity*.

The postulates of *black hole complementarity* [10, 11] are

- *The process of formation and evaporation of a black hole, as viewed by a distant observer, can be described entirely within the context of standard quantum theory. In particular, there exists a unitary S -matrix which describes the evolution from infalling matter to outgoing Hawking-like radiation.*
- *Outside the stretched horizon of a massive black hole, physics can be described to good approximation by a set of semi-classical field equations.*
- *To a distant observer, a black hole appears to be a quantum system with discrete energy levels. The dimension of the subspace of states describing a black hole of mass M is the exponential of the Bekenstein entropy $S(M)$.*

A similar idea to the first postulate was first thought of by 't Hooft [31]. The second postulate makes sure there are quantum corrections to the classical equations of motion so that Hawking radiation can arise. Finally the third postulate deals with black hole thermodynamics. A fourth postulate is predicted by general relativity, which was discussed in the aforementioned works. It was explicitly added to the postulates in [16],

- A freely falling observer experiences nothing out of the ordinary when crossing the horizon.

The first three postulates refer to what an outside observer sees, whereas the fourth deals with the infalling observer.

Various consistency checks of black hole complementarity were considered [32, & references therein]. For instance, one thought experiment describes preparing an entangled state outside the black hole, and throwing one part into the black hole while keeping the other part outside. At some point the exterior observer can extract the information of the qbit that fell in from the radiation, and then dive in the black hole to find the original qbit. It seems that one observer has two copies of the same qbit, which would imply observable quantum cloning. It was however argued in [32, 33] that this is impossible.

The reason why this is actually impossible is the following. We call a system scrambled when information about the initial state, that was initially pure, can only be retrieved by studying at least half the degrees of freedom. That is, any subsystem smaller than half of the size system has close to maximum entanglement entropy. When a single qbit is added to a pure state that has been scrambled, the time it takes for the information to diffuse over the degrees of freedom is defined as the scrambling time [33]. As we mentioned before, after half of the initial entropy has been radiated away the state purifies and information can be retrieved easily from the radiation. If we throw in a qbit, it can be recovered in a time as short as the scrambling time [30]. However short this time may be, the qbit that was thrown in will have hit the singularity before its information is deciphered from the radiation [32, 33].

It is conjectured that black holes are the fastest scramblers in nature, that is, no other system thermalizes as quickly as a black hole does [34]. Since the infalling qbit will hit the singularity before the scrambling time, and the scrambling time is the shortest time possible to obtain information from the radiation, black hole complementarity is a safe resolution of the information paradox. Boosting the qbit that fell in, to hover close to the horizon for a long time to avoid the singularity would require trans Planckian energy, therefore we do not consider this option.

2.3 Strong subadditivity, small corrections and firewalls

Now we present new arguments that revived the information paradox, seemingly contradicting with complementarity. Instead of using qbits that we throw in, we look at naturally produced Hawking pairs. It appears that the situation changes dramatically according to AMPS [16]. In this section we shall review some of the arguments.

2.3.1 Entanglement and the theorem of strong subadditivity

The strong subadditivity theorem of three *separate* quantum mechanical systems (A , B and C) is given in two forms by [35]

$$S(A + B) + S(B + C) \geq S(A) + S(C), \quad (2.33)$$

and

$$S(A + B) + S(B + C) \geq S(B) + S(A + B + C). \quad (2.34)$$

Summing the subsystems means that we compute the entropy of these systems taken together. Mathur and AMPS discussed in two different ways some properties of Hawking radiation. AMPS argued that late radiation cannot be maximally entangled with both the interior and early radiation, which is actually necessary to smoothly cross the horizon [16]. Mathur argued that small corrections to the radiation are not enough to purify the state in [15], and comes up with a slightly different argument of the paradox.

Entropy and entanglement

We label the early Hawking modes A and the late Hawking mode B with C its interior partner mode. After Page time the entropy has to go down, hence

$$S(A + B) < S(A). \quad (2.35)$$

The entropy $S(A)$ of the early, thermal, hawking mode is greater than zero. And since the modes across the horizon are maximally entangled which is required to smoothly cross the horizon we have

$$S(B + C) = 0, \quad (2.36)$$

which leads to

$$S(A + B + C) = S(A). \quad (2.37)$$

Putting all of this together in (2.34) we obtain

$$S(A) \geq S(B) + S(A). \quad (2.38)$$

Which is clearly inconsistent since $S(A)$ and $S(B)$ are positive, because the state of the late outgoing radiation B is thermal, hence $S(B) > 0$. The theorem is even stronger when Page's argument is considered, namely that the entropy goes down maximally after the Page time t_{Page} ; $S(A + B) = S(A) - S(B)$ and thus

$$S(A) \geq 2S(B) + S(A), \quad (2.39)$$

The inequality implies that $S(B) < 0$, which clearly contradicts with Hawking's conclusion, namely that the radiation appears thermal. Mathur argued in [15] that small corrections are not enough to purify the state. The identity (2.33), together with (2.35) and

$$S(B) = S(C), \quad (2.40)$$

which follows from (2.36), are seemingly inconsistent.

A firewall at the horizon

The arguments above led people to believe that the postulates of black hole complementarity cannot all be true. When we assume the AdS/CFT correspondence to be true, the evaporation process of a black hole has to be unitary. Since the curvature is small around a sufficiently heavy black hole there is no reason for EFT to break down, but it implies that the radiation escapes from a membrane that is a Planck length outside the horizon, known as the stretched horizon. Purity of the radiation implies that new Hawking modes are maximally entangled with the early radiation, smoothness of the horizon implies that modes across the horizon are maximally entangled, which seems to be contradictory. Giving up entanglement across the horizon seems like the more conservative compared to giving up unitarity, the consequence for the infalling observer encountering a hot membrane of highly excited particles just outside the horizon. This means that the horizon becomes a special place in space, which is radically different from what general relativity predicts.

2.4 A new tool: the AdS/CFT correspondence

In this section we shall give a lightning introduction to the AdS/CFT correspondence [6–8]. We shall motivate the correspondence and discuss some aspects that are useful to understand the rest of the thesis. This section is by no means intended to give an exhaustive review of the duality.

One can take two approaches to motivate the AdS/CFT correspondence, either starting from a strongly coupled gauge theory and argue that it can be related to string theory, or by taking the low energy decoupling limit of string theory.

2.4.1 Flux tubes and the large N limit

Quantum chromodynamics describes the strong interaction between quarks and gluons, it is a gauge theory based on $SU(3)$, where three is the number of quark colors. The coupling constant runs, that is, at low energies QCD is strongly coupled (confinement) whereas at high energies it is asymptotically free.

Let us consider a confined quark, anti-quark pair, the flux is believed to be squeezed to spread minimally over space. Unlike in quantum electrodynamics where the field lines of electrons spread over space and thus fall off as $1/r$, the flux tube of gluons is believed not to spread out. The flux tube of gluons has a constant energy density. When the quarks are separated by a greater distance the energy in the tube will grow linearly and hence the quarks are confined by a linear potential. This flux tube could play the role of an open string.

Since one cannot use perturbation theory when it is strongly coupled another trick had to be invented. 't Hooft proposed that the theory simplified when we take the number of colors N to infinity, which is known as the large N limit, and consequently set N equal to three [36].

In the Feynman diagram expansion there is a free index in the loops, which runs over the number of colors, which is taken to infinity in the large N limit. This problem can be cured by using the 't Hooft limit [36]. From the diagram drawn in figure 2.5c we see that to keep the propagator finite we need $\lambda = Ng_{YM}^2$ to be constant. This is known as the 't Hooft coupling which consists of a double scaling limit where $N \rightarrow \infty$ and $g_{YM} \rightarrow 0$ so that the $Ng_{YM}^2 = \lambda = \text{cst.}$

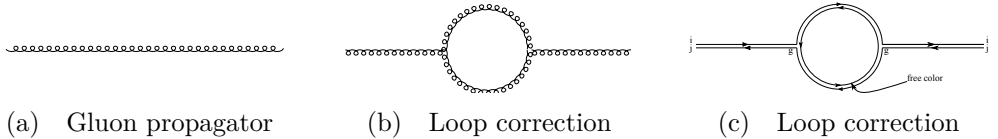


Figure 2.5: A gluon propagator and a loop correction in two notations; a Feynman diagram and the same diagram in 't Hooft his double line notation 2.5c.

The Lagrangian of a QFT with fields Φ_i^a , with a an index in the adjoint representation $SU(N)$ and i for instance a flavor index, can be schematically written as

$$\mathcal{L} \sim \text{Tr} (d\Phi_i d\Phi_i) + g_{YM} c^{ijk} \text{Tr} \Phi_i \Phi_j \Phi_k + g_{YM}^2 d^{ijkl} \text{Tr} \Phi_i \Phi_j \Phi_k \Phi_l. \quad (2.41)$$

Here c^{ijk} and d^{ijkl} are constants. The field Φ_i could also be taken to be the gauge field, since it transforms under the adjoint representation. The three point interaction vertex is proportional to the coupling constant and the four point vertex goes with the coupling constant squared. To see the scaling with the 't Hooft coupling and N we rescale the fields as $\tilde{\Phi}_i \equiv g_{YM} \Phi_i$ so the Lagrangian becomes

$$\mathcal{L} \sim \frac{N}{\lambda} \left(\text{Tr} (d\tilde{\Phi}_i d\tilde{\Phi}_i) + c^{ijk} \text{Tr} \tilde{\Phi}_i \tilde{\Phi}_j \tilde{\Phi}_k + d^{ijkl} \text{Tr} \tilde{\Phi}_i \tilde{\Phi}_j \tilde{\Phi}_k \tilde{\Phi}_l \right). \quad (2.42)$$

To simplify the Feynman diagram expansion we introduce the double line notation [36], where each line corresponds to a color index. In the scaling limit described before there are no diagrams with external lines that are diverging, which can be easily seen from the double line diagrams. Here planar diagrams scale with λ to the power of loops. Let us now consider a non-planar diagram and a planar one as in 2.6.

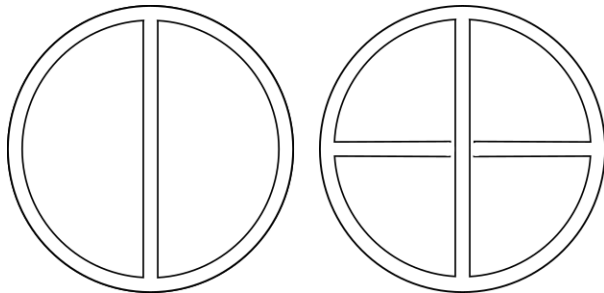


Figure 2.6: A planar diagram with three loops (left), and a non-planar diagram (right) with two loops, in double line notation.

The diagram on the left has three color indices, one for each loop, and two couplings g_{YM} . The right diagram has two free color indices and four couplings g_{YM} . Hence the left diagram scales as $O(N^2)$ whereas the right scales as $O(1)$. Therefore in the large N expansion we only need to consider the planar diagrams.

The diagrams in double line notation can be thought of as triangulated Riemann surfaces. We can then relate V (vertices) to the number of vertices, E (edges) to the number of propagators and F (faces) to the number of loops. Euler his formula for a polyhedron which is topological invariant is given by

$$V - E + F = 2 - 2g \quad (2.43)$$

where g is the genus. We then find that planar diagrams have the topology of a sphere, that is genus zero. Non-planar diagrams have $g \geq 1$.

$$\begin{aligned} \text{propagators} & \left(\frac{N}{\lambda}\right)^E \\ \text{vertices} & \left(\frac{\lambda}{N}\right)^V \\ \text{closed loops} & N^F \end{aligned} \quad (2.44)$$

So that

$$\left(\frac{N}{\lambda}\right)^E \left(\frac{\lambda}{N}\right)^V N^F = N^{V-E+F} \lambda^{E-V} = N^{2-2g} \lambda^{E-V} \quad (2.45)$$

From this we can see that the planar diagrams have a contribution of N^2 whilst higher order diagram contributions will be suppressed by a factor $1/N^2$.

The connection with string theory

The flux tube between a quark anti-quark pair could play the role of an open string. The different vibrational modes of the string represent different mesons. Glue balls could represent closed strings [37], which contains the graviton. Now let us make the connection with string theory by considering diagrams in which two strings evolve into two strings, with string coupling constant g_s . In quantum field theory we sum over all fields running in the loop while in string theory we have n strings going to n strings where we have to integrate over all geometries for every genus. This is one way to motivate the relation between a strongly coupled gauge theory and gravity. In the section below we take another approach.

2.4.2 String theory and the AdS/CFT correspondence

In string theory we have open and closed strings. There are two types of boundary conditions that can be imposed on the endpoints of an open string, the von Neumann boundary condition $\partial_\sigma X^\mu = 0$, at $\sigma = 0$, which implies that there is no restriction on δX and hence the endpoints can move freely. The Dirichlet boundary condition is given by $\delta X^\mu = 0$, at $\sigma = 0$, fixing the endpoints of the string at a particular location in space. Combining these boundary conditions was an insight of Polchinski [38], considering $p+1$ von Neumann boundary conditions and $D-1-(p+1)$ Dirichlet boundary conditions fixes the endpoints of the string to live on a $p+1$ dimensional hypersurface, which is called a Dp -brane with p denoting the amount of spatial dimensions. The endpoints of the string on the D -brane carry a $U(1)$ charge. When we stack N D -branes together, and considering a string that can start on one brane and end at another, we need two indices running from one to N to describe it. Implied in the low energy limit that it is described by a $U(N)$ gauge theory.

Supergravity is the low energy limit of string theory. It contains black p -branes, which are generalized black hole-like solution of supergravity whose horizon is space filling in p dimensions. A black 0-brane without charge and angular momentum would be the Schwarzschild black hole. The p -brane is surrounded by a $D - p - 2$ dimensional sphere, where D denotes the dimensionality of spacetime and the two other dimensions are time and the radial direction. At strong coupling the stack of D -branes backreact on the geometry in such a way that it is described by an extremal black brane geometry [39], which is the

higher dimensional equivalent of the extremal Reissner-Nordstrom black hole. Strominger and Vafa [3] computed the entropy of this type of black hole, not only finding the correct number as well as the functional dependence on the charges. This result, obtained from two completely different approaches, feeds the idea that black holes actually consist of D-branes as reviewed in [40].

The decoupling limit

We now review the logic that Maldacena followed to conjecture the AdS/CFT correspondence. We consider N D3 branes stacked together, extending along three spatial dimensions and in time. We will look at this setup at strong string coupling $g_s N \gg 1$, which is the closed string perspective and at weak coupling $g_s N \ll 1$ which is the open string perspective. Type IIB string theory contains open and closed strings. The former have their endpoints on the D-branes whereas the latter are excitations of empty space.

The effective low energy action of the massless modes of the string can schematically be written as

$$S = S_{\text{bulk}} + S_{\text{brane}} + S_{\text{int}}. \quad (2.46)$$

Where the bulk action lives in ten dimensional flat space. In the low energy limit it is the action of supergravity. The massive fields have been integrated out since their energy is too high. The brane action lives on a $(3+1)$ dimensional worldvolume, containing the $\mathcal{N} = 4$ super-Yang-Mills. In the low energy limit the interaction terms go to zero, which we knew already from gravity becoming free at long distances. One can show that the interaction between bulk and brane vanishes in this limit as well, so that we remain with $\mathcal{N} = 4$ *U(N) gauge theory in 3+1 dimensions* and a free supergravity theory in the bulk;

$$\text{IIB SUGRA in } 10\text{d flat space} \times 4\text{d } U(N) \text{ gauge theory; } \mathcal{N} = 4\text{SYM} \quad (2.47)$$

The D3 branes at strong coupling $g_s N$ backreact on the geometry, the supergravity solution is given by

$$ds^2 = \left(1 + \frac{R^4}{r^4}\right)^{-\frac{1}{2}} (-dt^2 + dx_1^2 + dx_2^2 + dx_3^2) + \left(1 + \frac{R^4}{r^4}\right)^{\frac{1}{2}} (dr^2 + r^2 d\Omega_5^2), \quad (2.48)$$

where $R^4 = 4\pi g_s l_s^4 N$. The energy that an observer measures at infinity is redshifted by the time component of the metric, that is, $E_\infty = \sqrt{g_{tt}} E_{\text{local}}$.

Therefore when an excitation is brought closer to the center its energy at infinity appears lower. The distant observer sees two types of low energy excitations; massless particles propagating in the bulk and excitations that originate close to $r = 0$. These two excitations decouple because the bulk excitations will have a wavelength much longer than the size of the throat, that is created by the D-branes. From the point of view of the branes, excitations near $r = 0$ will find it increasingly hard to climb the potential created by the branes and escape. Near $r = 0$ the metric can be expanded to find

$$ds^2 = \frac{r^2}{R^2} \left(-dt^2 + d\vec{x}^2 \right) + \frac{R^2}{r^2} \left(dr^2 + r^2 d\Omega_5^2 \right). \quad (2.49)$$

With the coordinate change $r = \frac{R^2}{z}$ the above becomes

$$ds^2 = R^4 \left[\frac{-dt^2 + dz^2 + d\vec{x}^2}{z^2} \right] + R^2 d\Omega_5^2, \quad (2.50)$$

where in the first term we recognize the metric of the *Poincaré patch of AdS* depicted in 2.7b and c. Again we remain with two decoupled pieces; free bulk supergravity and near horizon dynamics.

$$\text{IIB SUGRA in 10d flat space} \times \text{IIB string theory on } \text{AdS}_5 \times S^5 \quad (2.51)$$

In both the weak and strong coupling $g_s N$ regime we found that in the low energy limit dynamics decouple in two pieces. The two different theories de-

IIB SUGRA in 10d flat space	×	U(N) gauge theory; $\mathcal{N} = 4$ SYM
↕		↕
IIB SUGRA in 10d flat space	×	IIB string theory on $\text{AdS}_5 \times S^5$

Table 2.2: The decoupling limit from two perspectives that describe the same underlying physics.

scribe the same physics. That is, IIB string theory on $\text{AdS}_5 \times S^5$ is equivalent to $\mathcal{N} = 4$ Super Yang-Mills. The parameters of both theories are related to each other. On the AdS side we have the dimensionless string coupling g_s , with $g_s = g_{YM}^2$, and the curvature scale R/l_s in string units. On the CFT side we have the N which is the rank of the gauge group and the 't Hooft coupling

$\lambda \equiv g_{YM}^2 N$ where g_{YM} denotes the Yang-Mills coupling. The relation is given by

$$R^4 = 4\pi g_s l_s^4 N = 4\pi \lambda l_s^4. \quad (2.52)$$

Expressed in the Planck length $l_P = l_s g_s^{1/4}$ this becomes

$$\boxed{\frac{R}{l_P} \sim N^{1/4}} \quad \boxed{\frac{R}{l_s} \sim \lambda^{1/4}} \quad (2.53)$$

The symmetries of both theories are identified with each other. Where

$\mathcal{N} = 4$ Super Yang Mills	IIB String theory on $AdS_5 \times S^5$
N colors	N units of F_5 flux
g_{YM}^2	g_s
$SO(2,4)$	$SO(2,4)$ of AdS_5
$SO(6)$ (R-symmetry)	$SO(6)$ (of the S^5)
$16 Q \bar{Q} + 16 S \bar{S}$	32 supercharges

Table 2.3: Corresponding symmetries on both sides of the correspondence.

$SU(4)$ is the R symmetry of the CFT. The CFT carries 16 supercharges, which is the maximum amount of fermionic generators without having a spin-2 particle, and their 16 super conformal partners which are dual to the 32 supercharges that live on the gravity side. In the bulk we see the sphere S^5 , which is the maximally symmetric solution to the Einstein equations with positive cosmological constant, which has an isometry $SO(6)$. We know that the Lie algebra of $SU(4)$ which we find on the boundary is isomorphic to the Lie algebra of $SO(6)$.

A scalar field in AdS

In this section we will consider a very specific example of an AdS/CFT computation, consisting of computing a correlator, to derive some properties of the scalar field in AdS that will prove to be useful later. The linear equations of motion on the $AdS_5 \times S^5$ background for the scalar field are given by

$$\frac{1}{\sqrt{g}} \partial_\mu (\sqrt{g} g^{\mu\nu} \partial_\nu) \phi(t, x, z) = m^2 \phi(t, x, z), \quad (2.54)$$

where the mass m depends on the radius of the 5-sphere by compactification. Using the Poincaré patch of AdS (2.50) in Euclidean signature this can be written as

$$\frac{1}{\sqrt{g}}\partial_z(\sqrt{g}g^{zz}\partial_z)\phi(t,x,z) + \frac{1}{\sqrt{g}}\partial_i(\sqrt{g}g^{ii}\partial_i)\phi(t,x,z) = m^2\phi(t,x,z). \quad (2.55)$$

Due to the symmetry properties of the metric an ansatz for the solution of the form $\phi(t,x,z) = f(z)e^{ikx}$ is used, giving

$$z^2 f''(z) - (d-1)zf'(z) - (k^2 z^2 + m^2)f(z) = 0, \quad (2.56)$$

It is useful to study the behavior of the solution near the boundary at $z = 0$ using a power law series $f(z) = z^a(1 + z + \dots)k$, giving

$$a(a-1)z^a - a(d-1)z^a - k^2 z a + 2 - m^2 z^a = 0. \quad (2.57)$$

The third term can be dropped because it goes to zero faster than the other terms due to the higher power. Solving for the leading term in z^a and dividing by z^a gives

$$a(a-1) - a(d-1) - m^2 = 0, \quad (2.58)$$

giving $a_{\pm} = \frac{d}{2} \pm \sqrt{\frac{d^2}{4} + m^2}$. We now identify the scaling dimension Δ of an operator living in the boundary conformal field theory with the positive solution containing the mass of the bulk field

$$\Delta = \frac{d}{2} \pm \sqrt{\frac{d^2}{4} + m^2}. \quad (2.59)$$

For fields with positive mass squared we take the positive solution. The solution that falls off as z^{Δ} near the boundary is called the *normalizable mode*, the solution that blows up is given by $a_- = d - \Delta$. Solutions with $\Delta < d$ are called *relevant*, the one with $\Delta = d$ is *marginal* and with $\Delta > d$ is the *non normalizable solution*.

Let us now look at Lorentzian Anti-de Sitter space. The metric in global coordinates is given by

$$ds^2 = -\cosh^2 \rho dt^2 + d\rho^2 + \sinh^2 \rho d\Omega_{d-1}^2, \quad (2.60)$$

where ρ denotes the radial direction of the cylinder ranging from zero at the center to infinity at the boundary, and the CFT lives on the $S^{d-1} \times t$. This is depicted in 2.7a.

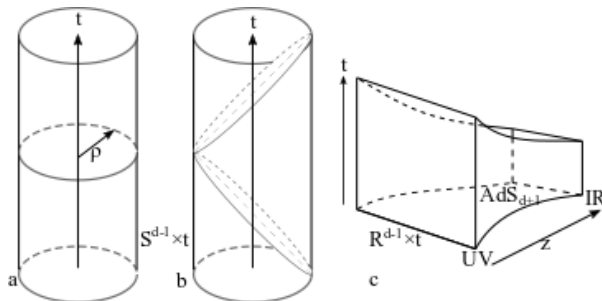


Figure 2.7: a depicts the cylinder whose interior corresponds to AdS spacetime, the boundary of the cylinder corresponds to its conformal boundary. In b and c the Poincaré patch is depicted.

The Hilbert space can be generated by all local operators of the theory using the state operator map. Primary operators with scaling dimension Δ correspond to massive fields in the bulk. Demanding regularity at the center and normalizability at the boundary (which in these coordinates is at infinity) leads to a discrete spectrum, whose modes are given by

$$\omega = \frac{\Delta + l + 2n}{R}, \quad \text{with } n = 0, 1, 2, \dots \quad (2.61)$$

with l the angular momentum on S^{d-1} . The obvious difference with flat space being the discrete spectrum, coming from AdS acting as a big box. The state operator map of the CFT dictates that the energy of an operator at the center is given by $E_{CFT} = \frac{\Delta}{R}$. Then $\square^n \partial_{[i_1} \dots \partial_{i_l]} \mathcal{O}$ gives the modes of a scalar field in the bulk. The number of uncontracted derivatives corresponds to the angular momentum l of the bulk field. The set of states is isomorphic to that of AdS. Increase in n corresponds to radially moving particles in AdS. A single particle corresponds to a single trace operator in the CFT, two particles to a double trace operator $\mathcal{O}\mathcal{O}$ with dimension $2\Delta + O(1/N^2)$.

Since AdS can be viewed as a box from which nothing can escape, once we keep on adding particles at some point a black hole will be created due to

gravitational collapse. By taking the coordinate transformation $r = \sinh \rho$ the metric becomes

$$ds^2 = -f(r)dt^2 + f(r)^{-1}dr^2 + r^2 d\Omega_{d-1}^2, \quad (2.62)$$

with $f(r) = 1 + r^2$ for empty AdS, and $f(r) = 1 + r^2 - c \frac{GM}{r^{d-2}}$ for an AdS-Schwarzschild black hole. Introducing a black hole in AdS results in a continuous spectrum, since we do not need to impose the regularity constraint at the center. Due to the presence of the black hole the frequencies are gravitationally redshifted hence the continuous spectrum. On the boundary a black hole corresponds to a state with many particles that is a singlet under gauge transformations, a thermal state of the quark gluon plasma. The entropy of the QGP corresponds to the black hole entropy. From the gauge theory side it is clear that the entropy is determined by the microstates of the QGP.

2.5 Complementarity revised using AdS/CFT

We mentioned that the late outgoing Hawking mode has to be entangled with the early radiation to ensure unitary evaporation, whilst it has to be entangled with its interior partner so that the horizon can be crossed smoothly. Using Rindler space as an explicit example we shall show why the entanglement is necessary to safely cross the horizon without encountering a firewall. We will focus on the modes behind the horizon of a black hole, and we will study it in the setting of the AdS/CFT correspondence. For reasons that shall become clear in the next sections we will call operators that describe modes behind the horizon *mirror operators*.

An interpretation of black hole complementarity is that interior degrees of freedom are contained in the radiation in a scrambled form. That is, the Hilbert space of the interior is encoded in that of the radiation. In this section we shall provide a way to mathematically incorporate the ideas of complementarity. Papadodimas and Raju double the degrees of freedom of a single sided black hole in AdS to ensure a safe passing of an infalling observer, whilst maintaining unitary evaporation [18].

To understand this we first consider Rindler space as an example before we treat black holes. When we compare the Penrose diagrams of Rindler space and that of the eternal black hole in figure 2.8 the similarities are obvious. This

black hole connects two universes, that each have a dual field theory living on their respective boundaries [19].

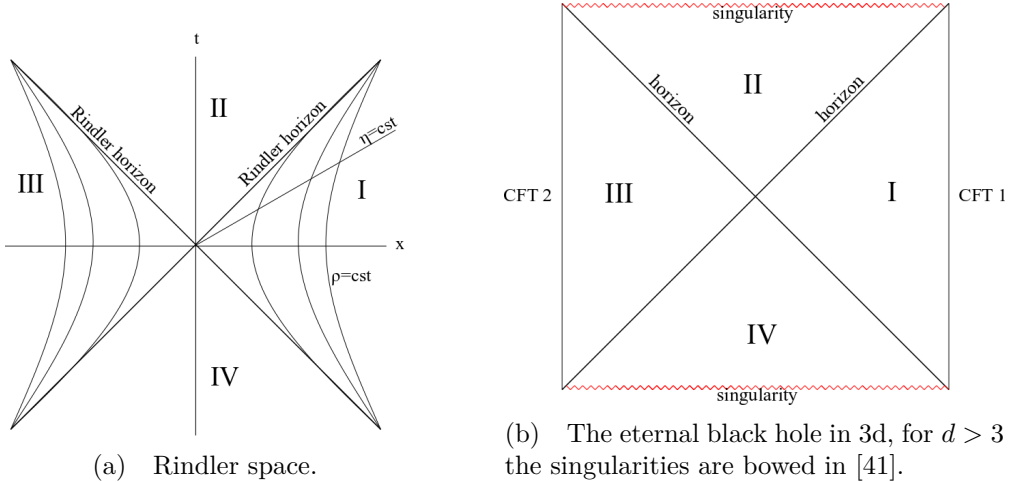


Figure 2.8: Penrose diagrams of various spacetime geometries

2.5.1 Rindler space as an example

In this section we shall demonstrate that in Rindler space we have to take the modes from the left *and* the right wedge into account when crossing the horizon. If we do not, an observer will see something similar to a firewall when crossing the Rindler horizon. We start with the quantization of a massive scalar field in Rindler space. The metric in three dimensions is given by

$$ds^2 = -\rho^2 d\eta^2 + d\rho^2 + dz^2. \quad (2.63)$$

The Klein Gordon equation for a massive scalar field is given by

$$(\square - m^2)\phi = 0, \quad \text{with} \quad \square = \frac{1}{\sqrt{-g}} \partial_\mu (\sqrt{-g} g^{\mu\nu} \partial_\nu) \quad (2.64)$$

with g the determinant of the metric. The differential equation becomes

$$\left[\frac{-1}{(\rho)^2} \partial_\eta \partial_\eta + \frac{1}{\rho} \partial_\rho + \partial_\rho \partial_\rho + \partial_z \partial_z - m^2 \right] \phi(\eta, \rho) = 0 \quad (2.65)$$

As an ansatz we use $\phi(\eta, \rho, z) = e^{-i\omega\eta + ikz} f(\rho)$. After massaging the expression a bit we obtain

$$\frac{\omega^2}{\rho^2} f(\rho) + \frac{1}{\rho} f'(\rho) + f''(\rho) - (m^2 + k^2) f(\rho) = 0. \quad (2.66)$$

The solution consists of a sum of two Bessel functions.

$$f(\rho) = C_1 J_{i\omega}(\mu\rho) + C_2 Y_{i\omega}(-i\mu\rho), \quad (2.67)$$

with $\mu = \sqrt{k^2 + m^2}$. The two solutions behave badly independently; the first one blows up at the “boundary” whereas the other diverges at the “center”, therefore we take a particular linear combination that gives a well behaved solution everywhere

$$f(\rho) = K_{i\omega}(\mu\rho). \quad (2.68)$$

Since this function is real we can expand the field as

$$\phi(\eta, \rho, z) = \int_0^\infty d\omega \int_{-\infty}^\infty dk C K_{i\omega}(\mu\rho) \left(e^{-i\omega\eta + ikz} a_\omega + e^{+i\omega\eta - ikz} a_\omega^\dagger \right). \quad (2.69)$$

The equal time commutation relations were used to fix the normalization $C = \sqrt{\frac{1}{\omega\Gamma(i\omega)\Gamma(-i\omega)}}$, where the Bessel functions were expanded in leading order around $\rho = 0$. Putting everything together we find that the field in the right wedge is given by

$$\phi^I(\eta, \rho, z) = \frac{1}{2\pi} \int_0^\infty d\omega \int_{-\infty}^\infty dk \frac{K_{i\omega}(\mu\rho)}{|\Gamma(i\omega)|} \frac{1}{\sqrt{\omega}} \left(a_\omega e^{-i\omega\eta + ikz} + a_\omega^\dagger e^{i\omega\eta - ikz} \right). \quad (2.70)$$

In the left wedge the expansion is given by

$$\phi^{III}(\eta, \rho, z) = \frac{1}{2\pi} \int_0^\infty d\omega \int_{-\infty}^\infty dk \frac{K_{i\omega}(\mu\rho)}{|\Gamma(i\omega)|} \frac{1}{\sqrt{\omega}} \left(\tilde{a}_\omega e^{+i\omega\eta + ikz} + \tilde{a}_\omega^\dagger e^{-i\omega\eta - ikz} \right). \quad (2.71)$$

In the left wedge the quantization is analogous to the right wedge. In the future wedge however we have the following expression for the line element

$$ds^2 = \rho^2 d\eta^2 - d\rho^2 + dz^2. \quad (2.72)$$

We note that ρ now behaves timelike and η spacelike. Again we choose an ansatz of the form $\phi(\eta, \rho, z) = e^{-i\omega\eta + ikz} f(\rho)$ to obtain

$$\frac{-\omega^2}{\rho^2} f(\rho) - \frac{1}{\rho} f'(\rho) - f''(\rho) - (\mu)f(\rho) = 0. \quad (2.73)$$

Which has Bessel functions as solutions as well, however these are complex; $J_{i\nu}(x)^* = J_{-i\nu}(x)$. When we write the field expansion we therefore need to consider all possible combinations, and hence we double the amount of modes in comparison to the right wedge. We denote the annihilation operators by c and d , and the creation operators by their respective hermitian conjugates

$$\phi(\eta, \rho, z) = \int_0^\infty d\omega \int_{-\infty}^\infty dk C J_{i\omega}(\mu\rho) e^{-i\omega\eta + ikz} c_\omega + J_{-i\omega}(\mu\rho) e^{-i\omega\eta + ikz} d_\omega + \text{h.c.} \quad (2.74)$$

Fixing the normalization according to

$$\begin{aligned} [\phi(\rho, z), \pi(\rho' z')] &= \int_0^\infty d\omega d\omega' \int_{-\infty}^\infty dk dk' C^2(i\omega) \\ &J_{i\omega}(\mu\rho) J_{-i\omega}(\mu'\rho') e^{i(kz - k'z')} [c_\omega, c_{\omega'}^\dagger] + J_{-i\omega}(\mu\rho) J_{i\omega}(\mu'\rho') e^{i(k'z' - kz)} [c_{\omega'}, c_\omega^\dagger] + \\ &J_{-i\omega}(\mu\rho) J_{i\omega}(\mu'\rho') e^{i(kz - k'z')} [d_\omega, d_{\omega'}^\dagger] + J_{i\omega}(\mu\rho) J_{-i\omega}(\mu'\rho') e^{-i(kz - k'z')} [d_{\omega'}, d_\omega^\dagger]. \end{aligned} \quad (2.75)$$

Cross terms vanish because when we expand the Bessel functions and do not take the cross terms into account because the integral over the expanded $J_{i\omega}(\mu\rho)$, which are Gamma functions, is zero. The usual commutation relations apply for the creation and annihilation operators so that we obtain a $\delta(\omega - \omega')\delta(k - k')$ so that the results simplifies to

$$\begin{aligned} [\phi(\rho, z), \pi(\rho' z')] &= \int_0^\infty d\omega \int_{-\infty}^\infty dk C^2(i\omega) \\ &J_{i\omega}(\mu\rho) J_{-i\omega}(\mu\rho') e^{ik(z-z')} + J_{-i\omega}(\mu\rho) J_{i\omega}(\mu\rho') e^{ik(z'-z)} + \\ &J_{-i\omega}(\mu\rho) J_{i\omega}(\mu\rho') e^{ik(z-z')} + J_{i\omega}(\mu\rho) J_{-i\omega}(\mu\rho') e^{-ik(z-z')}. \end{aligned} \quad (2.76)$$

After expanding the Bessel functions and integrating over k gives a delta function with a prefactor. Transforming to a Tortoise like coordinate and demanding that the commutator gives a delta function leads to fixing the constant to $C = \frac{\sqrt{\Gamma(1+i\omega)\Gamma(1-i\omega)}}{8\pi\omega}$. Putting everything together we obtain for the field in the future wedge

$$\begin{aligned} \phi^{II}(\eta, \rho, z) &= \int_0^\infty d\omega \int_{-\infty}^\infty dk \frac{1}{8\pi} \sqrt{\frac{\Gamma(1+i\omega)\Gamma(1-i\omega)}{\omega}} \\ &\left(b_\omega e^{-i\omega\eta + ikz} J_{i\omega}(\mu\rho) + c_\omega e^{-i\omega\eta + ikz} J_{-i\omega}(\mu\rho) + \text{h.c.} \right). \end{aligned} \quad (2.77)$$

Matching at the horizon

We want to express the operators behind the horizon in terms of operators in the left and right wedges. For a smooth transition of one wedge to the other we demand that the fields match at the horizons, which is also known as regularity of the horizon. To do this we expand the Bessel functions around $\rho = 0$ and move to lightcone coordinates. All expansions have a factor in common, $\Omega \equiv m^{i\omega} 2^{-i\omega}$, which we will take out. The coordinates in the respective wedges become

$$\begin{array}{lll}
 \text{Wedge I} & \text{Wedge III} & \text{Wedge II} \\
 u = -\rho e^{-\eta} & u = \rho e^{-\eta} & u = \rho e^{-\eta} \\
 v = \rho e^{\eta} & v = -\rho e^{\eta} & v = \rho e^{\eta}
 \end{array} \tag{2.78}$$

To match the fields we use the *Riemann Lesbesgue lemma* which states that the integral of a rapidly oscillating functions goes to zero as the number of oscillations goes to infinity.

$$\boxed{\hat{f}(z) := \int_{\mathbb{R}} f(x) e^{-izx} dx \rightarrow 0 \quad \text{as } z \rightarrow \infty} \tag{2.79}$$

Because the coordinates are the same in all quadrants, and hence so is their dual frequency we can match mode by mode. Expanding the fields near the horizon gives

$$\begin{aligned}
 \phi^I \sim \frac{1}{\sqrt{\omega \Gamma(i\omega) \Gamma(-i\omega)}} & \left(\Omega \Gamma(-i\omega) (-u)^{i\omega} a_{\omega} + \Omega^{-1} \Gamma(i\omega) (v)^{-i\omega} a_{\omega} + \right. \\
 & \left. \Omega \Gamma(-i\omega) (v)^{i\omega} a_{\omega}^{\dagger} + \Omega^{-1} \Gamma(i\omega) (-u)^{-i\omega} a_{\omega}^{\dagger} \right)
 \end{aligned} \tag{2.80}$$

and

$$\begin{aligned}
 \phi^{II} \sim \sqrt{\omega \Gamma(i\omega) \Gamma(-i\omega)} & \left(\frac{\Omega}{\Gamma(1+i\omega)} (u)^{i\omega} b_{\omega} + \frac{\Omega^{-1}}{\Gamma(1-i\omega)} (u)^{-i\omega} b_{\omega}^{\dagger} + \right. \\
 & \left. \frac{\Omega^{-1}}{\Gamma(1-i\omega)} (v)^{-i\omega} c_{\omega} + \frac{\Omega}{\Gamma(1+i\omega)} (v)^{i\omega} c_{\omega}^{\dagger} \right),
 \end{aligned} \tag{2.81}$$

where we defined the common factor $\Omega \equiv m^{i\omega} 2^{-i\omega}$. When we approach the horizon going from I to II along constant v and $u \rightarrow 0^-$ we can use (2.79) to show that we can discard the u coordinate since

$$(-u)^{i\omega} = \exp[\ln((-u)^{i\omega})] = \exp[i\omega \ln(-u)],$$

when u approaches zero from below the exponent goes to $-\infty$ and the Riemann Lebesgue lemma tells us the contribution goes to zero. Similarly we approach $u \rightarrow 0^+$ from II to I and also here the u dependence vanishes so that we find $c_\omega = -ia_\omega$, and the hermitian conjugate. When we go from wedge III to II we can keep the expansion we found (2.81). We now approach the horizon along constant u and $v \rightarrow 0^+$ from III to II and $v \rightarrow 0^-$, using the same procedure as above we find $b_\omega = i\tilde{a}_\omega^\dagger$. When we substitute these results in the expansion (2.77) we find the expression for the field in the future wedge

$$\begin{aligned} \phi^{II}(\eta, \rho, z) = & \int_0^\infty d\omega \int_{-\infty}^\infty dk \frac{1}{8\pi} \sqrt{\frac{\Gamma(1+i\omega)\Gamma(1-i\omega)}{\omega}} \\ & \left(-i\tilde{a}_\omega e^{+i\omega\eta - ikz} J_{-i\omega}(\mu\rho) - ia_\omega e^{-i\omega\eta + ikz} J_{-i\omega}(\mu\rho) + \text{h.c.} \right). \end{aligned} \quad (2.82)$$

Two point functions across the Rindler horizon

To compute the two point correlation function across the horizon we use the expression of the fields in the right and future wedge. We shall show that when we only use the non-tilde modes behind the horizon the two point function diverges, whereas when we take the mirror modes into account the function is well behaved.

The two point function that includes modes from the left wedge is written below. For clarity we write down the expectation values on the Minkowski vacuum explicitly. We are interested in the small wavelength limit; therefore we already take this limit for the Bessel functions

$$\begin{aligned} {}_M \langle 0 | \phi^{II}(\eta', \rho', z') \phi^I(0, \rho, z) | 0 \rangle_M = & \\ i \int_{\omega > 0} d\omega d\omega' dk dk' \Big(& J_0(\mu\rho') K_0(\mu\rho) e^{-i\omega\eta + ik(z'-z)} \frac{1}{e^{\pi\omega} - e^{-\pi\omega}} \\ & - J_0(\mu\rho') K_0(\mu\rho) e^{+i\omega\eta - ik(z'-z)} \frac{1}{e^{\pi\omega} - e^{-\pi\omega}} \\ & - J_0(\mu\rho') K_0(\mu\rho) e^{-i\omega\eta + ik(z'-z)} \frac{1}{1 - e^{-2\pi\omega}} \\ & + J_0(\mu\rho') K_0(\mu\rho) e^{+i\omega\eta - ik(z'-z)} \frac{1}{e^{2\pi\omega} - 1} \Big). \end{aligned} \quad (2.83)$$

It is easy to observe, after clubbing together the terms and expanding for small omega, the integrand is well behaved and yields a finite result. When we do not

take into account the modes from wedge III we obtain the following expression

$$\begin{aligned}
{}_M \langle 0 | \phi^{II}(\eta', \rho', z) \phi^I(0, \rho, z) | 0 \rangle_M = \\
\int_{\omega > 0} d\omega d\omega' dk dk' \left(-J_0(\mu\rho') K_0(\mu\rho) e^{-i\omega\eta + ik(z'-z)} \frac{1}{1 - e^{-2\pi\omega}} \right. \\
\left. + J_0(\mu\rho') K_0(\mu\rho) e^{+i\omega\eta - ik(z'-z)} \frac{1}{e^{2\pi\omega} - 1} \right). \tag{2.84}
\end{aligned}$$

This will blow up logarithmically for small frequencies. When we compute a correlator of two points that both lay behind the horizon, using only modes from the left or the right wedge the divergence will be stronger. The integrand then goes as $\frac{1}{\omega^2}$ [18].

We see that the entanglement of the modes between the left and right wedge exactly conspire to cancel the divergences. Therefore to smoothly cross the Rindler horizon the entanglement between the left and right wedge is crucial.

2.5.2 Rindler space and the eternal black hole

This section covers the background material from [18] and motivation for chapters 3 and 4. The need for mirror operators to ensure a safe passage for the infalling observer was motivated above. First we shall briefly describe how to relate boundary operators to local bulk fields living in empty AdS. In this setup the dual field theory is in the ground state. Then we review what happens when we study a black hole in AdS, which corresponds to a thermal state on the boundary. A special case is considered, namely the eternal black hole. In the last section we discuss a theorem that shares interesting features with the idea of complementarity.

Bulk reconstruction for empty AdS

In this section we shall motivate, following [18, 42], that local bulk fields in AdS can be written in CFT operators in flat space. An assumption we use in this set up is that thermal correlators of generalized free fields factorize in a $1/N$ expansion

$$\begin{aligned}
\langle 0 | \mathcal{O}(x_1) \mathcal{O}(x_2) \dots \mathcal{O}(x_{2n}) | 0 \rangle = \\
\frac{1}{2^n} \sum_{\pi} \langle 0 | \mathcal{O}(x_{\pi_1}) \mathcal{O}(x_{\pi_2}) | 0 \rangle \dots \langle 0 | \mathcal{O}(x_{\pi_{2n-1}}) \mathcal{O}(x_{\pi_{2n}}) | 0 \rangle + \frac{1}{N} \dots \tag{2.85}
\end{aligned}$$

That is, we can write a $2n$ -point correlation function in terms of a product of two-point functions, where we sum over all permutations. For the expansion to work it is important, amongst other things, that the number of operators does not scale with N , since then the 't Hooft counting might not work. The Fourier modes of $\mathcal{O}(x)$ are defined as

$$\mathcal{O}(\omega, \vec{k}) = \int dt d^{d-1} \vec{x} \mathcal{O}(t, \vec{x}) e^{i\omega t - i\vec{k}\vec{x}} \quad (2.86)$$

In signature $(-, +, + \dots)$. From the analysis of the Wightman two-point function

$$\langle \mathcal{O}(\tau, \vec{x}) \mathcal{O}(0, \vec{0}) \rangle = \left(\frac{1}{\tau^2 + \vec{x}^2} \right)^\Delta, \quad (2.87)$$

with Δ the conformal dimension it was found that at leading order in $1/N$ the operators $\hat{\mathcal{O}}(\omega, \vec{k})$ satisfy

$$\left[\hat{\mathcal{O}}(\omega, \vec{k}), \hat{\mathcal{O}}^\dagger(\omega', \vec{k}') \right] = \delta(\omega + \omega') \delta^{d-1}(\vec{k} + \vec{k}'). \quad (2.88)$$

Which is the algebra of free oscillators. Where we have to keep in mind that for this to work the number of insertions should not scale with N . The AdS Poincare patch is described by the metric

$$ds^2 = \frac{-dt^2 + d\vec{x}^2 + dz^2}{z^2}, \quad (2.89)$$

on which we can solve the Klein-Gordon equation. The solution can be expanded in different bases. For the purpose of writing bulk fields in terms of boundary operators it is convenient to take the normalizable mode, on which we shall elaborate further in section 2.4.2. The CFT operator can then be written in terms of the Fourier modes \mathcal{O} and the normalized mode expansion ξ that obey the Klein Gordon equation in the bulk as

$$\phi(t, \vec{x}, z)_{CFT} = \int_{\omega > 0} \frac{d\omega d^{d-1} \vec{k}}{(2\pi)^d} \left[\mathcal{O}_{\omega, \vec{k}} \xi_{\omega, \vec{k}}(t, \vec{x}, z) + \mathcal{O}_{\omega, \vec{k}}^\dagger \xi_{\omega, \vec{k}}^*(t, \vec{x}, z) \right]. \quad (2.90)$$

The ladder operators are replaced by their dual operators. The above is a non-local operator, evident from the dependence on the radial depth z , which can be thought of as a smearing parameter. The expansion above is the same as that of a free massive field in AdS, therefore in the large N limit it has to behave as one as well.

Doubling of modes

The analogy between Rindler space and the eternal black hole is immediately clear when we look at the Penrose diagram of both spacetimes 2.8. The eternal black hole has two exterior “universes” that are both described by their respective CFTs, that are in a specific entangled state [19]. For a sufficiently large black hole at late time, the geometry can be approximated by that of the eternal black hole, since the dynamics of the collapse become irrelevant [18].

When we put a black hole in AdS, the CFT is in a thermal state whose temperature is given by the Hawking temperature of the black hole. The $2n$ -point function can still be factorized in the large N limit in a product of two point functions. An eternal black hole has two exterior universes, with on the boundary of each universe a CFT. For the eternal black hole these CFTs are in a special entangled state; the thermofield doubled state, the setup is depicted in 2.8b. The scalar field can be quantized in the AdS black hole background that in the Poincaré patch that given by the metric

$$ds^2 = \frac{-f(z)dt^2 + d\vec{x}^2 + f(z)^{-1}dz^2}{z^2}, \quad (2.91)$$

with $f(z) = (1 - z^d/z_0^d)$ and z_0 the location of the horizon. The Klein Gordon equation can easily be solved using the symmetries of t and \vec{x} , with mode expansion

$$f_{\omega, \vec{k}}(t, \vec{x}, z) = e^{-i\omega t + i\vec{k}\vec{x}} g_{\omega, \vec{k}}(z), \quad (2.92)$$

which can be found in regions I and III (the right and left exterior respectively in the figure). There are two sensible normalization schemes, either fixing the constant using the commutator or by taking an expansion near the boundary. For our purpose it is useful to have well behaved fields at the boundary since we want to connect operators on the CFT. Again we relate $f_{\omega, \vec{k}}(t, \vec{x}, z)$ with an operator $\mathcal{O}_{\omega, \vec{k}}$ so that we obtain an operator in the CFT which is non-local but that obeys the Klein Gordon equation in the bulk. The fields can be expanded in modes in their respective wedges. Because all regions of the Kruskal diagram are covered by the boundary operators \mathcal{O} and $\tilde{\mathcal{O}}$ at large N the n point function at the boundary can be written as

$$\frac{1}{Z(\beta)} \text{Tr} \left[e^{-\beta H} \phi_{CFT}(t_1, \vec{x}_1, z_1) \dots \phi_{CFT}(t_n, \vec{x}_n, z_n) \right] = \langle \phi(t_1, \vec{x}_1, z_1) \dots \phi(t_n, \vec{x}_n, z_n) \rangle_{HH}. \quad (2.93)$$

where the subscript HH denotes the Hartle-Hawking vacuum. The two point function across the horizon in terms of boundary operators can now be written down. For this we use the same relations of the correlator expectation value as we derived in the previous section, where we replace the ladder operators a_ω by $\mathcal{O}_{\omega, \vec{k}}$. The same conditions that we had for the ladder operators apply, and in addition the mirror operators approximately commute with the normal operators, namely

$$\left[\mathcal{O}_{\omega, \vec{k}}, \tilde{\mathcal{O}}_{\omega, \vec{k}} \right] = \left[\mathcal{O}_{\omega, \vec{k}}^\dagger, \tilde{\mathcal{O}}_{\omega, \vec{k}} \right] = \left[\mathcal{O}_{\omega, \vec{k}}^\dagger, \tilde{\mathcal{O}}_{\omega, \vec{k}}^\dagger \right] \approx 0 \quad (2.94)$$

The number of mirror operators is equal to the number of normal operators. The computed integral has the same properties as the one we found in Rindler space, it seems to diverge, however when one takes the \mathcal{O} and $\tilde{\mathcal{O}}$ into account this divergence will cancel. That is, we take

$$\begin{aligned} \phi_{CFT}^{II}(t, \vec{x}, z) = \int_{\omega > 0} \frac{d\omega d^{d-1}\vec{k}}{(2\pi)^d} & \left(\mathcal{O}_{\omega, \vec{k}}(t, \vec{x}, z) f_{\omega, \vec{k}}^{I'}(t, \vec{x}, z) + \right. \\ & \left. \tilde{\mathcal{O}}_{\omega, \vec{k}}(t, \vec{x}, z) f_{\omega, \vec{k}}^{II'}(t, \vec{x}, z) + h.c. \right), \end{aligned} \quad (2.95)$$

and when we take all terms into account we do not find any divergence. Now, crossing a Rindler horizon is not the same as crossing a black hole horizon, since the Rindler horizon has an infinite entropy and it does not evaporate. Therefore we can pass through Rindler horizons all the time without burning up [16].

From the CFT point of view we can understand the above as follows. Operators living in the CFT that is dual to a typical one sided black hole can be divided into simple and complex operators by dividing the Hilbert space into coarse grained and fine grained observables. For a typical state they are entangled. A heuristic argument for this entanglement is that when we take two systems with each N degrees of freedom in a non entangled state we need $2N$ numbers to fix the states. For an entangled state we need N^2 numbers. For a large enough system $N \gg 1$ there are many more entangled states, hence when we pick a state there is a large possibility it is entangled.

When the state is entangled we can go to the Schmidt basis in which the entanglement is diagonal. For every operator acting on the first part we can simply write down a “mirror operator” acting on the other state. However this is only straightforward in the Schmidt decomposition. When we transform to

the normal basis the mirror operators become complicated. Furthermore the transformation that takes us from the Schmidt basis to a general basis depends on the state. Hence the mirror operators become state dependent [20, 43].

To summarize, the mirror operators have the following properties

- For every simple operator \mathcal{O} there is a mirror operator $\tilde{\mathcal{O}}$.
- The algebra of the mirror operators is isomorphic to the algebra of the simple operators \mathcal{O} .
- The mirror operators commute with the simple operators.
- The mirror operators are entangled with the simple operators in such a way that correlators reproduce (at large N) those of the thermofield doubled state.

Connection with the Tomita-Takesaki theorem

There is a prescription that one can follow to obtain mirror operators which follows from the Tomita-Takesaki theorem, which is used in studying operator algebras [44]. The theorem deals with Von Neumann algebras, but when we talk about black holes and a subset of operators, this is not a proper algebra. It *is* however an excellent physical, and probably mathematically the most rigorous, example of black hole complementarity.

The procedure starts by defining a small algebra $\mathcal{A}_{\text{small}}$, where we put an upper bound on the number of operators that are allowed in multiplication, which makes it a “truncated” algebra instead of a proper algebra. When we consider a large N gauge theory we can restrict ourselves to the set of single trace operators, and let the number of operators in a product not scale with N . If the operators in the algebra satisfy certain conditions we can apply the Tomita-Takesaki theorem to find the commutant of the small algebra. The commutant corresponds to the mirror operator we discussed before. When applying the theorem one also constructs something called the modular Hamiltonian, it makes sure that operators stay within the small algebra [20]. For the ground state of Rindler space the modular Hamiltonian is the boost generator [45].

Generally this operator is quite complicated and non local, however for the ground state of symmetric spaces it simplifies tremendously. In its exact form

the theorem would invalidate the idea of complementarity. When the constructed mirror operator commutes exactly with all other operators the Hilbert spaces would be independent and the strong subadditivity theorem would hold, and hence there could be something like a firewall present at the horizon. When we talk about an approximate algebra and an approximate commutant then the Hilbert spaces are not exactly independent and thus the arguments that support the firewall argument are not valid [20].

Conclusions

The constructed mirror operators that describe the interior of the black hole are not independent from the operators describing the exterior. While at the semi classical level the Hilbert spaces of the interior and exterior are independent, fundamentally they are not, which means that the theorem of strong subadditivity cannot be applied. The argument of Mathur that we quoted above does not hold for this case and hence it is possible that small corrections purify the state [18].

A question is what physical interpretation we can give to the mirror operators. The mirror operators describe the fine grained degrees of freedom whilst the ‘normal’ operators describe the coarse grained degrees of freedom. In chapter 3 we will show that mirror operators arise naturally in a single CFT in the ground state, that is dual to empty AdS. The difference with the mirror operators described above being the state dependence. The state dependence was objected in [46]. Some aspects remain open for further research.

3

A toy model for black holes

This chapter is based on our published paper [47].

3.1 Introduction

Recent discussions of the information paradox [15–17, 48] have revived interest in the idea of black hole complementarity [10, 11]. In a colloquial sense, this is the idea that degrees of freedom inside the black hole are “scrambled” combinations of degrees of freedom outside. A precise version of this idea was developed in [20, 43, 49, 50]. In this construction, a local operator inside the black hole can be represented as a sufficiently complicated combination of $\mathcal{O}(S_{BH})$ operators outside the black hole, where S_{BH} is the black hole entropy. This is indicated by

$$\phi(x_{in}) \cong P(\phi(x_2), \phi(x_3), \dots), \quad (3.1)$$

where $\phi(x_{in})$ is a local field located inside the black hole and P is a suitably complicated polynomial comprised entirely of fields localized at points $x_{out} \equiv \{x_2, x_3, \dots\}$ outside the black hole that are spacelike to x_{in} . (See figure 3.1.)

It is apparent that such a relation implies a radical loss of causality and locality in correlators with $\mathcal{O}(S_{BH})$ insertions. However, the analysis of [20, 43, 49, 50] left two questions unanswered. First, what is the precise form of P that we must pick in order to observe this loss of locality, and in what sense is the field inside equal to the polynomial? Second, while positing such a loss of locality resolves various aspects of the information paradox, what is the independent evidence that this is indeed a physical feature of quantum gravity?

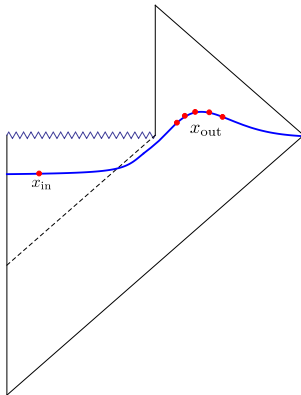


Figure 3.1: *Degrees of freedom at x_{in} are identified with complicated combinations of those at x_{out} .*

The objective of this chapter is to investigate these questions in a simpler setting. We describe, in the context of the AdS/CFT correspondence [6–8], how such a loss of locality is not only physical but can even be seen in empty AdS in the absence of black holes. In particular, given a local field operator $\phi(x_1)$, we will explicitly find “complicated” polynomials, \mathcal{P} made up of field operators with support on points that are all spacelike with respect to x_1 , but with the property that $\phi(x_1) \doteq \mathcal{P}$. In this equation the symbol \doteq means that we can approximate $\phi(x_1)$ as accurately as we wish, but true equality can only be obtained by taking the limit of an infinite sequence of polynomials. This makes (3.1) precise and thus demonstrates non-locality in a calculable setting.

Our setup of this chapter is as follows. We consider a large N CFT with a bulk AdS dual. In this CFT, we consider the set of boundary operators defined in a short time band. Now, if this time band is shorter than the light-crossing time of AdS, it naturally divides the bulk spacetime into two regions: a causal diamond near the center of AdS that is causally disconnected from the time band, and its complement. (See figure 3.2.)

We argue that the CFT dual of this division is that operators in the CFT can be naturally divided into two classes: simple operators —which consist of single trace operators and polynomials of an $\mathcal{O}(1)$ number of single trace operators— and complex operators, where the number of single-trace components starts scaling as a function of N . While the region of AdS near the boundary is reconstructed by simple operators, we argue that the region near the center of AdS

is reconstructed by complicated ones. The two sets approximately commute in the large N limit and on a given class of states. However, their commutator is not zero as an operator equation, and in fact, complicated operators can in principle be reconstructed by many simple operators.

To demonstrate this feature, we identify the specific complicated operators that probe the diamond at the center of AdS. It turns out that the key ingredient we need for these operators are the polynomials

$$\mathcal{P}_{\alpha,p_c} = \sum_{p=0}^{p_c} (-1)^p \frac{(\alpha H)^p}{p!}, \quad (3.2)$$

specified by two adjustable cutoffs, α, p_c that we can choose freely, provided we take them to be large enough. For example, as we describe below, one sufficiently large choice is $\alpha = \ln(N)$ and $p_c = N \ln(N)$. Here H is the CFT Hamiltonian, shifted appropriately so that the ground state has energy 0. Note that

$$\lim_{\alpha \rightarrow \infty} \lim_{p_c \rightarrow \infty} \mathcal{P}_{\alpha,p_c} = P_0, \quad (3.3)$$

where $P_0 = |0\rangle\langle 0|$ is the projector onto the CFT vacuum. We show that combining these complicated polynomials with other simple polynomials of single-trace operators allows us to probe regions which, in the bulk, are causally disconnected from the time band.

These observations demonstrate several important physical points: in order to understand locality in AdS/CFT, we have to distinguish between simple and complicated experiments. Since effective field theory only requires locality to hold for simple experiments, we can indeed have significant violations of locality once we consider complicated operators in the theory.

A second important point is the relation between radial depth, complexity and time-dependence. The fact that we have locality in the emergent radial direction in AdS/CFT is related to the fact that at any given moment in time, the information of the quantum state of the CFT is partly contained in simple and partly in complicated operators. It is hard for a boundary observer to extract the information in the complicated operators, which is geometrically related to the fact that she does not have direct access to points deep in AdS. Under time evolution the dynamics of the CFT shuffles the information between simple and complex operators. For states near the vacuum of AdS, the shuffling time is of the order of the AdS light crossing time.

Hence complicated operators inside a short time band can become simple operators at later points outside the band. On the other hand, if the state corresponds to a black hole in the bulk, then the information gets trapped in complicated operators for a very long time, until it manages to escape via Hawking evaporation.

It is remarkable that the study of CFT operators in the short-time band can also capture some of the essential physics of black hole complementarity. We believe that this model deserves further attention.

Before we close this section, we would like to mention that the same setup of a spherical hole in AdS was first considered in [51]. (See [52, 53] for related work.) There it was proposed that the decomposition of the bulk into \mathcal{D} and $\overline{\mathcal{D}}$ could be understood in the CFT by covering the time band \mathcal{B} with a set of overlapping causal diamonds, whose size was determined by that of \mathcal{B} , and considering the information that could be recovered by localized measurements in these diamonds. The proposal in this work differs in that it concentrates on the decomposition of the boundary algebra into simple and complicated operators.

Second, this work has overlap with questions discussed in [54–58]. The “code subspace” introduced in [57] is similar to the subspace created by acting with the small algebra on the ground state of the CFT. As noted there, this construction was, in turn, related to a similar subspace—termed \mathcal{H}_Ψ , and obtained by acting with the small algebra on an equilibrium black hole state — that played a role in the reconstruction of the black hole interior [18, 20, 43, 49, 50]. However, we do not consider the question of the spatial localization of the information in the CFT and the possible connection to quantum error correction that was a central part of the discussion in [57].

There is also significant discussion in the literature on reconstructing the bulk from a subregion on the boundary that does have a causal complement. It was proposed in [59] that this region is dual to bulk region called the “entanglement wedge”, and we refer the reader to [45, 60, 61] for some recent work on this proposal. The Reeh-Schlieder theorem has also been previously considered in the context of AdS/CFT in the paper [62] that considered the algebra of operators on the boundary of bulk wedges.

Our emphasis in this chapter is somewhat different from the papers above because we are considering an entire band on the boundary. The “entanglement wedge” dual to this contains an entire Cauchy slice for the bulk. The reason

we nevertheless are able to define a consistent subalgebra on the boundary is because of our division of boundary operators into simple and complicated operators.

This chapter is organized as follows. In section 3.2 we describe our setup in more detail. In section 3.3 we describe the division of this algebra into simple and complicated operators in a more precise manner. We also prove a version of the Reeh-Schlieder theorem for operators confined to a finite band in time. In section 3.4, we describe how operators near the center of AdS that are causally disconnected from the time band, can nevertheless be constructed in terms of operators in the time band using suitably complicated operators. Some additional implications are discussed in section 3.5.

3.2 The setup

We consider a large N CFT with a holographic dual, defined on $S^{d-1} \times [\text{time}]$. We take the CFT in the ground state $|0\rangle$. The dual spacetime is AdS_{d+1} in global coordinates

$$ds^2 = -\left(1 + r^2\right) dt^2 + \frac{dr^2}{1 + r^2} + r^2 d\Omega_{d-1}^2 \quad (3.4)$$

We are working in units where both the radius of S^{d-1} and of AdS_{d+1} are set to 1.

We consider a time band \mathcal{B} in the CFT that is defined to be the set of points $S^{d-1} \times [0, T]$. We are interested in the case where this band is short, and in particular shorter than the light crossing time in AdS: $T < \pi$.

The bulk points that are causally disconnected from boundary points in \mathcal{B} constitute a causal diamond \mathcal{D} in the center of AdS as depicted in figure 3.2. The base of the diamond extends in the r coordinate up to

$$r_d = \tan \left[\frac{\pi - T}{2} \right] \quad (3.5)$$

As we make the length T of the band longer, the diamond gets smaller in size and for $T \geq \pi$ the diamond disappears altogether. The causal complement of the diamond defines an annular domain in the bulk that is denoted as $\bar{\mathcal{D}}$ in figure 3.2.

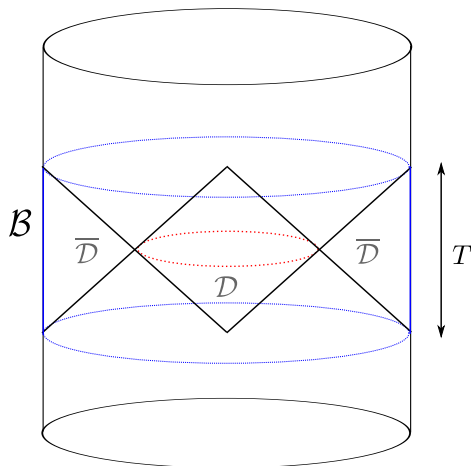


Figure 3.2: The time band \mathcal{B} of length $T < \pi$ on the boundary of AdS spacetime, the diamond shaped region \mathcal{D} in the bulk and its causal complement, the annular region $\overline{\mathcal{D}}$.

If we were dealing with a non-gravitational QFT on a fixed AdS background then the two domains $\mathcal{D}, \overline{\mathcal{D}}$ would correspond to a decomposition of the bulk Hilbert space in two factors. Here, we are neglecting UV divergences, and so the situation would be similar to the decomposition of the Minkowski Hilbert space into two Rindler wedges. More precisely the operator algebras $\mathcal{A}(\mathcal{D})$ and $\mathcal{A}(\overline{\mathcal{D}})$ would be well defined and independent. In a theory with gravity we do not expect to have sharply defined local observables, so these algebras will make sense only in an approximate sense, in the large N limit. Our goal in this chapter is precisely to explore this loss of locality.

In some sense the set-up resembles a black hole. For the observer confined to the time band, there is a spherical horizon located at $r = r_d$. Approximately local degrees of freedom at smaller values of r are not easily accessible to this observer. However, as we show below, just as in the case of black hole complementarity, this observer can access the interior of \mathcal{D} , using sufficiently complicated operators.

While we will elaborate on this answer shortly, we first point out how local operators in $\mathcal{A}(\overline{\mathcal{D}})$ can be related to simple operators inside the time band \mathcal{B} on the boundary.

Consider a free scalar field ϕ in $\overline{\mathcal{D}}$, satisfying $(\square - m^2)\phi = 0$. We impose normalizable boundary conditions for this field in the time band, and additionally impose the boundary condition that a suitably rescaled field tends to the boundary operator within the time band. This corresponds to

$$\lim_{r \rightarrow \infty} r^\Delta \phi(t, r, \Omega) = \mathcal{O}(t, \Omega), \quad (3.6)$$

and fixes the form of ϕ within $\overline{\mathcal{D}}$.

More precisely, we can write the bulk field within $\overline{\mathcal{D}}$ as

$$\phi(t, r, \Omega) = \sum_{k, \ell} \mathcal{O}_{k, \ell}^T e^{-i2\pi k t/T} \zeta_{k, \ell}(r) Y_\ell(\Omega) + \text{h.c.}, \quad (3.7)$$

where $Y_\ell(\Omega)$ are spherical harmonics, and

$$\mathcal{O}_{k, \ell}^T = \frac{1}{T} \int_0^T dt \int d^{d-1}\Omega \mathcal{O}(\tau, \Omega) e^{i2\pi k t/T} Y_\ell^*(\Omega). \quad (3.8)$$

These modes $\mathcal{O}_{k, \ell}^T$ should not be confused with the global AdS modes $\mathcal{O}_{n, \ell}$ that appear later and are defined in (3.34). Another technicality, which is irrelevant here, is that since we have defined these modes by convoluting the boundary operators with a function that drops sharply to 0 at the end-points 0 and T , the action of $\mathcal{O}_{k, \ell}^T$ creates states that have high energy tails and are non-normalizable.

The radial modes $\zeta_{k, \ell}$ appropriate for this setting are calculated by imposing (3.6) and are found to be

$$\zeta_{k, \ell}(r) = \left(\frac{r^2}{1+r^2} \right)^{\frac{\omega_k}{2}} r^{-\Delta} {}_2F_1 \left(\frac{1}{2}(2-d-\ell-\omega_k+\Delta), \frac{1}{2}(\ell-\omega_k+\Delta); 1-\frac{d}{2}+\Delta; -\frac{1}{r^2} \right), \quad (3.9)$$

where $\omega_k \equiv \frac{2\pi k}{T}$. Note that at large ℓ the hypergeometric function in the expression for the bulk mode grows exponentially, so that

$$\zeta_{k, \ell}(r) \xrightarrow{\ell \rightarrow \infty} c \ell^{\frac{d-1}{2}-\Delta} \exp \left[\ell \operatorname{arccosh} \left(\frac{r^2+2}{2r^2} \right) \right], \quad (3.10)$$

where c is an ℓ -independent constant.

While (3.7) gives an explicit formula for the bulk to boundary map in momentum space, it is not possible to Fourier transform this expression back to

position space as a result of the exponential growth in the mode function at large ℓ . This means we cannot write the bulk field in terms of a convolution of the boundary operator with an ordinary function in position space on the boundary.

$$\nexists K_T, \text{ such that } \phi(t, r, \Omega) = \int_0^T dt' \int d^{d-1} \Omega' \mathcal{O}(t', \Omega') K_T(t', \Omega'; t, r, \Omega).$$

This can also be related to the existence of bulk null geodesics that do not intersect the time band \mathcal{B} [63]. The same technical complication arises in the reconstruction of the AdS-Rindler wedge and of the exterior of an AdS black hole. As was first explained in [18] and then elaborated in [62], we must understand K_T as a distribution that is integrated only against correlators in the CFT. Leaving aside this subtlety, the bottom line is that we expect local operators in $\overline{\mathcal{D}}$ to be related to simple CFT operators in the time band.

Note that no such direct construction is possible for operators inside the diamond \mathcal{D} within effective field theory. Except for Gauss law tails, which appear because the energy and other conserved charges can all be measured at infinity, local operators inside \mathcal{D} commute with simple single-trace operators within the time band on the boundary.

One may wonder why it would not be possible to simply apply (3.7) for points inside \mathcal{D} . While the hypergeometric function in (3.7) is well defined everywhere except for $r = 0$, the field that we would obtain by means of this formal extension would not obey (3.6) for $t > T$. So, it would differ from the correct bulk field operator inside \mathcal{D} . The extension of the field from $\overline{\mathcal{D}}$ to \mathcal{D} is not uniquely determined by boundary conditions on \mathcal{B} , since we can have solutions with support in \mathcal{D} that are zero everywhere on \mathcal{B} ; so if we restrict ourselves to single-trace operators, we need information from the boundary region $[T, \pi]$ to construct the field in \mathcal{D} .

In section 3.4, we will write down an explicit formula for operators inside \mathcal{D} , but this requires us to go beyond the single-trace sector considered above.

3.3 Operator algebras in time bands

In this section, we will analyze the algebra of operators $\mathcal{A}(\mathcal{B})$ more closely. We show that when this algebra is appropriately defined, then we can prove a

version of the Reeh-Schlieder theorem. In this context, the theorem states that all effective field theory excitations in AdS, including those in \mathcal{D} and those in $\overline{\mathcal{D}}$ can be obtained by acting with operators within \mathcal{B} .

In formula (3.7) we have already related individual field operators to smeared single-trace operators. Now, in ordinary QFT, we can multiply field operators to obtain other field operators. This gives rise to an algebra of local operators. We can do the same by multiplying single-trace operators on the boundary smeared with functions that have support only inside the time band.

Before we proceed, we pause to emphasize an important point. In a general QFT, there is no sense in which we can associate an algebra of operators with a time band. The set of all operators at a given time constitutes all operators in the theory. This is evident in any Hamiltonian formulation of the theory, and is formalized by the *time-slice axiom* [44].

The reason that we can define an algebra corresponding to a time band for CFTs with a holographic dual is because they have a special class of operators called generalized free fields [64–66]. These are local operators with a small operator dimension with the property that their correlators factorize. We will denote such a field by $\mathcal{O}(t, \Omega)$. We would like to consider all kinds of fields, including tensor fields, but for simplicity we omit the tensor indices. We also assume that $\mathcal{O}(t, \Omega)$ is Hermitian. The condition of factorization means that

$$\begin{aligned} \langle 0 | \mathcal{O}(t_1, \Omega_1) \dots \mathcal{O}(t_{2n}, \Omega_{2n}) | 0 \rangle &= \frac{1}{2^n} \sum_{\pi} \langle 0 | \mathcal{O}(t_{\pi_1}, \Omega_{\pi_1}) \mathcal{O}(t_{\pi_2}, \Omega_{\pi_2}) | 0 \rangle \dots \\ &\times \langle 0 | \mathcal{O}(t_{\pi_{2n-1}}, \Omega_{\pi_{2n-1}}) \mathcal{O}(t_{\pi_{2n}}, \Omega_{\pi_{2n}}) | 0 \rangle + \mathcal{O}\left(\frac{1}{N}\right), \end{aligned} \quad (3.11)$$

where the sum is over all permutations of $(1 \dots 2n)$. These operators are called generalized free fields because while they share the property of factorization with perturbative free fields, they do not obey a perturbative equation of motion.

In a large N gauge theory, generalized free fields are low dimension single trace conformal primary operators. For example, in $N=4$ Super Yang Mills theory, the operators $\text{tr}(F^2)$ and the stress tensor, $T^{\mu\nu}$ are both generalized free fields.

We now define *simple operators* to be those that can be written as low-order polynomials in generalized free fields. *Complicated operators* are those that can

only be expressed as polynomials of a very high order — this includes large multi-trace operators of dimension $\mathcal{O}(N)$ and also operators that change the Hamiltonian by a small amount, or not at all, such as P_0 .

It is convenient to define the modes of generalized free fields on the sphere through

$$\mathcal{O}_\ell(t) = \int_{S^{d-1}} d^{d-1}\Omega \mathcal{O}(t, \Omega) Y_\ell^*(\Omega), \quad (3.12)$$

where $Y_\ell(\Omega)$ are the spherical harmonics on S^{d-1} .

We now consider the set of all polynomials in these modes

$$\mathcal{A}_{\text{small}}(\mathcal{B}) = \text{span of} \{ \mathcal{O}_{\ell_1}(t_1), \mathcal{O}_{\ell_2}(t_2) \mathcal{O}_{\ell_3}(t_3), \dots, \mathcal{O}_{\ell_4}(t_4) \mathcal{O}_{\ell_5}(t_5) \cdots \mathcal{O}_{\ell_{\mathcal{D}_m}}(t_{\mathcal{D}_m}) \}. \quad (3.13)$$

We write an element of this “small algebra” as $A_a \in \mathcal{A}_{\text{small}}$, where the time argument of the operators on the RHS must be localized in \mathcal{B} .

Several comments are in order. First, we introduce a cut-off in the number of operators in the product by demanding that the degree of each polynomial should not be larger than \mathcal{D}_m . We must ensure that

$$\mathcal{D}_m \mathcal{L} N. \quad (3.14)$$

Hence the set $\mathcal{A}_{\text{small}}(\mathcal{B})$ is an algebra in a restricted sense, since arbitrary multiplications can take us outside the set. We also limit the highest allowed angular momentum mode that can enter the algebra, $\ell \leq \ell_{\text{max}} \mathcal{L} N$.

These cutoffs are important for realizing the idea of complementarity: while for simple operators, which are dual to effective field theory experiments in the bulk, the cutoff in the definition of $\mathcal{A}_{\text{small}}(\mathcal{B})$ is not important, at a fundamental level the set $\mathcal{A}_{\text{small}}(\mathcal{B})$ is not a closed sub-algebra of the CFT. We will continue calling this set an “algebra”, but the reader should keep this important limitation in mind.

We now establish some key properties of this small algebra with respect to the vacuum. First, consider the Hilbert space \mathcal{H}_{EFT} of all states in EFT that can be thought of as AdS with a small number of excitations. This is produced by acting with polynomials of generalized free fields, both inside and outside the band.

$$\mathcal{H}_{\text{EFT}} = \text{span of} \{ \mathcal{O}_{\ell_1}(t_1)|0\rangle, \mathcal{O}_{\ell_2}(t_2) \mathcal{O}_{\ell_3}(t_3)|0\rangle, \dots, \mathcal{O}_{\ell_4}(t_4) \mathcal{O}_{\ell_5}(t_5) \cdots \mathcal{O}_{\ell_{\mathcal{D}_m}}(t_{\mathcal{D}_m})|0\rangle \}. \quad (3.15)$$

The difference between (3.13) and the expressions above is that the time coordinates now are not limited to the time band and we have $0 \leq t_i \leq \pi$.

We will now prove an analogue of the *Reeh-Schlieder* theorem [44] for local algebras for the small algebra defined above.

$$\mathcal{H}_{\text{EFT}} \doteq \mathcal{A}_{\text{small}}|0\rangle, \quad (3.16)$$

i.e. the set of states obtained by acting with the small algebra $\mathcal{A}_{\text{small}}$ is dense in the full Hilbert space of effective field theory. This is the statement that the the CFT ground state $|0\rangle$ is a *cyclic* vector for this Hilbert space with respect to the small algebra.

In the bulk, the property (3.16) can be thought of as the version of Reeh-Schlieder theorem for region $\overline{\mathcal{D}}$. On the boundary this is a version of Reeh-Schlieder for finite time-domains. As explained above, this statement is non-trivial only in a situation where we can naturally define the notion of a small algebra in a time domain, for instance in large N CFTs.

We first establish this result in the large N limit, $N \rightarrow \infty$, namely the free field limit when there is no interaction. These results can easily be generalized away from the free-field limit, within perturbation theory in $\frac{1}{N}$ as we indicate subsequently.

Let us consider smearing $\mathcal{O}_\ell(t)$ in time by a smearing function f whose support is confined inside the time band. This defines operators X_f as

$$X_f = \int dt f(t) \mathcal{O}_\ell(t) \quad , \quad f(t) = 0 \quad \text{for } t \notin [0, T]. \quad (3.17)$$

These operators can be thought of as generators of the small algebra $\mathcal{A}_{\text{small}}(\mathcal{B})$ of simple operators in the time band. We do not display the dependence of X on the angular momentum quantum number ℓ because it will not play much of a role below.

In the large N limit, the space of simple bulk states has the structure of a Fock space. As a consequence of this, the statement (3.16) can be established by simply showing that any single particle state can be well approximated by a state of the form $X_f|0\rangle$. More precisely, any single particle state can be written as

$$|\Psi\rangle = \int_0^\pi dt g(t) \mathcal{O}_\ell(t) |0\rangle, \quad (3.18)$$

for an appropriate choice of the function $g(t)$. Then the claim is that we can find a sequence of functions f_1, \dots, f_n, \dots , such that

$$\lim_{n \rightarrow \infty} X_{f_n} |0\rangle \equiv \lim_{n \rightarrow \infty} \int_0^T \mathcal{O}_\ell(t) f_n(t) |0\rangle = \int_0^\pi g(t) \mathcal{O}_\ell(t) |0\rangle. \quad (3.19)$$

To prove this, we consider its converse. If (3.19) did not hold, then there would exist a non-vanishing state of the form (3.18) orthogonal to all states produced by operators of the form (3.17). This in particular would require that $\langle 0 | \mathcal{O}_\ell(t) | \Psi \rangle = 0$ for all $t \in [0, T]$ and for all ℓ . We consider the function

$$R(t) \equiv \langle 0 | \mathcal{O}_\ell(t) | \Psi \rangle. \quad (3.20)$$

Given the positivity of the energies in the CFT this function can be analytically continued in the $\text{Im}[t] < 0$ half-plane. We then have a meromorphic function $R(t)$ in the lower half plane with the property that $\lim_{\text{Im}[t] \rightarrow 0^-} R(t) = 0$ for all $\text{Re}[t] \in [0, T]$. Then the “edge of the wedge” theorem implies that $R(t)$ vanishes everywhere. This is inconsistent with the assumption that $|\Psi\rangle$ was a non-vanishing state of the form (3.18), we have thus reached a contradiction.

Having thus established that general bulk single-particle states of the form (3.18) can be arbitrarily well approximated by states produced by operators of the form (3.17), it is easy to show that in the large N limit the same can be done for multi-particle bulk states by induction. Say that we have proved that all n -particle states can be obtained by acting with operators inside \mathcal{B} . Then the space of $(n+1)$ -particle states is spanned by states of the form

$$|\Psi_{n+1}\rangle = \int_0^\pi \mathcal{O}_\ell(t) g(t) |\Psi_n\rangle, \quad (3.21)$$

where $|\Psi_n\rangle$ is a n particle state and $g(t)$ is arbitrary as above. Once again, it is possible to construct this using

$$|\Psi_{n+1}\rangle = \lim_{n \rightarrow \infty} X_{f_n} |\Psi_n\rangle, \quad (3.22)$$

for an appropriately chosen sequence of functions f_n with support in $[0, T]$. If this has not been possible we would have $\langle \Psi_n | \mathcal{O}_\ell(t) | \Psi_{n+1} \rangle = 0$ for all $t \in [0, T]$. By the edge of the wedge theorem, this would require $\langle \Psi_n | \mathcal{O}_\ell(t) | \Psi_{n+1} \rangle = 0, \forall t \in [0, \pi]$, but this is in contradiction with (3.21).

This property of cyclicity is a somewhat surprising property, and we can gain intuition for it by examining the structure of the norm on the space of

single-particle states. Indeed, it is clear that a general function in $[0, \pi]$ cannot be well-approximated by a function in $[0, T]$ in the usual L^2 norm. What allows us to approximate a state produced by a function on $[0, \pi]$ with another state produced by functions on $[0, T]$ is the structure of the norm.

Notice that given two such states

$$|\Psi_1\rangle = \int_0^\pi dt_1 g_1(t_1) \mathcal{O}_\ell(t_1) |0\rangle, \quad |\Psi_2\rangle = \int_0^\pi dt_2 g_2(t_2) \mathcal{O}_\ell(t_2) |0\rangle, \quad (3.23)$$

we have

$$\langle \Psi_1 | \Psi_2 \rangle = \int_0^\pi dt_1 \int_0^\pi dt_2 g_1^*(t_1) G_\ell(t_1 - t_2) g_2(t_2). \quad (3.24)$$

Therefore the inner-product on the Hilbert space induces a bilocal product on function space that depends on the Wightman function in the ground state

$$\langle 0 | \mathcal{O}_\ell(t_1) \mathcal{O}_{\ell'}(t_2) | 0 \rangle \equiv G_\ell(t_1 - t_2) \delta_{\ell\ell'}, \quad (3.25)$$

where the delta function in the angular momentum comes from the rotational invariance of the vacuum. Note that in the correlator above, we have picked an ordering in the Lorentzian theory. This is a Wightman function, and not a time-ordered correlator.

For any given mode, it is straightforward to compute this Wightman function explicitly. For example for the modes of a scalar field of dimension Δ , we have

$$\langle 0 | \mathcal{O}_\ell(t_1) \mathcal{O}_{\ell'}(t_2) | 0 \rangle = \frac{2^{2-\Delta-l} \pi^d \Gamma(\Delta + l)}{\Gamma(d/2) \Gamma(d/2 + l) \Gamma(\Delta)} \cos^{-\Delta-\ell} [t_{12} - i\epsilon] \quad (3.26)$$

$$\times {}_2F_1 \left(\frac{\Delta + l}{2}, \frac{\Delta + l + 1}{2}; \frac{d}{2} + l; \cos^{-2} [t_{12} - i\epsilon] \right) \delta_{\ell\ell'}, \quad (3.27)$$

where $t_{12} = t_1 - t_2$. Here we have suppressed the hopefully obvious dependence on the remaining angular momentum quantum numbers characterizing operators within the given representations ℓ, ℓ' .

The Fourier transform, $G_\ell(\omega) = \frac{1}{2\pi} \int dt e^{i\omega t} G_\ell(t)$, can be obtained by expanding the 2-point function in a complete set of energy eigenstates we find

$$G_\ell(\omega) = \sum_E \delta(E - \omega) |\langle 0 | \mathcal{O}_\ell(0) | E \rangle|^2. \quad (3.28)$$

From this we learn that on general grounds $G_\ell(\omega) \geq 0$. Moreover at large N the function $G_\ell(\omega)$ has support only on single-particle states in the bulk whose energies are $E = \Delta + 2n + \ell$, where ℓ is the angular momentum of the mode.

$$G_\ell(\omega) = \sum_{n=0}^{\infty} G_{n,\ell} \delta(\omega - \Delta - 2n - \ell). \quad (3.29)$$

where the coefficients $G_{n,\ell}$ are the Fourier transform of (3.26) and have the form

$$G_{n,\ell} = \frac{4\pi^d \Gamma(\Delta + n + \ell) \Gamma(\Delta + n + 1 - d/2)}{\Gamma(d/2) \Gamma(n + 1) \Gamma(\Delta) \Gamma(\Delta + 1 - d/2) \Gamma(d/2 + n + \ell)}. \quad (3.30)$$

The important property to notice above is that $G_{n,\ell} = 0, \forall n < 0$. So, to reconstruct a state of the form (3.18), using (3.19), we need the sequence of functions f_n to match only the positive Fourier components of g and not to match the function in general. This is what allows us to create any state by acting within the time band and allows (3.16) to hold.

Although we have phrased our entire discussion within free-field theory, most of the discussion above remains unchanged in its essentials when $\frac{1}{N}$ corrections are added. This is because within perturbation theory, we can write the Heisenberg operators in the $\frac{1}{N}$ expansion as linear combinations of the free-field operators. Note that this statement is only correct perturbatively, and in terms of the action of these operators on states with energies much less than N . Therefore, it is clear that, in the perturbative approximation, the span of these operators is the same as the span of the original operators. So, we conclude vacuum remains a cyclic vector with respect to $\mathcal{A}_{\text{small}}$.

We will write the fact that we generate the state $|\Psi\rangle$ by acting with an operator with compact support as

$$X_f|0\rangle \doteq |\Psi\rangle, \quad (3.31)$$

where it is understood that this corresponds to taking a sequence of functions in $[0, T]$ and then taking the limit.

The reason we are careful to write \doteq instead of $=$ is that, in fact, one can show that while by acting within $[0, T]$ it is possible to approximate the state $|\Psi\rangle$ arbitrarily well, one cannot always go to the limit and obtain a state that

is equal to $|\Psi\rangle$. A closely related result is that we cannot exactly annihilate the vacuum by acting with operators smeared with functions in $[0, T]$.

More precisely, we have the result

$$\nexists f(t), f \neq 0, \quad \text{such that } \int_0^T f(t) \mathcal{O}_\ell(t) |0\rangle = 0. \quad (3.32)$$

The theorem (3.32) is sometimes framed by stating that the vacuum is a *separating* vector for the small algebra. We provide two pieces of caution the reader while interpreting (3.32). First, while we cannot exactly annihilate a state from within the time band, we can get arbitrarily close to 0; Second, we note that (3.32) only holds for generalized free fields that do not correspond to short representations of the conformal algebra. If we are considering generalized free fields like the stress tensor or conserved currents, then it is possible to annihilate the vacuum, as we show below.

We now prove (3.32). Say that a function $f(t)$ with compact support in $[0, T]$ existed so that we could use it to annihilate the vacuum. Then we must have

$$X_f |0\rangle = \int_0^T f(t) \mathcal{O}_\ell(t) |0\rangle = \int_0^\pi f(t) \mathcal{O}_\ell(t) |0\rangle = \pi \sum_{n=-\infty}^{\infty} f_{-n} \mathcal{O}_{n,\ell} |0\rangle = 0, \quad (3.33)$$

where we have first used the fact that f has compact support to expand the region of integration, and then used a Fourier transform, with

$$\mathcal{O}_{n,\ell} = \frac{1}{\pi} \int_0^\pi \mathcal{O}_\ell(t) e^{i(\Delta+\ell+2n)t}; \quad f_n = \frac{1}{\pi} \int_0^\pi f(t) e^{i(\Delta+\ell+2n)t}. \quad (3.34)$$

Now, unless \mathcal{O} belongs to a short representations of the conformal algebra, then by the state operator map the action of $\mathcal{O}_{0,0}$ on the vacuum creates the primary state of this representation while $\mathcal{O}_{n,\ell} |0\rangle$ with non-positive n corresponds to descendants. Since these descendants are orthogonal, we see that for (3.33) to hold, we must have $f_n = 0, \forall n \geq 0$. But then f is an analytic function in the lower t plane, and since $f(t) = 0$ for $t \in [T, \pi]$, by the edge of the wedge theorem, we see that $f(t) = 0, \forall t$. This proves (3.32).

This proof evidently fails for operators corresponding to short representations. Here, we can annihilate the vacuum by integrating the operator with a

specific spherical harmonic and then smearing it appropriately in time so as to extract the null descendant. For example we clearly have

$$\int d^{d-1}\Omega \int dt T^{00}(t, \Omega) f'(t) |0\rangle = 0, \quad (3.35)$$

where T is the stress-tensor, and f is a function that vanishes smoothly at the end-points $[0, T]$. Similar relations hold for other conserved currents.

As mentioned above, a related statement is that there exist states $|\Psi\rangle \in \mathcal{H}_{\text{EFT}}$ that can be arbitrarily well approximated but not necessarily quite attained using the operators X_f . More specifically, there are states $|\Psi\rangle \in \mathcal{H}_{\text{EFT}}$ with the property that while we can find a sequence of functions f_1, \dots, f_n, \dots , such that $\lim_{n \rightarrow \infty} \int_0^T \mathcal{O}_\ell(t) f_n(t) |0\rangle = |\Psi\rangle$ we also have

$$\nexists f(t), \text{ such that } \int_0^T f(t) \mathcal{O}_\ell(t) |0\rangle = |\Psi\rangle. \quad (3.36)$$

For example, consider a state $|\Psi\rangle$ that is a superposition of global AdS modes with a maximum n_{max} . For such a $|\Psi\rangle$, we can prove (3.36) just as we proved (3.32). If such an f existed, then $e^{it(\Delta + \ell + 2n_{\text{max}})} f(t)$ would lead to a function that was analytic in the lower t -plane. But any such function that vanishes in $[T, \pi]$, must vanish everywhere, and so f would have to be 0. This is absurd, and so f cannot exist.

The relations (3.32) and (3.36) may be understood as one important difference between the algebra of operators in $[0, T]$ and in $[0, \pi]$ at infinite N . In the former case, we cannot produce exact energy eigenstates or annihilate the vacuum exactly, whereas in the latter we can.

Note that both (3.32) and (3.36) continue to be true at finite N . This is because we may write the action of an operator on the vacuum at finite N as

$$A_a |0\rangle = A_a^0 |0\rangle + \frac{1}{N} A_a^1 |1\rangle + \dots, \quad (3.37)$$

where $A_a^0 |0\rangle$ is the state that we would have obtained at infinite N , and the remaining terms are perturbative corrections. Now, we see that since all the terms multiplying the powers of $\frac{1}{N}$ are manifestly independent of N , $A_a |0\rangle = 0 \Rightarrow A_a^0 |0\rangle = 0$. Since we have proved that the latter cannot happen, we conclude that perturbatively the vacuum remains a separating vector. Similarly, it is not possible to generate an exact energy eigenstate through the action of the small algebra.

However, at finite N , the relations (3.32) and (3.36) are less of a distinguishing factor between $\mathcal{A}_{\text{small}}$ and the algebra of single trace operators in the interval $[0, \pi]$ since at finite N we cannot annihilate the vacuum, or produce exact energy eigenstates even by considering simple operators from the larger time-range.

3.3.1 Explicit construction of arbitrary states using operators in the band

We now turn to the explicit construction of a sequence of functions f_n that, through the operators in (3.17), can approximate any state $|\Psi\rangle$ in the larger time band. Let $b_k(t)$ be a complete basis of functions with compact support in $[0, T]$, where $k = 0, 1, \dots, \infty$. Then we consider the set of trial states

$$X_{f_n}|0\rangle = \sum_{k=0}^n \alpha_k \int_0^T \mathcal{O}_\ell(t) b_k(t) dt |0\rangle, \quad (3.38)$$

and choose α_k to minimize

$$r_n = ||X_{f_n}|0\rangle - |\Psi\rangle||^2 \quad (3.39)$$

for each n . Note that as n increases the value of this minimum must decrease monotonically, since at each n , we have the choice of obtaining the previous minimum by just taking $\alpha_n = 0$. By the theorem of cyclicity above, we also see also that as we take $n \rightarrow \infty$ this norm must tend to 0.

If we denote the inner-product matrix between the elements of the b_k basis G_{qk}^T

$$G_{qk}^T \equiv \int_0^T dt_1 \int_0^T dt_2 b_q^*(t_1) G(t_1 - t_2) b_k(t_2), \quad (3.40)$$

then to minimize r_n we require

$$\sum_k \alpha_k G_{qk}^T - \int_0^\pi dt_2 \int_0^T dt_1 b_q^*(t_1) g(t_2) G(t_1 - t_2) = 0, \forall q. \quad (3.41)$$

We note that by showing that the state is separating, we have also shown that G_{qk}^T is invertible. We now denote the inverse of G_{qk}^T by I_{pq}^T , which has the property that

$$\sum_{q=0}^n I_{pq}^T G_{qk}^T = \delta_{pk}, \quad (3.42)$$

where we remind the reader that n is the length of the sequence that appears in the trial wave function (3.38). This allows us to solve the equation above through

$$f_n(t) = \sum_{q,k=0}^n I_{qk} b_q(t) \int_0^\pi dt_2 \int_0^T dt_1 g(t_2) G(t_1 - t_2) b_k^*(t_1). \quad (3.43)$$

The specific choice of the basis $b_k(t)$ may be made according to convenience and does not affect the validity of the formula above.

The same procedure can easily be used to create multi-particle states with operators that have support only within the time band.

3.4 Interior operators and precursors

We now move on to the question of how to represent CFT bulk operators, which are inside the diamond \mathcal{D} , using operators in the time band. From bulk effective field theory, this might seem impossible. Bulk locality implies that CFT operators in the time band should commute, up to Gauss law tails, with operators in the diamond, since they are spacelike separated. On the other hand the *time slice axiom* of quantum field theory implies that all CFT operators are contained in the set of operators at a given time. Therefore, if the CFT has operators that represent the interior of the diamond, they must be present in the time band. (This point was also discussed in [57].)

Although this seems to be a contradiction, it is resolved by the fact that bulk locality is an emergent concept. Operators inside \mathcal{D} are made up of complicated operators from the time band. These complicated operators have the property that they commute with the simple operators that make up operators inside $\overline{\mathcal{D}}$.

In this section, we will show how to explicitly reconstruct these complicated operators. Although this construction clearly conflicts with bulk locality, we will show that it can be done in a straightforward manner by adding the complicated polynomials (3.2), that approximate $P_0 = |0\rangle\langle 0|$, to the algebra.

The operators inside the diamond are also called precursors [67]. This terminology arises as follows. Consider the excited state,

$$|\text{exc}\rangle = \exp \left[i \int_{S^{d-1}} d\Omega \phi(r=0, t=\frac{T}{2}, \Omega) \right] |0\rangle, \quad (3.44)$$

which corresponds to the vacuum excited with an S-wave at the center of the diamond. Then, this state has the property that

$$\langle \text{exc} | A_\alpha | \text{exc} \rangle = \langle 0 | A_\alpha | 0 \rangle, \quad \forall A_\alpha \in \mathcal{A}_{\text{small}}. \quad (3.45)$$

This makes it appear that an observer restricted to measuring simple operators inside the time band cannot detect the presence of this excitation.

On the other hand, an observer who has access to the entire boundary, can simply wait till the time $t = \pi$, and detect the presence of the excitation in $|\text{exc}\rangle$ in (3.45). Below, we will directly construct $\phi(r = 0, t = \frac{T}{2}, \Omega)$ using complicated operators from the time band. These operators are called precursors because they give us information about points deep in the bulk, before this information can causally propagate to the boundary.

Before we start, it is worth mentioning that there is a simple way to construct precursors by using operators from only the time band. This is to consider the set of operators $U(t) = e^{iHt}$, for all values of t . This fact was also emphasized by Marolf [55], who argued directly from the bulk that information present in any Cauchy slice of the boundary could be recovered from any other slice. Note that if we have access to arbitrarily complicated operators at $t = 0$, then the Hamiltonian can be evaluated on that time-slice and we can reconstruct $U(t)$. Using $U(t)$, we can then reconstruct the Heisenberg operators at all values of time. However, this construction is somewhat formal, and does not give insight into the nature of the “complicated operators” that enter into expressions for local operators in the interior of the diamond. It also suggests that we need an infinite sequence of complicated operators, labelled by different values of t , to reconstruct precursors. This turns out to be unnecessary in the approach that we follow below.

Our construction proceeds in three steps. First, we remind that reader that it is possible to write the bulk field at any point in AdS, including the center of the diamond as

$$\begin{aligned} \phi(t, r, \Omega) &= \sum_n c_{n,\ell} \mathcal{O}_{n,\ell} e^{-i(2n+\ell+\Delta)t} Y_\ell(\Omega) \chi_{n,\ell}(r) + \text{h.c.}, \\ \chi_{n,\ell}(r) &= r^\ell (r^2 + 1)^{-\frac{\Delta+2n+\ell}{2}} {}_2F_1\left(-n, -\Delta - n + \frac{d}{2}; \frac{d}{2} + \ell; -r^2\right), \\ c_{n,\ell} &= \frac{\Gamma\left(\frac{1}{2}(d - 2\Delta - 2n)\right) \Gamma\left(\frac{1}{2}(d + 2\ell + 2n)\right)}{\Gamma\left(\frac{d}{2} - \Delta\right) \Gamma\left(\frac{d}{2} + \ell\right)}. \end{aligned} \quad (3.46)$$

This formula follows from the standard analysis of the bulk to boundary smearing function and we refer the reader to [68–72] for details and to [18] for a review. Notice that, unlike the expansion (3.7), the wave functions above do not grow as $\ell \rightarrow \infty$ and so we can write (3.46) in position space as well.

Therefore, if we could reconstruct the operators

$$\mathcal{O}_{n,\ell} = \frac{1}{\pi} \int_0^\pi dt \int d^{d-1}\Omega \mathcal{O}(t, \Omega) Y_\ell^*(\Omega) e^{i(n+\ell+2\Delta)t} \quad (3.47)$$

using operators from the time band, we would be able to reconstruct the local field.

Projector on the Vacuum

We now show that to reconstruct $\mathcal{O}_{n,\ell}$, we need to add only one operator to the algebra to obtain precursors. This is the operator

$$P_0 = |0\rangle\langle 0|. \quad (3.48)$$

This operator can clearly be constructed using local operators in the CFT within the time band $[0, T]$. For example, we could write

$$P_0 = \lim_{\alpha \rightarrow \infty} e^{-\alpha H}, \quad (3.49)$$

where H is the CFT Hamiltonian that is simply obtained by integrating the local stress energy tensor

$$H = \int T^{00}(t, \Omega) d^{d-1}\Omega - E_0, \quad (3.50)$$

and shifted by a constant, E_0 , to ensure that the ground state is annihilated by H .

But, it is important, that for our purposes we do not need the exact operator (3.49) but any approximation of the form

$$\mathcal{P}_{\alpha,p_c} = \sum_{p=0}^{p_c} \frac{(-1)^p (\alpha H)^p}{p!}, \quad (3.51)$$

will also suffice provided we take α and p_c to be large enough.

To see how large these values have to be, note that we must take α large enough so that, if $|E_{\min}\rangle$ is the lowest energy state above the vacuum, we have $|P_{\alpha,p_c}|E_{\min}\rangle|^2\mathcal{L}1$. This requires $e^{-\alpha E_{\min}}\mathcal{L}1$. Now, since every holographic theory contains the graviton, the first excited state has an energy that cannot be larger than d , $E_{\min} \leq d$. Second, consider the highest energy state E_{\max} for states in \mathcal{H}_{EFT} . We must keep enough terms in the polynomial to ensure that (3.51) is a good approximation to the exponential for this state as well. This implies that the two conditions on the cutoffs are

$$e^{-\alpha d}\mathcal{L}1, \quad p_c \gg \alpha E_{\max}. \quad (3.52)$$

We expect that $E_{\max}\mathcal{L}N$, since for states with higher energy than this, our description of the physics in terms of generalized free fields breaks down. Moreover, since we are working at leading order in N , it is sufficient to suppress the lowest excited state by a factor of $\frac{1}{N}$. Therefore, one choice of cutoffs that meets the condition (3.52) is $\alpha = \ln(N)$ and $p_c = N \ln(N)$. The reader may choose to work with different cutoffs provided that (3.52) is satisfied.

It is important to understand that no choice of cutoffs on \mathcal{H}_{EFT} will allow us to include a good approximation to P_0 within our simple algebra. For example, let us say we attempt to take $p_c = \mathcal{D}_m$ to include an expansion of the form (3.51) in the algebra, where we remind the reader that \mathcal{D}_m is the largest allowed degree of a polynomial in the simple algebra. But now we see that $E_{\max} \geq d\mathcal{D}_m$, and for states with this energy, and the cutoff $p_c = \mathcal{D}_m$, the expansion (3.51) does not approximate P_0 well.

Construction of $\mathcal{O}_{n,\ell}$

We now show how to use P_0 , or alternately the polynomials \mathcal{P}_{α,p_c} from (3.51), to construct $\mathcal{O}_{n,\ell}$

As we have discussed, at large N , the Hilbert space has the structure of a Fock space. In this limit, we introduce a natural basis of states for \mathcal{H}_{EFT} by writing

$$|p_{n_1,\ell_1} \cdots p_{n_j,\ell_j} \cdots\rangle = \prod_{j=0}^{\mathcal{D}_m} \left(\Gamma(p_{n_j,\ell_j} + 1) G_{n_j,\ell_j} \right)^{-\frac{1}{2}} \left(\mathcal{O}_{n_j,\ell_j} \right)^{p_{n_j,\ell_j}} |0\rangle, \quad (3.53)$$

where the product above ranges over all allowed descendants of the primary operator \mathcal{O} , which are limited by \mathcal{D}_m by our cutoff above. In this basis, the

operator $\mathcal{O}_{n,\ell}$ has the natural simple harmonic oscillator form

$$\mathcal{O}_{n,\ell} = \sum_{\{p_{n_j,\ell_j}\}} \sqrt{p_{n,\ell} G_{n,\ell}} |p_{0,0} \dots p_{n,\ell} - 1 \dots \rangle \langle p_{0,0}, \dots p_{n,\ell} \dots|, \quad (3.54)$$

where the sum ranges over all allowed p_j .

But note that we already know how to construct the states in the Fock space using operators in the time band. Let us introduce some notation to represent this. We denote the operator $X \in \mathcal{A}_{\text{small}}$ that creates the state (3.53) by

$$X[p_{n_1,\ell_1} \dots p_{n_j,\ell_j} \dots] |0\rangle \doteq |p_{n_1,\ell_1} \dots p_{n_j,\ell_j} \dots\rangle. \quad (3.55)$$

With this notation, we see that the mode of the boundary operator can be written as

$$\mathcal{O}_{n,\ell} \doteq \sum_{\{p_{n_j,\ell_j}\}} \sqrt{p_{n,\ell} G_{n,\ell}} X[p_{0,0} \dots p_{n,\ell} - 1 \dots] P_0 X[p_{0,0} \dots p_{n,\ell} \dots]^\dagger. \quad (3.56)$$

We can now simply write the field operator as

$$\begin{aligned} \phi(t, r, \Omega) \doteq & \sum_{n,\ell} \sum_{\{p_{n_j,\ell_j}\}} \sqrt{p_{n,\ell} G_{n,\ell}} X[p_{0,0} \dots p_{n,\ell} - 1 \dots] P_0 X[p_{0,0} \dots p_{n,\ell} \dots]^\dagger \\ & \times c_{n,\ell} \chi_{n,\ell}(r) e^{-i(\Delta+2n+\ell)t} Y_\ell(\Omega) + \text{h.c.} \end{aligned} \quad (3.57)$$

We remind the reader that we use \doteq because the operators in the time band can reproduce a given state only in the limit shown in (3.19). Except for P_0 , all the other operators that appear above explicitly belong to the simple algebra and P_0 itself can be obtained as a limit of a sequence of polynomials \mathcal{P}_{α,p_c} .

Note that to obtain this result, we had to use the important result of cyclicity from the discussion above: the set of states obtained by acting with the small algebra is dense in the full Hilbert space. Therefore any state obtained by the action of $\mathcal{O}_{n,\ell}$ on the vacuum can also be obtained by the action of an appropriate operator from the time band.

The statement of cyclicity by itself does not allow us to represent the operator $\mathcal{O}_{n,\ell}$ in terms of operators from the time band. Rather, it tells us about its action on the state $|0\rangle$. By inserting the projector $P_0 = |0\rangle\langle 0|$ and sandwiching it between a sequence of operators $X[p_{0,0} \dots]$ above, we are able to

reproduce the entire operators $\mathcal{O}_{n,\ell}$, and in turn the local field in the interior of the diamond.

We believe that the expression (3.57) gives a remarkably simple expression for precursors in terms of boundary operators.

3.5 Conclusion and discussion

In this chapter, we have essentially focused on two results. One of them is that large-scale non-locality is an essential feature of quantum-gravity. Such a loss of causality is an ingredient in proposals of black-hole complementarity. In previous work, two of us showed that several recent versions of the information paradox could be resolved by accepting that simple local operators at a point in the interior of the black hole could be identified with complicated operators near the boundary of AdS that were causally disconnected from that point.

Here, we see that this phenomenon is evident in empty AdS. In particular, our formula (3.57) shows that one can write the field at a point in the center of AdS purely in terms of a complicated polynomial of operators in a time band $T < \pi$, even though all of these are causally disconnected from the center of the AdS.

A related question has to do with the approximation in which locality arises within effective field theory. Here, we argued that the correct way to understand this is in terms of an approximate “algebra” of simple operators in the time band. It is possible to define such an algebra, only in the large N limit where there is a parametric separation between light generalized free fields and more complicated multi-trace operators comprised of polynomials of N such fields. We showed that, if one makes a distinction between simple and complicated operators, then simple operators in a time band of width $T < \pi$ on the boundary obey a version of the Reeh-Schlieder theorem. This is the dual of the Reeh-Schlieder theorem for the region in the bulk that is causally connected to this time band.

One interesting question, which we hope to explore further has to do with whether it is possible to define a natural modular Hamiltonian for the time-band. This can be done entirely algebraically on the boundary using the techniques of Tomita-Takesaki theory as follows. We can define the following anti-

linear operator

$$SA_\alpha|0\rangle = A_\alpha^\dagger|0\rangle, \quad A_\alpha \in \mathcal{A}_{\text{small}}, \quad (3.58)$$

which is well defined on \mathcal{H}_{EFT} because the vacuum is cyclic and separating with respect to $\mathcal{A}_{\text{small}}$. Then the modular Hamiltonian can be defined through $H_{\text{mod}} = -\log(S^\dagger S)$. It would be interesting to check that this should correspond to the bulk modular Hamiltonian for $\overline{\mathcal{D}} - D$.

Precursors have been discussed extensively in the literature. In [73], it was proposed that Wilson loops may act as precursors building on the intuition that the bulk duals of Wilson loops are string worldsheets that extend into the bulk, and may therefore detect excitations in the interior. Although this is a natural guess, as pointed out [74], this is incorrect. Wilson loops are dual to operators that create a perturbative string excitation in the bulk. To the extent that perturbative string theory is local, Wilson loop operators in a region of the boundary cannot detect information from a causally disconnected region in the bulk. In the presence of such an excitation, Wilson loops cannot be computed through a minimal area surface any longer. As explained in [75], this is not dissimilar to the fact that, in the vacuum, correlation functions can be computed in a geodesic approximation. However, while bulk geodesics do respond to bulk excitations, this does not imply that boundary correlators are precursors; all that happens is that the duality between correlators and geodesics duality breaks down in the presence of a bulk excitation.

It is now believed, based on the HRT formula for the entanglement entropy of a region [76] that the entanglement entropy does provide an example of a precursor that is sensitive to bulk dynamics in the “entanglement wedge” of the region. A related proposal was made in [75], where it was proposed that the modular Hamiltonian for a region was dual to the Area operator for the minimal bulk surface. As we mentioned earlier, an important difference between previous work and our study is that we are considering a boundary region that has no non-trivial causal complement. Nevertheless, locality emerges when we focus on simple operators, whereas non-local information is stored in complex polynomials.

It is rather remarkable that we are able to construct a toy model of black hole complementarity in this simple setting. In empty AdS, we can only examine non-locality on length scales that are the AdS radius. We believe that, in their essentials, these ideas should also apply to flat-space black holes, where we require non-locality over the the distance that radiation travels in the evapora-

tion time of the black hole. However, it would be very interesting to understand this in greater detail.

4

Black hole formation

This chapter is based on our published paper [77].

4.1 Introduction

Over the last few decades black holes have been the primary window into the manifestation of quantum effects in gravity. In particular a huge amount of research in the last few years has been devoted to the understanding of the conflict between black hole physics and quantum mechanical expectation in the light of AdS/CFT correspondence [6].

An ideal set up to address this problem is the quantum gravity theory in three-dimensional Anti de Sitter spacetime. The dual field theory being a two dimensional CFT. It becomes easier, technically, to do explicit field theory computations exploiting the Virasoro algebra. Furthermore, qualitatively the static and stationary black hole solution in AdS_3 , namely the BTZ black hole [78] has most of its qualitative features very similar to higher dimensional AdS black holes and hence one expects to get a lot of insights on the black hole information problem solely from the study of black hole physics in AdS_3 ¹

In the previous chapter we studied operators behind a static horizon. In this chapter we will study a black hole that is formed by collapse. Due to the time

¹One might wonder that the black holes in AdS_2 might be even easier technically to study. However, AdS_2 spacetime has its own pathologies [79]. It does not support any finite energy excitations keeping the asymptotic properties fixed. Nonetheless, there has been a surge of work in understanding information loss paradox with simple one dimensional quantum mechanical toy models with nearly AdS_2 duals [80, 81]. We hope to have a more complete understanding of the AdS_2 story in this context in near future.

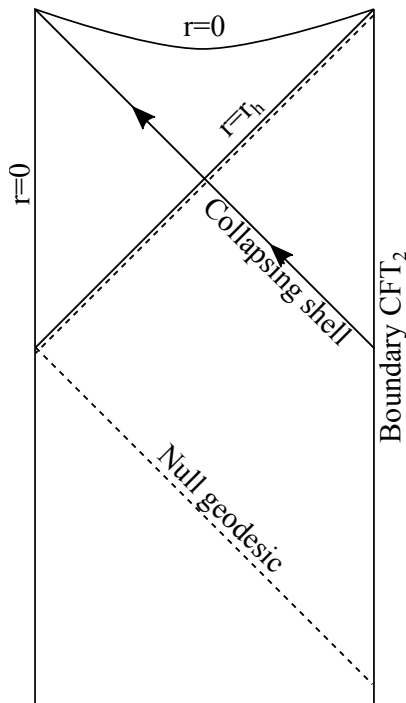


Figure 4.1: Geometry of a collapsing shell in AdS. The solid line denotes in-falling matter while the dashed line denotes the formation of horizon.

dependent nature this a challenging problem, however it could provide insights on, for instance, the trans-Planckian problem. In three dimensional Anti de Sitter spacetime this was attempted by tracing back a scalar field from just outside the black hole horizon along a null geodesic to the boundary. This was done using numerics in [82]. The set up is depicted in figure 4.1 and described more elaborately in appendix C. We focus on the CFT aspects of this problem, and some bulk aspects are elaborated on in the appendix.

Black holes are identified as localized high energy states in a quantum gravity theory. Therefore in the framework of $\text{AdS}_3/\text{CFT}_2$ correspondence, it would be tempting to create a heavy state in CFT and understand under which conditions the late time behavior of the correlators evaluated on the state are indistinguishable to the expected thermal correlators in the black hole spacetime. In principle, from the eigenstate thermalization hypothesis [83] this late time

thermal behavior of high energy states is expected for any dynamical complex system. However, one important feature of black hole thermalization is that it is characterized by a particular temperature, namely the Hawking temperature which is a purely geometric quantity. It would therefore be challenging to identify the quantity in the dual CFT construction which captures this universality. This is one of the goals of this work.

Our starting point will be to construct a heavy state dual to a collapsing black hole in AdS_3 . Our initial state would correspond to arbitrary mass distributions in the bulk in the form of some random distribution of conical defects or even colliding black holes. This CFT construction has its application beyond the understanding of the thermalization properties of black holes. This is in fact the set up where addressing the information loss paradox is most challenging. We will however take the first small step towards this in this work where we would contemplate on the collapse of this arbitrarily heavy state into a thermal background and measures to identify the collapse from a purely CFT perspective.

The first study in this line was done in [84] where the authors constructed a collapse state in CFT_2 by insertion of a large n number of local primary operators corresponding to a large number of dust particles constituting a massive null shell in AdS_3 . Other work in this direction include [85, 86]. In the limit $n \rightarrow \infty$ this yields a state with a well-defined uniform stress-energy tensor. The simple form of the “averaged” stress-energy tensor simplifies the computations of correlation functions drastically as demonstrated in their work. They specifically considered CFTs with large central charge, c and having a sparse spectrum at low energy, the gravity dual of which corresponds to having an AdS_3 space-time with a very large radius compared to the Planck length $c \sim \frac{\mathcal{R}_{\text{AdS}}}{L_P}$. For such CFTs the collapse state was constructed and the correlation functions were studied as a perturbative expansion in $\frac{1}{c}$.

We however adopt an alternative and a more generic scenario where a black hole in AdS_3 is created through collision of a finite number of heavy particles. In the perspective of the dual CFT_2 the possible dual set up is the creation of a high energy state through insertion of primary operators with high scaling dimension. For this dual picture to make sense the scaling dimension of the inserted operators need to scale with c in the limit $c \rightarrow \infty$. Furthermore, in view of having a static black hole as the final state of the time-evolution, every pair of operators need to be inserted at antipodal points with respect to one another.

In our work, we however, consider more general black hole states starting with arbitrary initial energy configurations. While studying the problem numerically we will consider two separate cases, namely operator insertions resulting in a static black hole or an oscillating final black hole state.

Once the background is created, the immediate interest will be to understand the measures of the black hole collapse at late Lorentzian time. It turns out that the most natural and simplest detector of the heavy state collapsing into a thermal black hole state is the correlation functions of the form

$$\mathcal{A}_{N_Q} = \langle V | Q(z_1) Q(z_2) \cdots Q(z_{N_Q}) | V \rangle, \quad (4.1)$$

where $|V\rangle$ is the heavy state created by insertion of heavy primaries as discussed above. $Q(z_i)$'s are probe operators which are attributed to the property that the scaling dimensions of these operators do not scale with c in the limit $c \rightarrow \infty$. These probe operators, typically termed as “light operators” therefore do not back-react on the heavy state. A heavy state created through insertion of N_H number of heavy primaries, (4.1) amounts to evaluating a $(2N_H + N_Q)$ point correlation function in the vacuum state. This correlator can be evaluated using conformal block techniques and as we will argue, the dominant contribution to the correlator comes from the vacuum Virasoro block which effectively captures the pure gravitational interactions in the bulk. This fact greatly simplifies the computation of the correlation function, (4.1). However, if N_H is a finite number of heavy operators naively it looks like the perturbative expansion in $\frac{1}{c}$ breaks down and it becomes hard to extract out even the leading order semi-classical behavior of the correlators, (4.1).

In a series of work initiated with [21] and later developed further in [22], the authors proposed a trick to save the perturbative expansion in $\frac{1}{c}$. Their prescription was to put the CFT_2 on a non-trivial background geometry. However, in $d = 2$ any geometry is related to the flat space geometry by a Weyl rescaling. The proposal was to choose an appropriate Weyl scaling or equivalently, a conformal transformation, $z \rightarrow w(z)$ such that in the new coordinates, w , it becomes possible to write down the correlator as a power series expansion in $\frac{1}{c}$ again.

This procedure of resumming the divergences in the perturbation series at large c , known as the “uniformization problem” in literature, is mathematically equivalent of sewing local coordinate patches around the punctures of a n -punctured Riemann sphere to construct a smooth covering manifold. However, the actual implementation of the mechanism increases in difficulty with

the increase in the number of punctures. In the language of the correlation functions, this number denotes the number of heavy operator insertions required for creating the heavy background state.

For our case we need at least four heavy operators (two heavy operators and their adjoints) to create a static black hole configuration at late time which amounts to solving the “uniformization problem” for a four-punctured Riemann sphere. Unfortunately, this problem does not have an analytic solution and therefore it is not possible to write down the conformal transformation $z \rightarrow w(z)$ for our case ².

The main claim of this chapter is that so long as one is concerned with the late time behavior of the Lorentzian correlator (4.1), one can actually get around this problem of finding explicit solutions to the uniformization problem which in our case amounts to solving a second order differential equation of Fuchs’ class. We show that most of the relevant information about the late time thermalization is already encoded in the monodromy matrix of the solutions along a curve on the unit circle. In particular the temperature of the final state is related to the eigenvalue of the monodromy matrix. However, finding the monodromy matrix explicitly for a general Fuchsian equation is technically as daunting as solving the original uniformization problem. But in this work we introduce two completely different tricks to establish the precise connection between the eigenvalues of the monodromy matrix at late Lorentzian time and the final black hole temperature even without knowing the explicit matrix.

The first approach relies on finding a conformal transformation that preserves the structure of the monodromy matrix while leading to a new Fuchs equation which is much easier to solve. In fact this transformation leads to a stress-energy wave function similar to one obtained in the continuum limit of [84] discussed earlier. For the hyperbolic class of monodromy matrices, this yields a precise relation between the eigenvalue of the monodromy matrix and the Hawking temperature of the black hole in the late Lorentzian time limit.

The second approach exploits the the representation of the monodromy ma-

²We have found some literature like [87] where the authors made an attempt to glue different coordinate patches defined locally, in the vicinity of the punctures of a four-punctured Riemann sphere. They used local series solutions of the uniformization equation near each puncture and finally matched the series solution at intermediate points. However, the variables they used had limited range of validity and the local series expansions, limited radius of convergences, both the facts not very useful for our purpose.

trix in terms of a path ordered integral over a flat connection [88]. We then use the Chern-Simons formulation of pure gravity to relate this path ordered integral to the area of horizon of the black hole. Upon using Bekenstein-Hawking formula this finally yields the same relation between the eigenvalue of the monodromy matrix and the Hawking temperature of the black hole after collapse.

The first of our proofs tells us something more about the final state of the Lorentzian time evolution. In fact, at late Lorentzian time, it is also possible to obtain a black hole dressed with soft gravitational hair. This soft hair corresponds to “boundary gravitons”, namely some non-propagating graviton degrees of freedom localized near the asymptotic boundary of the AdS_3 spacetime. From the perspective of dual CFT, these modes can be understood as acting with a raising Virasoro generator which affects the energy of the state, however, without modifying the temperature associated with the state. Therefore only looking at the temperature of the final state it is not possible to distinguish between a black hole state and a black hole state dressed with boundary graviton modes. The conformal transformation we used in our first approach has the holographic interpretation of a (monodromy preserving) large diffeomorphism that precisely chops off this hair to yield a pure black hole as the final state of collapse.

In this work, we present a numerical scheme to show that for generic initial state there can indeed be a large difference in energy between the initial energy injected to the system and the energy of a black hole final state estimated using thermodynamics of the black hole, with the difference in energy interpreted as the amount of energy stored in boundary gravitons.

Recently there has been a surge of work in understanding the role of soft gravitational hair in the context of black hole information paradox for flat space black holes. Interested readers can look at [89–92]. As we discussed, in AdS_3 , already at the semiclassical limit, these boundary gravitons play an important role in the late time thermalization. It is therefore natural to expect that beyond this limit, the boundary graviton modes might also play some role in understanding the black hole information paradox in the present set up. We postpone a more detailed investigation in this direction for future work.

This chapter is organized as follows. In section 4.2 we introduce our set up and the conformal block techniques which is an immensely useful tool that simplifies the problem greatly in the limit of large central charge.

The first part of section 4.3 is devoted to the understanding of the analytic

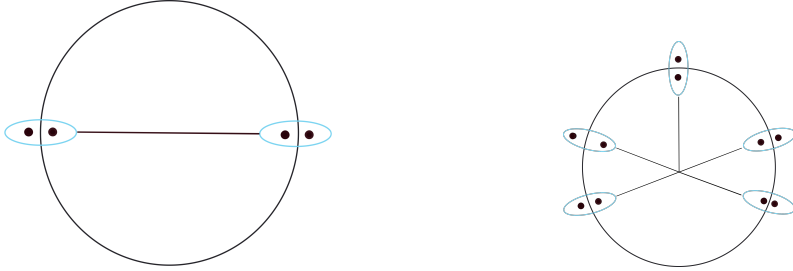
continuation of the correlator to Lorentzian signature. We present here the form of the analytically continued correlator in the limit of late Lorentzian time. We also discuss in this section how to associate the behavior of the correlator at late Lorentzian time to the monodromy matrix using a gauge connection. By introducing monodromy preserving diffeomorphisms in section 4.3.2 we establish the precise relation between the monodromy eigenvalues and the temperature of the final state black hole.

In section 4.4, we present another proof of this relation using the Chern-Simons interpretation of pure gravity in AdS_3 .

Section 4.5 contains a numerical analysis for our problem for different operator distributions. We estimate the energy of the final black holes and notice a significant deficit in energy as compared to the initial injected energy. We identify this deficit as the fraction stored in boundary gravitons. In this numerical set up we distinguish between polyhedral and non-polyhedral distributions of operators on the circle and discuss the consequences in either case. This chapter has three appendices.

4.2 A lightning review of the uniformization problem

In this section we shall set up our problem and introduce the computational tools we shall be using in the rest of the chapter. First we shall present the configuration of a finite number of heavy operators that represents an arbitrarily heavy state. Each of these heavy operator insertions is dual to adding a conical defect or a black hole in the bulk AdS_3 . We are interested in studying the final collapse states achieved through collisions among those defects or black holes at late Lorentzian time. This collapse is captured by measuring certain correlators of probe operators in the heavy background. As we shall review, the conformal block decomposition techniques in CFT_2 simplifies computations of these correlation functions greatly. After presenting these techniques, the rest of the section will be devoted to presenting the main technical obstacle that we would like to overcome in this chapter, namely the “uniformization problem” in our set up.



(a) Four punctures, corresponding to the (b) Surface corresponding to a Riemann Heun equation. surface with ten punctures.

Figure 4.2: This diagram displays the type of mirror pair configurations under consideration, and displays the OPE channel used. The dots represent heavy operator insertions on the radial plane. The left configuration potentially forms a stationary black hole, the right configuration is expected to not be stationary at late time.

4.2.1 Basic set up

We consider a generic heavy state $|V\rangle$ created by acting with heavy primary operators, O_H of scaling dimensions $H = \mathcal{O}(c)$ at the same time but at different points in space. In radial quantization,

$$|V\rangle = O(x_1) \dots O(x_n) |0\rangle, \quad |x_n| = 1 - \sigma_n. \quad (4.2)$$

Here x_i 's are complex coordinates in Euclidean CFT_2 so that the CFT states lie on a unit circle. To avoid UV divergences, we regularize our operator insertions x_n by shifting them a small distance σ away from the unit circle ($|x_n| = 1 - \sigma_n$) [84]. The respective adjoint operators contained in the bra-state $O^\dagger(1/\bar{x}_n)$ are therefore located on the circle with radius $(1 - \sigma_n)^{-1}$. We call a heavy primary insertion and its adjoint together, a “mirror pair”. We shall frequently use this nomenclature later in this work. We consider arbitrary distribution of these mirror pairs on the circle. Configuration of these mirror pairs of operators in a regular polyhedral distributions on the circle is a sufficient condition that the resulting black hole after collision will be at rest with respect to the center of AdS while relaxing the same yields oscillating black holes in the final state of evolution. Both these configurations are shown in figure 4.2. Using numerical techniques, later in this work, we will show the physical consequences of and

difference between having a static and a non-static configurations of operators explicitly.

As we mentioned before, we want to study the propagation of small probes on this heavy background that can be interpreted as undergoing gravitational collapse to a black hole state. To achieve we will be interested in the qualitative properties of correlators of the form (4.1). In particular, we shall focus on 2-point correlation function

$$\mathcal{A} = \langle V|Q(z_1)Q(z_2)|V\rangle, \quad (4.3)$$

where $Q(z_i)$'s are light operators with scaling dimensions $h_Q\mathcal{L}c$ and do not backreact on the background heavy state.

At this point it is worth reminding ourselves that, to reach the collapse state, we need to study evolution of the correlation function, (4.3) to late Lorentzian time. This requires analytic continuations of (4.3) to different Lorentzian correlators corresponding to different operator orderings. As we shall discuss in next section, for our purpose we will specifically need out-of-time-ordered correlation functions.

The leading semi-classical information about the final collapse state is encoded in the regime of large central charge. In order to extract this information, it is convenient to use the monodromy method developed in [93] and used in [84] in a related context. However, it is worth mentioning here once again that the continuous state limit considered in [84] stands as a very special case of the generic scenario we consider in this work. As discussed in the introduction, the large number of operator insertion, $n \rightarrow \infty$, as opposed to the finite number of heavy operator insertions we consider in (4.2), drastically simplifies the computation. The “heaviness” of inserted operators in our case naively destroys the perturbative expansion at large c . In the next subsections we shall review this problem and an effective solution thereof prescribed in a set of papers, [21, 22]. However, as mentioned earlier, we allow an arbitrary initial energy distribution corresponding to insertions of any finite number of heavy operators. We will, therefore, find that the afore-mentioned prescription does not completely fix the semi-classical correlator for us, although it simplifies our problem to a large extent.

4.2.2 The vacuum block and semiclassical correlation functions

In a 2d CFT with large central charge and sparse spectrum of low-lying operators, the method of conformal block decomposition provides the most efficient way to study the correlator given in (4.3). In general, in any quantum field theory, a correlator can be rewritten by inserting a projection operator made out of a complete set of states as

$$\begin{aligned}\mathcal{A}(x_1, \dots, x_n) &\equiv \langle O(x_1) \dots O(x_n) O(\bar{x}_1^{-1}) \dots O(\bar{x}_n^{-1}) Q(z_1) Q(z_2) \rangle \\ &= \sum_{\alpha} \langle O(x_1) \dots O(x_n) O(\bar{x}_1^{-1}) \dots O(\bar{x}_n^{-1}) | \alpha \rangle \langle \alpha | Q(z_1) Q(z_2) \rangle\end{aligned}$$

In a 2d CFT, in particular, one can arrange the states into irreducible representations of the conformal algebra, namely the Virasoro algebra. We can formally decompose the projector into a sum over partial projectors associated with each irreducible representation contained in the CFT spectrum. The full conformal algebra in $d = 2$ consists of two copies of Virasoro algebra. In what follows, we will present formulae only for the holomorphic sector, however, keeping in mind that all these statements will have anti-holomorphic counterparts.

$$P = \sum_h P_h = \sum_h \sum_{\{n_i, k_i\}} \frac{L_{-m_n}^{k_n} \dots L_{-1}^{k_1} |h\rangle \langle h| L_1^{k_1} \dots L_{m_n}^{k_n}}{\langle h| L_1^{k_1} \dots L_{m_n}^{k_n} L_{-m_n}^{k_n} \dots L_{-1}^{k_1} |h\rangle}, \quad (4.4)$$

where we have used the fact that a single Verma module of the conformal algebra can be generated by acting on the primary state with all ordered combinations of raising Virasoro generators

$$\mathcal{V}_h = \{L_{-n}^{k_n} \dots L_{-1}^{k_1} |h\rangle\}.$$

The denominator in (4.4) is the normalization factor. In order to avoid an over-complete basis, one needs to adopt an ordering convention. The conventional choice is given by $m_1 > m_2 > \dots > m_n$. The modes, L_n are subject to the usual Virasoro algebra

$$[L_n, L_m] = (n - m)L_{n+m} + \frac{c}{12}n(n^2 - 1)\delta_{n, -m}. \quad (4.5)$$

The projection of a correlator on one particular irreducible representation of the conformal algebra constitutes a single conformal block. Schematically, for the holomorphic part

$$\langle O(x_1) \dots O(x_n) O(\bar{x}_1^{-1}) \dots O(\bar{x}_n^{-1}) P_h Q(z_1) Q(z_2) \rangle = \mathcal{C} \alpha_h \mathcal{F}_h, \quad (4.6)$$

where \mathcal{C} denotes a choice of normalization and α_h , a kinematic factor given by a product of OPE coefficients in a particular OPE channel of interest. \mathcal{F}_h is the holomorphic conformal block which, on the other hand, is entirely fixed by the Virasoro symmetry. A similar expression also holds for the anti-holomorphic part. Each of the representations of the Virasoro algebra is associated with a primary operator, $\mathcal{O}_{h,\bar{h}}$ that creates the state $|h\rangle$ acting on the vacuum state,

$$\mathcal{O}_{h,\bar{h}}|0\rangle = |h\rangle \otimes |\bar{h}\rangle. \quad (4.7)$$

Substituting the holomorphic part of (4.7) in (4.6), one can express the conformal block in terms of factorized correlators in the vacuum.

In general the computation of conformal blocks in 2d CFT simplifies greatly in the regime where the central charge becomes very large, i.e the semi-classical regime. The simplification most clearly appears when the representation of the Virasoro block contains operators, $\mathcal{O}(x_i)$ and intermediate operators, $\mathcal{O}_{h,\bar{h}}$ whose scaling dimensions h, \bar{h} are small with respect to the central charge c . In this case, while the numerator of (4.4) does not scale with c , from the conformal algebra, (4.5), the denominator provides factors of c when the generators are not contained within the global conformal group ($\{L_{-1}, L_0, L_1\}$). In the large c limit, the leading semi-classical result can therefore be extracted solely from the global conformal block. Contribution from higher descendents will be suppressed by factors of c .

However, as mentioned before, we shall be considering heavy states created by a finite number of heavy operators, i.e. operators whose scaling dimension is proportional to the central charge c . As a result the numerator factors of (4.4) will contain operators with scaling dimensions scaling with c . However, if we allow this, the numerator of (4.4) will produce factors scaling with powers of c that can overcome the suppression from the denominator. This can be demonstrated by noting that the Virasoro generators are defined as the coefficients of the Laurent series of the stress-energy tensor $\mathcal{T}(z)$.

$$\mathcal{T}(z) = \sum_{n=-\infty}^{\infty} z^{-n-2} L_n, \quad L_n = \frac{1}{2\pi} i \oint dz z^{n+1} \mathcal{T}(z)$$

We can therefore construct a generating function for correlators containing

Virasoro generators

$$\begin{aligned} & \langle O(x_1) \dots O(x_n) O(\bar{x}_1^{-1}) \dots O(\bar{x}_n^{-1}) L_{-n_m} \dots L_{-n_1} \mathcal{O}_h(0) \rangle \\ &= \oint dz_1 \dots dz_m z_1^{n_1+1} \dots z_m^{n_m+1} \langle O(x_1) \dots O(x_n) O(\bar{x}_1^{-1}) \dots O(\bar{x}_n^{-1}) \mathcal{O}_h(0) \mathcal{T}(z_1) \dots \mathcal{T}(z_m) \rangle. \end{aligned} \quad (4.8)$$

By means of the Virasoro Ward identity we can see that the right-hand side will contain terms proportional to powers of the scaling dimensions of operators which in turn scale as powers in c .

Under the circumstances, it becomes impossible to extract the leading behavior from the global conformal block as the perturbative suppression of contributions coming from higher descendent states no longer works.

In [21] and [22], the authors came up with an idea to circumvent this problem. They established that the lack of suppression of the terms containing higher numbers of Virasoro modes is not a fundamental problem but rather signifies a poor choice of conformal frame. The authors exploited the fact that any metric in a 2-dimensional spacetime is conformally related to the flat space. The proposal was to choose an appropriate geometry, or equivalently employ a conformal transformation on the complex coordinates, $z \rightarrow w(z)$ in such a way that the correlator in the new “ w ”-coordinate system,

$$\langle O(x_1) \dots O(x_n) O(\bar{x}_1^{-1}) \dots O(\bar{x}_n^{-1}) \mathcal{O}_h(w) \mathcal{T}(w_1) \dots \mathcal{T}(w_m) \rangle \quad (4.9)$$

does not scale with positive powers of c . This can be done by exploiting the inhomogenous transformation of the stress energy tensor under conformal transformation, namely

$$\mathcal{T}(w) = \left(\frac{dz}{dw} \right)^2 \mathcal{T}(z(w)) + \frac{c}{12} S[z(w), w], \quad (4.10)$$

where $S[z(w), w]$ is the Schwarzian derivative defined by

$$S[z(w), w] \equiv \frac{z'''(w)}{z'(w)} - \frac{3}{2} \left(\frac{z''(w)}{z'(w)} \right)^2. \quad (4.11)$$

The Schwarzian extension of the transformation (4.10) ensures that in the new coordinate system the projector states constructed out of the global conformal

block give $O(1)$ contributions, while contributions coming from the states outside of the global block remain suppressed by factors of $1/c$. Furthermore, it can be proved using the $\mathcal{T}(w_1)\mathcal{T}(w_2)$ OPE that if the correlator with a single stress energy tensor insertion, $\langle O(x_1)\dots O(x_n)O(\bar{x}_1^{-1})\dots O(\bar{x}_n^{-1})\mathcal{O}_h(w)\mathcal{T}(w)\rangle$ can be expressed as a systematic expansion in $\frac{1}{c}$, similar expansion for an arbitrary number of stress energy tensor insertions as in (4.9) is automatically guaranteed.

One simplification that we adopt in our analysis is that we focus on the vacuum block corresponding $h = 0, \bar{h} = 0$ operators, namely the identity operator. This is reflected in the OPE channel depicted in figure 1 where all operators are fused with their adjoint and the resulting identity operator are in turn fused as indicated by the lines. From the gravitational bulk perspective of the $\text{AdS}_3/\text{CFT}_2$ correspondence, all graviton modes are expected to correspond to descendant states of the vacuum. Thus all exchanged gravitational modes are encompassed within the exchange of this one particular conformal block. From the perspective of CFT this is a consequence of large c and sparse spectrum of low-lying single trace operators. For certain conformal field theories this can be explicitly proved [93, 94]. We will assume this to work for generic CFTs having holographic duals since the afore mentioned properties typically hold in those CFTs [64–66].

In this case the irreducible representation of the global conformal group contains the vacuum state only. It would therefore be sufficient to choose a conformal transformation that renders correlators with single stress-energy tensor insertion vanish identically, namely,

$$\langle O(w(x_1))\dots O(w(x_n))O(w(\bar{x}_1^{-1}))\dots O(w(\bar{x}_n^{-1}))\mathcal{T}(w)\rangle = 0. \quad (4.12)$$

If this property holds for the coordinate system $w(z)$ this will ensure that it is only the contributions to the partial projector from the global conformal group that survive the limit $c \rightarrow \infty$. As a result, in the new w -coordinate system, the vacuum conformal block corresponds to the factorized correlator

$$\begin{aligned} A_0(w_1, w_2) &= \langle O(w(x_1))\dots O(w(x_n))O(w(\bar{x}_1^{-1}))\dots O(w(\bar{x}_n^{-1}))P_0 Q(w_1)Q(w_2)\rangle \\ &= \langle O(w(x_1))\dots O(w(x_n))O(w(\bar{x}_1^{-1}))\dots O(w(\bar{x}_n^{-1}))\rangle \langle Q(w_1)Q(w_2)\rangle. \end{aligned}$$

The correlation function factor containing the heavy operators does not contain any dependance on w_i so it is an overall factor that we will henceforth ignore.

We can transform back to the original z -coordinates by means of the usual transformation rule of primary operators

$$A_0(z_1, z_2) = \left(\frac{dw}{dz_1} \right)^{h_Q} \left(\frac{dw}{dz_2} \right)^{h_Q} (w(z_1) - w(z_2))^{-2h_Q}, \quad (4.13)$$

this will be the object that will be studied for the remainder of this chapter.

4.2.3 The defining equation for the uniformizing coordinates

In this subsection we will focus on how to construct these uniformizing coordinates. It is known that the stress-energy tensor satisfies the following transformation law given by (4.10) and (4.11).

Let us define the “stress-energy function”

$$T(z) = \frac{\langle O(x_1) \dots O(x_n) O(\bar{x}_1^{-1}) \dots O(\bar{x}_n^{-1}) \mathcal{T}(z) \rangle}{\langle O(x_1) \dots O(x_n) O(\bar{x}_1^{-1}) \dots O(\bar{x}_n^{-1}) \rangle} \quad (4.14)$$

The defining property of the uniformizing coordinates (4.12) can be transformed back to the original radial plane coordinates z by means of the transformation law

$$T(z) z'(w)^2 + \frac{c}{12} \left(\frac{z'''(w)}{z'(w)} - \frac{3}{2} \left(\frac{z''(w)}{z'(w)} \right)^2 \right) = 0. \quad (4.15)$$

where in the term between brackets we recognize the Schwarzian derivative defined by

$$S[z(w), w] \equiv \frac{z'''(w)}{z'(w)} - \frac{3}{2} \left(\frac{z''(w)}{z'(w)} \right)^2. \quad (4.16)$$

As a first step we invert the differential equation, so that $T(z(w))$ is a function of the variable, instead of being a variable in the equation. This is done by means of the substitution $f(z(w)) = \frac{dz(w)}{dw} = \frac{1}{w'(z)}$, where the prime denotes the derivative with respect to w . After some trivial manipulations one obtains

$$\frac{12}{c} T(z) + \frac{f''}{f} - \frac{1}{2} \frac{(f')^2}{f^2} = 0.$$

By adding and subtracting $\frac{1}{2} \frac{(f')^2}{f^2}$ we can simply replace the combination $\frac{f''}{f} - \frac{(f')^2}{f^2}$ by $\frac{d}{dz} \frac{f'(z)}{f(z)}$, this way we can obtain an equation that can be easily rewritten

into a well known form

$$\frac{12}{c}T(z) + \frac{d}{dz}\frac{f'}{f} + \frac{1}{2}\frac{(f')^2}{f^2} = 0. \quad (4.17)$$

The previous expression can be simplified by defining the new function $g(z) = \frac{f(z)'}{f(z)}$. Substituting this into the expression above an equation of Riccati type is obtained,

$$g'(z) + \frac{1}{2}g(z)^2 + \frac{12}{c}T(z) = 0. \quad (4.18)$$

The Riccati type equation can be rewritten to a linear equation of Fuchsian type by defining $g(z) = 2\frac{u'(z)}{u(z)}$ and substituting we obtain a second order linear differential equation of Fuchs class.

$$u''(z) + \frac{6}{c}T(z)u(z) = 0, \quad (4.19)$$

where $u(z)$ is given by $u(z)^{-2} = dw/dz$. Typically $T(z)$ is a meromorphic function whose poles are regular singular points of the differential equation, but we will consider as an example the case of [84] where this analyticity condition is relaxed. In terms of $u(z)$ the vacuum conformal block (4.13) can be written as

$$A_0(z_1, z_2) = u(z_1)^{-2h_Q} u(z_2)^{-2h_Q} \left(\int_{z_1}^{z_2} u(z)^{-2} dz \right)^{-2h_Q}. \quad (4.20)$$

In the next section we will demonstrate that a lot of qualitative properties can be derived from the form of this formula without the need to actually explicitly solve the Fuchs type equation (4.19) above.

4.3 Lorentzian time-evolution on the radial plane

The goal of this chapter is to describe the dynamics of probe correlators at asymptotically late Lorentzian times. This matter is complicated by the fact that the probe correlators

$$\langle V(0)|Q(t_1)Q(t_2)|V(0)\rangle = \langle V|e^{-iHt_1}Qe^{-iH(t_2-t_1)}Qe^{-iHt_2}|V\rangle \quad (4.21)$$

are out of time order³. A consequence of the reconstruction theorems of quantum field theory [95,96] states that all operator orderings within a correlator are

³For notational convenience we gave the state $|V(0)\rangle$ a single time label. As mentioned in the previous section we do not want to restrict ourselves to heavy operators inserted at the

related to each other through analytic continuation [97]. Hence the problem is to evaluate the full analytically continued correlator on the correct branch. To distinguish the correct branch we give the operator locations small imaginary parts corresponding to their ordering within the correlator. The Heisenberg picture above elucidates the signs and relative magnitudes of the imaginary parts as there exists a unique choice of either upper or lower half plane to which the time differences can be extended in order to obtain a convergent correlator on the extended domain. In this case we will give the Lorentzian times small imaginary parts, which can equivalently be thought of as giving them small real shifts in Euclidean time instead. This suggests the following algorithm⁴

- Give all Lorentzian times imaginary parts such that the time differences fall within the appropriate extended domain.
- Set all real parts of the Lorentzian times equal to zero, the resulting correlator is purely Euclidean and can be computed using standard CFT techniques.
- As a final step bring all real parts of Lorentzian time (or equivalently imaginary parts of Euclidean time) back to their original values. The imaginary parts will prescribe how to circumnavigate all encountered branch points and the associated multi-valuedness of the Lorentzian correlator.

This method provides our strategy to deriving results at late Lorentzian time. As mentioned before, we evaluate our correlator in radial quantization. We make use of the exponential map to see how our shifts in Euclidean time manifest on the radial plane.

$$z = e^{\tau+i\phi}, \quad \bar{z} = e^{\tau-i\phi}.$$

One can see that a small shift in Euclidean time corresponds to a small radial shift on the radial plane. This justifies the σ_i regularization scheme presented in the last section. If the heavy state operators and their adjoints are respectively shifted radially away from or toward the origin while maintaining the position

same time, therefore the appropriate way to think of $t = 0$ is as the time of the latest heavy operator inserted and the effect of all other heavy operators on the state $|V(0)\rangle$ is included through a path integral.

⁴ See [98] for an explicit demonstration of Lorentzian continuation of Euclidean correlators in a similar context.

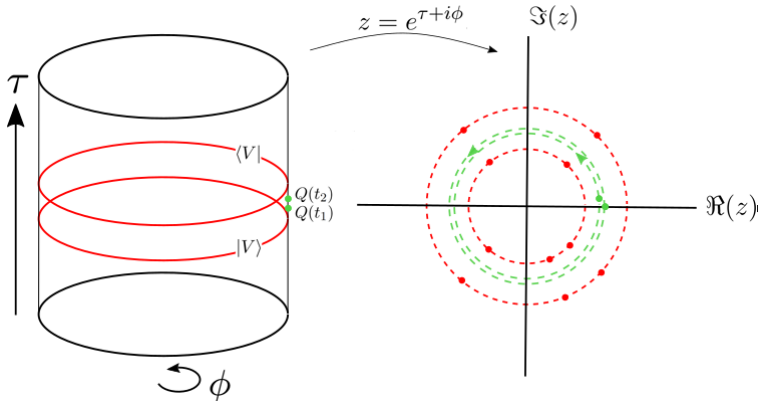


Figure 4.3: This diagram illustrates the effect of the exponential map on states created on the Euclidean cylinder. The red dots correspond to the insertions of heavy operators while the green dots denote light probe operators.

of the probe operators on the unit circle we ensure that we are on the right branch after reinstating the appropriate Lorentzian times. Hence from then onwards Lorentzian time-evolution of the probe correlators simply corresponds to letting them perform cycles along the unit circle.

This implies that this cycle needs to possess a non-trivial monodromy in the case where the correlation function is not expected to be periodic in time. Let us return to the Fuchsian equation (4.19), it is a second-order linear differential equation which means that its general solution is a linear combination of two particular solutions

$$u(z) = c_1 u_1(z) + c_2 u_2(z). \quad (4.22)$$

Since $T(z)$ is not analytic everywhere on the unit disk the linear space spanned by the particular solutions possesses a non-trivial flat connection on the unit circle. This statement can be made visible by rewriting the single second-order ODE (4.19) into two coupled first-order ODEs [88]

$$\partial_z U(z) = a(z) U(z), \quad (4.23)$$

here $U(z)$ is the fundamental matrix of solutions and $a(z)$ is the connection matrix

$$U(z) = \begin{pmatrix} u_1(z) & u_2(z) \end{pmatrix}, \quad a(z) = \begin{pmatrix} 0 & 1 \\ -\frac{6}{c} T(z) & 0 \end{pmatrix}. \quad (4.24)$$

In principle the general solution of this set of ODEs can be written as an initial value problem

$$U(z) = \mathcal{P} \left\{ e^{\int^z dz' a(z')} \right\} U(0), \quad (4.25)$$

here \mathcal{P} designates the path-ordered integral. Hence the monodromy relevant for Lorentzian time-evolution is given by

$$M \sim \mathcal{P} \left\{ e^{\oint_{|z|=1} dz a(z)} \right\}, \quad (4.26)$$

here \sim indicates equal up to a similarity transformation. From the fact that $a(z)$ is always traceless we can establish the general property that the monodromy matrix M possesses unit determinant, i.e. as a matrix M is contained within the group $SL(2, \mathcal{C})$. In principle one can go further, the symmetric distribution of heavy operators and their adjoints around unit circle provides the following reflection property

$$T(z) = z^{-4} \overline{T(1/\bar{z})}. \quad (4.27)$$

As rather elegantly proved in [99], this property implies that in general the monodromy matrix M is up to a similarity transformation contained within the group $SU(1, 1)$. Since similarity transformation do not effect the eigenvalues this restricts the eigenvalues of M to be either pure phase or purely real (see figure 4.4). This divides M into one of three classes purely real eigenvalues, purely imaginary eigenvalues and two cross-over point at 1 and -1 where the eigenvalues are degenerate.

The path-ordered integral over the flat connection above has a natural interpretation in the Chern-Simons formulation of gravity in AdS_3 . We will exploit this interpretation in section 4.

4.3.1 Late-time behavior of the correlators

It is interesting to see what kind of algebraic effect the considerations of the previous section have on (4.3) in the late-time limit which is obtained by letting the probe correlator undergo a large number of cycles on the unit circle. Let us assume a basis of solutions that diagonalizes the monodromy matrix around the unit circle⁵. Since the monodromy has to have unit determinant, it only

⁵This can be done whenever the eigenvalues are non-degenerate, which are our cases of interest

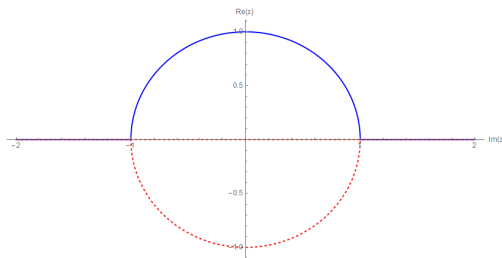


Figure 4.4: The restriction of the unit circle monodromy matrix to $SU(1,1)$ restricts the eigenvalues it can possess to be either purely real or pure phases. Since the eigenvalues are each others inverse $\lambda_1 = 1/\lambda_2$, the domain in which the eigenvalues can reside can be further split up into two independent domains indicated by the blue solid line and red dashed line.

has one free eigenvalue λ the other one has to be its inverse $1/\lambda$. After n cycles the general solution to the Fuchs equation will generically be given by

$$u\left(e^{2\pi i n} z\right)=\lambda^n c_1 u_1(z)+\lambda^{-n} c_2 u_2(z), \quad (4.28)$$

we here assume, without loss of generality, that $|\lambda| \geq |1/\lambda|$. There are two particular cases of interest. Either both eigenvalues are distinct and pure phase, in which case time-evolution in Lorentzian time will yield periodic correlation functions. The physical interpretation is that the system fails to collapse into a black hole and the heavy material will continue to oscillate forever around the center of AdS_3 . The monodromy falls into elliptic class by the classification in [100].

The second case is when $|\lambda| > 1$, which is most interesting scenario for us. Since n plays the role of a discretized time, the $u_1(z)$ mode acts as a stable mode, whereas $u_2(z)$ plays the role of a decaying mode. We find that the mode $u_1(z)$ should be given by a solution that corresponds to a BTZ black hole, since this is the situation that the collapse process should converge to at late times. Furthermore if both z_1 and z_2 make the same number of cycles the constant λ drops out of the correlator (4.3), corroborating the interpretation as a stable mode.

The eigenvalue is not purely a mathematical construct, it can be given a physical interpretation by considering the late-time limit. Consider $z_1 = e^{2\pi i n} z_0$; $z_2 = e^{2\pi i(n+m)} z_0$, where z_0 is some number on the unit circle on

the principle sheet and $n \gg 1$, the integer separation of the times is purely for notational convenience, we will take m to be large soon after which the remainder under a more general treatment would be a subdominant correction. By allowing z_2 to make a few more cycles compared to z_1 , corresponding to time-advancing $Q(z_2)$ we can obtain the following result for the correlator

$$\begin{aligned}
\langle O(x_1) \dots O(x_n) Q(z_1) Q(z_2(n)) \rangle &= u(z_1)^{-2h_Q} \lambda^{-2mh_Q} u(z_2)^{-2h_Q} \\
&\times \left(\int_{z_1}^{e^{2\pi i} z_1} u(z)^{-2} dz + \int_{e^{2\pi i} z_1}^{e^{4\pi i} z_1} \lambda^{-2} u(z)^{-2} dz + \dots + \int_{e^{2\pi i(m-1)z_1}}^{e^{2\pi i m} z_1} \lambda^{-2(m-1)} u(z)^{-2} dz \right)^{-2h_Q} \\
&= u(z_1)^{-2h_Q} u(z_2)^{-2h_Q} \lambda^{-2mh_Q} \left(\frac{\lambda^{-2m} - 1}{\lambda^{-2} - 1} \right)^{-2h_Q} \left(\int_{z_1}^{e^{2\pi i} z_1} u(z)^{-2} dz \right)^{-2h_Q}.
\end{aligned} \tag{4.29}$$

Hence as m becomes larger we note the approximate scaling law

$$\langle O(x_1) \dots O(x_n) Q(z_1) Q(z_2(m)) \rangle \sim \lambda^{-2mh_Q}. \tag{4.30}$$

It is worth noting that the scaling behavior is independent of n and only depends on the difference between the number of cycles which can be interpreted as the difference in time when the two operators are fixed at the same spatial point. Such a scaling relation at late times is suggestive of thermal behavior. In the upcoming sections we will support this observation by two separate arguments. Firstly we will demonstrate that when the eigenvalues are purely real we can construct a monodromy preserving diffeomorphism to a stress-energy tensor whose associated Fuchs equation can be solved.

Secondly we will demonstrate that the eigenvalue λ has a natural manifestation in the Chern-Simons formulation of $3d$ Einstein gravity, as being related to the temperature of the bulk black hole geometry associated to the boundary connection $a = \left(J_{-1} + \frac{6}{c} T(z) J_1 \right) dz$, where the J_i matrices are generators of $SL(2, \mathbb{R})$. Either way we will find out that the explicit relationship is given by

$$\log(|\lambda|) = 2\pi^2 T_{BH}, \tag{4.31}$$

with the black hole temperature T_{BH} . If we equate $2\pi m$ with time difference $(t_2 - t_1)$ we find the following asymptotic scaling

$$A_0(t_1, t_2) \sim e^{-2\pi h_Q T_{BH}(t_2 - t_1)}, \tag{4.32}$$

where we have put the two operators at the same spatial point. This is exactly the form of a thermal correlator with temperature T_{BH} . This provides our general conclusion, without strictly solving the Fuchs equation we find that at late Lorentzian time, under certain conditions, the probe correlator converges to a thermal correlator with a temperature identified with the temperature of the bulk theory black hole.

4.3.2 Monodromy preserving diffeomorphisms and their bulk interpretation as boundary gravitons

In this section we provide the first argument that the hyperbolic class of asymptotic Lorentzian correlators correspond to thermal black hole correlators. The proof provided here is the most straightforward of the two, but also the most abstract. As a consequence it clarifies that the bulk final state consists of a black hole dressed by boundary gravitons. Here we will exploit the fact that the stress-energy functions, $T(z)$ for which the associated Fuchs equations, (4.19) possess monodromy matrices around the unit circle with real eigenvalues must be contained within a specific Virasoro coadjoint orbit [101]. Different points in the orbit are related by conformal transformations. In the dual gravity picture, this orbit can be associated with a class of black hole solutions to the Einstein equations.

It is well-known that any asymptotically AdS_3 solution in the Fefferman-Graham gauge is given by the Banados geometries [102]

$$ds^2 = \frac{dr^2}{r^2} - \left(rdz - \frac{\bar{L}(\bar{z})}{r} d\bar{z} \right) \left(rd\bar{z} - \frac{L(z)}{r} dz \right), \quad (4.33)$$

where $L(z)$ and $\bar{L}(\bar{z})$ are single-valued functions related to the holomorphic and anti-holomorphic stress tensors of the boundary CFT. After fixing the Banados gauge there exists a residual symmetry that preserves the general form of this metric but changes the functions $L(z)$ and $\bar{L}(\bar{z})$. At $r \rightarrow \infty$ the vector fields generating these coordinate transformations are given by [103]

$$\zeta = \left(\xi(z) + \frac{1}{2r^2} \partial_z^2 \bar{\xi}(\bar{z}) \right) \partial_z + \left(\bar{\xi}(\bar{z}) + \frac{1}{2r^2} \partial_{\bar{z}}^2 \xi(z) \right) \partial_{\bar{z}} - \frac{r}{2} \left(\partial_z \xi(z) + \partial_{\bar{z}} \bar{\xi}(\bar{z}) \right) \partial_r. \quad (4.34)$$

The set of all these vector fields is parametrized by the two functions $\xi(z)$ and $\bar{\xi}(\bar{z})$. It was originally shown in [103] that under the infinitesimal coordinate

transformations generated by these vector fields the functions $L(z)$, $\bar{L}(\bar{z})$ transform according to the infinitesimal Virasoro Ward identity

$$\delta_\zeta L(z) = 2L(z)\partial_z \xi(z) + \xi(z)\partial_z L(z) - \frac{1}{2}\partial_z^3 \xi(z), \quad (4.35)$$

with a similar rule holding for $\bar{L}(\bar{z})$. From this it is natural to identify the functions parametrizing the Banados metric with the boundary stress tensor through $L(z) = \frac{c}{6}T(z)$. From this one can conclude that the dual description of (single-valued) conformal transformations is given by large diffeomorphisms⁶ that preserve the asymptotic boundary conditions of the AdS_3 . Hence stress tensors that are connected to each other through single-valued coordinate transformations correspond in the bulk to geometries that are related to each other through boundary gravitons.

Given a function $T(z)$ (correspondingly $L(z)$) it is natural to consider the set of all other functions $T(z)$ that can be obtained by single-valued conformal transformation. To remind ourselves the infinitesimal transformation law integrates to one of the form of (4.10), namely,

$$T(w) = \left(\frac{dz}{dw}\right)^2 T(z(w)) + \frac{c}{12}S[z(w), w], \quad (4.36)$$

for a finite conformal transformation. The orbits of $T(z)$ under all single-valued conformal transformations is directly related to the Virasoro coadjoint orbits discussed in the beginning of the section. The Virasoro orbits have all been classified in terms of the monodromy of the solutions Hills equation [104] (see table 4.1). Up to a change of variables Hill's equation is the Fuchs equation whose domain has been restricted to the unit circle. Each orbit is classified by a reference point, a function $T(z)$, usually of some convenient form, that can be reached by conformal transformation.

Of special interest are the the functions $T(z)$ that generate solutions to the Fuchs equation whose monodromy matrix has real eigenvalues, these coadjoint orbits contain a reference point that is the standard BTZ geometry [105–107]. From the CFT perspective this reference point corresponds to a stress tensor expectation value associated to a state created by acting on the vacuum with a primary operator whose scaling dimension satisfies $H > c/12$.

⁶Large in the sense that they do not drop off fast enough at infinity.

Class	eigenvalues	Coadjoint orbit	dual geometry
Elliptic	pure phase ($\lambda \neq 1, -1$)	\mathcal{C}_ν $0 < \nu < 1$	Conical defect
Parabolic	$\lambda = 1$ or -1	$\mathcal{P}_0^+, \mathcal{P}_1^-$	minimal mass BTZ
Hyperbolic	purely real	$\mathcal{B}_0(b)$	BTZ black hole
Exceptional	$\lambda = 1,$	\mathcal{E}_1	Vacuum

Table 4.1: A characterisation of the relevant monodromy classes their associated Virasoro coadjoint orbit and the geometry of the holographic dual. (following [104], [100])

From the boundary CFT perspective it is not entirely obvious that the generic stress tensor we are considering is contained within an orbit that contains as a reference point a stress tensor associated to a state created by a single primary operator. First of all, it would naively be expected that a generic heavy CFT state would correspond to a linear combination of energy eigenstates. However, on the other hand, the existence of the BTZ reference point suggests that even a generic heavy stress energy function is dominated by contributions coming from a single conformal family. These two apparently conflicting CFT statements can actually be justified in the large c limit.

Let us now provide some heuristic arguments to help obtain some scaling laws for the energy of the heavy states under consideration. These scaling laws provide us some intuition that we have applied in section 3 and 5 of the main body of the text. We will assume that if the separation of a mirror pair σ is very small that the gravitational binding energy between mirror pairs is negligible in the gravitational dual in the weak gravity regime. Therefore we expect that the total energy of a heavy state is proportional to the sum of energies of the isolated mirror pairs. The stress tensor wavefunction of a single mirror pair is given by a conformal three-point function and can therefore be calculated explicitly

$$\langle O(1+\sigma)T(z)O(1-\sigma) \rangle = \frac{H}{((1-z)^2 - \sigma^2)^2 (2\sigma)^{2H-2}},$$

note that we have implicitly assumed $\sigma \ll 1$. From this we find the expectation value

$$\langle T(z) \rangle = \frac{\langle O(1+\sigma)T(z)O(1-\sigma) \rangle}{\langle O(1+\sigma)O(1-\sigma) \rangle} = \frac{4H\sigma^2}{((1-z)^2 - \sigma^2)^2}.$$

We see that the energy is peaked around $z = 1$ with a value given by $\frac{4H}{\sigma^2}$, which drops off as z^{-4} as z goes to infinity, as we expect from a stress-energy tensor expectation value. The expression above will lead to the energy density of the state created by acting with the heavy operators. The following trick can be used to obtain the energy over the full Cauchy slice. First we map to the Euclidean cylinder

$$\begin{aligned}\langle O(1+\sigma)O(1-\sigma) \rangle &= e^{H \log(1+\sigma) + H \log(1-\sigma)} \langle O(\log(1+\sigma))O(\log(1-\sigma)) \rangle \\ &\sim \langle O(\sigma)O(-\sigma) \rangle,\end{aligned}$$

where we dropped all terms of order $\mathcal{O}(\sigma^2)$. After Wick rotating to Lorentzian signature

$$\langle O(i\sigma)O(-i\sigma) \rangle = \langle e^{-i(i\sigma)H} O e^{i(i\sigma)H} e^{-i(-i\sigma)H} O e^{i(-i\sigma)H} \rangle = \langle O e^{-2\sigma H} O \rangle,$$

we can compute the total energy simply taking a derivative

$$\frac{\langle OHO \rangle}{\langle OO \rangle} = \frac{-\frac{1}{2} \frac{d}{d\sigma} \langle O(i\sigma)O(-i\sigma) \rangle}{\langle O(i\sigma)O(-i\sigma) \rangle} = \frac{H}{\sigma}.$$

This expression is similar to the one in [84], note that it is only valid when σ is small. We can simply take the second-derivative to find the expectation value of the Hamiltonian squared

$$\frac{\langle OH^2O \rangle}{\langle OO \rangle} = \frac{H(2H+1)}{2\sigma^2}.$$

The standard deviation of the energy of the state is given by

$$\Delta E = \sqrt{\langle E^2 \rangle - \langle E \rangle^2} = \sqrt{\frac{H}{2\sigma^2}}.$$

This implies that our typical state has an energy variance that is wide enough for incorporating features like non-trivial quantum Poincaré recurrences. While $\frac{\Delta E}{E} = \frac{1}{\sqrt{2H}}$ is sufficiently small as to think of our resulting final state as a stationary black hole. As the energy of our state increases the variance in the energy increases as well. However, the variance increases parametrically less fast than the expectation value ($\sqrt{nh/\sigma}$ as opposed to nh/σ). As one can check, for a heavy state with an energy expectation at least of the order of the central charge the energy distribution can be well approximated as being

sharply peaked. This is of course directly analogous to the intuition of the eigenstate thermalisation hypothesis [83]. Therefore the general expectation is that a pure state created by acting with the heavy primary operators on the vacuum is dominated by the contribution of a single energy eigenstate.

Secondly, of course, a generic $T(z)$ does not correspond to a primary state, in fact in general it will be a generic element of the Virasoro orbit associated to a primary state. In principle all states within a Virasoro orbit are connected to each other by conformal transformations. So it remains to determine which primary state is associated to the conformal family that our heavy state $|V\rangle$ actually belongs to. This primary state should be related to our heavy state by some judiciously chosen single-valued conformal transformation [108]. The Fuchs equation mirrors this picture; the conjugacy class of the monodromy matrix around the unit circle remains invariant under the group of orientation preserving diffeomorphisms of the circle $\text{Diff}_0(S^1)$ [104]. This is due to the eigenvalue being related to the scaling weight of the primary state and is hence an orbit invariant. We will now construct an element of $\text{Diff}_0(S^1)$ similar to the one in [104] that brings us to the stress-energy tensor of a single primary operator inserted at the origin with a specific scaling dimension. We can connect to the intuition above by interpreting the diffeomorphism as the transformation that undoes the boundary gravitons. The Fuchs equation is given by

$$\psi''(z) + \frac{6}{c}T(z)\psi(z) = 0. \quad (4.37)$$

We assume that $T(z)$ is such that the monodromy along the unit circle of solutions falls in the hyperbolic class corresponding to real eigenvalues with $|\lambda| > 1$. A complete classification of the monodromy matrices is presented in Table 4.1. Consider the eigenbasis of solutions under the monodromy transformation along the unit circle

$$\psi_1(e^{2\pi i}z) = \lambda\psi_1(z), \quad \psi_2(e^{2\pi i}z) = \frac{1}{\lambda}\psi_2(z). \quad (4.38)$$

In this case it is clear that the ratio of these two solutions $f(z) = \psi_1(z)/\psi_2(z)$ has the following transformation property

$$f(e^{2\pi i}z) = \lambda^2 f(z). \quad (4.39)$$

From this transformation rule we can construct a function that is inherently single-valued on the unit circle

$$u(z) = e^{\frac{i\pi}{\gamma} \log(f(z))} = f(z)^{\frac{i\pi}{\gamma}}, \quad (4.40)$$

since this function simply adds a term $2\pi i$ to the exponent after making a full circle. Here γ is defined by $\gamma = \log(|\lambda|)$. To prove that the function above is an element of $\text{Diff}_0(S^1)$ we need to show further that it is smooth everywhere on the unit circle. The assumption that our stress-energy tensor is an element of a hyperbolic orbit and that the zero-mode of the stress-energy tensor is bounded from below restricts the orbit to the coadjoint orbit $B_0(b)$, as per the classification given in [104, 108]. The complete classification is briefly summarised in Table 4.1. It is known that if $T(z)$ is contained within $B_0(b)$, the eigenbasis of solutions to the Fuchs equations has no roots along the unit circle [106, 107]. This implies that the ratio of solutions $f(z)$ is forced to be smooth on the unit circle. Therefore we can conclude that $u(z) \in \text{Diff}_0(S^1)$. Next, with some algebra we will show that this function, $u(z)$ has a desirable property.

Taking the Schwarzian derivative of $u(z)$ and making use of the group structure of the Schwarzian derivative gives

$$S[u(f(z)), z] = S[f, z] + \left(\frac{df}{dz}\right)^2 S[u, f]. \quad (4.41)$$

From the theory of Fuchs equations we know that under the Wronskian normalization condition $\psi_2(z)\psi_1'(z) - \psi_1(z)\psi_2'(z) = 1$ the following identity holds

$$S[f, z] = \frac{12}{c} T(z), \quad (4.42)$$

in fact it is the inverted version of the Schwarzian ODE we started with. Inserting this identity in (4.41) and rearranging the terms a little bit yields

$$\begin{aligned} T(z) &= \left(\frac{du}{dz}\right)^2 \frac{c}{24\pi^2} (\gamma^2 + \pi^2) u(z)^{-2} + \frac{c}{12} S[u, z] \\ &\equiv \left(\frac{du}{dz}\right)^2 \tilde{H} u(z)^{-2} + \frac{c}{12} S[u, z] \end{aligned} \quad (4.43)$$

This is, therefore, exactly the coordinate transformation that yields a uniform stress-tensor component of the form \tilde{H}/u^2 , where the role of the scaling dimension is now played by

$$\tilde{H} \leftrightarrow \frac{c}{24\pi^2} (\gamma^2 + \pi^2), \quad (4.44)$$

Note that the scaling dimension has a minimum value given by $c/24$, this is enforced by the initial assumption that we are in a hyperbolic monodromy class, the minimum value corresponds to the zero mass BTZ state in the bulk. Given the primary stress-energy tensor the monodromy matrix can be computed by explicitly calculating the path-ordered integral [109]. But the associated Fuchs equation can also be solved explicitly. In fact in [21] the authors found uniformized correlator associated to these solutions and find that they produce a thermal correlator with temperature $T_H = \frac{1}{2\pi} \sqrt{24H/c - 1}$, inserting (4.44) and reinstating λ through $\gamma = \log(|\lambda|)$ gives us the relationship

$$|\lambda| = e^{2\pi^2 T_H}, \quad (4.45)$$

quoted in the previous section.

4.4 Chern-Simons interpretation of the monodromy

As shown in the previous section, the late-time behavior of the probe correlation function is controlled by a monodromy matrix. In this section we will demonstrate that this matrix has a natural manifestation in the Chern-Simons formulation of $3d$ gravity. The discussion in this section is heavily based on [109], additional references include [108, 110–112]. The topological nature of $3d$ gravity is most clearly expressed in terms of $so(2,2)$ connection field A [113],

$$\mathbf{A}_i = e_i^a \mathbf{P}_a + \omega_i^a \mathbf{J}_a,$$

here e_i^a and ω_i^a are respectively the vielbein and the spin connection associated to the Einstein-Hilbert action. P_a and J_a denote generators for translation and Lorentz transformations respectively. After imposing that A transforms as a non-abelian gauge field under local $SO(2,2)$ transformations it can be shown that the Chern-Simons action

$$S_{CS}[\mathbf{A}] = \frac{k}{4\pi} \int \text{Tr} \left(\mathbf{A} \wedge d\mathbf{A} + \frac{2}{3} \mathbf{A} \wedge \mathbf{A} \wedge \mathbf{A} \right),$$

is equivalent to the Einstein-Hilbert action with negative cosmological constant. The constant k is the level of the Chern-Simons theory. By means of the Brown-Henneaux formula it can be related to the central charge through $k = \frac{c}{6}$. It turns out to be convenient sometimes to use the decomposition of the gauge

group $SO(2, 2)$ as $SL(2, \mathbb{R}) \times SL(2, \mathbb{R})$. The connection field \mathbf{A} , accordingly, also assumes a decomposition in terms of a pair of $SL(2, \mathbb{R})$ connections, $\{A, \bar{A}\}$ defined as

$$A_i = \left(\omega_i^a + \frac{1}{R} e_i^a \right) J_a^{(+)} \\ \bar{A}_i = \left(\omega_i^a - \frac{1}{R} e_i^a \right) J_a^{(-)}$$

where $J_a^{(\pm)} = \frac{1}{2} (J_a \pm RP_a)$. With this decomposition the Einstein Hilbert action takes the form

$$S_{\text{EH}} = S_{\text{CS}}[A] - S_{\text{CS}}[\bar{A}],$$

and the constant, R gets a natural interpretation as the radius of the AdS_3 .

4.4.1 Wilson loops in Chern-Simons theory

In [109] Wilson lines were considered as geometrical probes for the bulk gravitational theory which act as the Chern-Simons analogue of massive probe particles traveling along geodesics in the bulk geometry. To make this statement quantitative

$$W_{\mathcal{R}}(C) \sim e^{-mL},$$

the \sim designates that this is an on-shell relation. Here C designates the curve along which the Wilson line is defined on the boundary of AdS_3 . m is the mass of the relevant probe and L as the proper length of the geodesic connecting the endpoints of the Wilson line supported at the boundary. The subscript \mathcal{R} denotes the $SL(2, \mathbb{R})$ representation in which the Wilson line falls. In order to allow for a continuous mass parameter for the probe the representation needs to be infinite dimensional, e.g. the highest weight representation of $SL(2, \mathbb{R})$ [109]. As we will find, the relation to the geodesic length, L stated above will turn out to be extremely useful. Given an appropriate bulk geodesic, this length will be interpreted as the horizon of the diffeomorphism-equivalent black hole which in turn is to its temperature by means of the Bekenstein-hawking formula.

The key point of [109] is that the expectation value of the Wilson line is given by the path integral over the following action

$$S(U, P, A, \bar{A})_C = \int_C ds \text{Tr}(PU^{-1}D_s U) + \lambda(s) \left(\text{Tr}(P^2) - \frac{1}{2}m^2 \right).$$

The Hilbert space of the quantum system described by the auxiliary field U and its conjugate momentum P corresponds to the vector space given by the carrier space of an infinite dimensional representation of $SL(2, \mathbb{R})$. s parametrizes the curve, C and D_s denotes covariant derivative with respect to s , defined as

$$D_s U = \frac{dU}{ds} + A_s U - U \bar{A}_s, \quad A_s \equiv A_\mu \frac{dx^\mu}{ds}.$$

We can choose the field U to live in the fundamental representation, this way we will connect to our monodromy matrix. Note that we are only integrating over the auxiliary fields and consider the Chern-Simons field A as a background field which fixes the background geometry. As a consequence, the probe mass can take any real positive value without affecting the dynamics. The equations of motion of this action are

$$U^{-1} D_s U + 2\lambda(s)P = 0, \quad \partial_s P + [\bar{A}_s, P] = 0,$$

while the Lagrange multiplier $\lambda(s)$ imposes the constraint

$$\text{Tr}(P^2) = \frac{1}{2}m^2.$$

On shell, the action reduces to a very simple form

$$S_{\text{on-shell}} = -m^2 \int_C ds \lambda(s).$$

When solving the equations of motion it is natural to define the function $\alpha(s)$ through $d\alpha/ds = \lambda(s)$. In this case the action simply becomes

$$S_{\text{on-shell}} = -m^2 \Delta\alpha,$$

the point is now clear, we need to solve for $\Delta\alpha$ and equate it to L/m . Note that $\Delta\alpha$ only depends on the endpoints of the curve. We will show below that knowledge of the boundary conditions is sufficient to solve for $\Delta\alpha$.

4.4.2 The nothingness trick

We will here follow steps very similar to those presented in [109]. The equations of motion are simple to solve in the ‘empty gauge’, i.e. $A = \bar{A} = 0$, so we will solve the equations of motion in that particular gauge and then gauge transform

the resulting solution to generate more solutions. One could ask, how many solutions are gauge connected to the empty gauge? The answer is that the bulk equation of motion of Chern-Simons theory imposes that A is locally flat, hence all solutions to the Einstein field equations have an associated connection field A that is gauge connected to the empty gauge. These gauge transformations will, however, be multivalued in general.

In the empty gauge the equations of motion are given by

$$U_0(s)^{-1}\partial_s U_0(s) + 2\lambda(s)P_0(s) = 0, \quad \partial_s P_0 = 0.$$

These equations are easily solved, their general solutions are given by

$$U_0(s) = u_0 e^{-2\alpha(s)P_0}, \quad P_0(s) = P_0,$$

here as before $d\alpha/ds = \lambda(s)$. Under $SL(2, \mathbb{R}) \times SL(2, \mathbb{R})$ gauge transformations the auxiliary field variables transform as

$$U(s) \rightarrow L(s)U(s)R(s), \quad P(s) \rightarrow R^{-1}(s)P(s)R(s), \quad (4.46)$$

where $L(s)$ and $R(s)$ are elements of the fundamental representation of $SL(2, \mathbb{R})$. In order to obtain the gauge transformation that brings us to the required connection, we need to find a transformation L and R such that

$$LdL^{-1} = A = b^{-1}ab + b^{-1}db = b^{-1} \begin{pmatrix} 0 & 1 \\ -\frac{6}{c}T(z) & 0 \end{pmatrix} b + b^{-1}db,$$

and similarly

$$R^{-1}dR = \bar{A} = b^{-1} \begin{pmatrix} 0 & 1 \\ -\frac{6}{c}\bar{T}(\bar{z}) & 0 \end{pmatrix} b + b^{-1}db.$$

Here a is the boundary connection defined as $a = \left(J_{-1} + \frac{6}{c}T(z)J_1\right) dz$. It is related to the full connection through $A = b^{-1}(a + d)b$, with $b = e^{\rho J_0}$. J_i denote $SL(2, \mathbb{R})$ generators with $i = \{1, 0, -1\}$. With some simple algebra it can be shown that a solution to the differential equation for L is given by

$$L = e^{-\rho J_0} \mathcal{P} \left\{ e^{-\int_0^s a(z) ds} \right\}. \quad (4.47)$$

One can similarly demonstrate that

$$R = \mathcal{P} \left\{ e^{\int_0^{s_f} \bar{a}(\bar{z}) ds} \right\} e^{-\rho J_0}. \quad (4.48)$$

We know what gauge transformation we want, the trick will be to apply it to the boundary conditions of the field variables. We are interested in Wilson loops (i.e. we want to find a geodesic that closes in on itself), therefore we have to impose periodic boundary conditions to the field variables

$$U(0) = U(s_f), \quad P(0) = P(s_f).$$

Using the gauge transformation (4.46) the boundary condition for P gives us

$$\left[P_0, R(s_f) R^{-1}(0) \right] = 0. \quad (4.49)$$

This condition implies that P_0 commutes with the path-ordered integral over the right-moving boundary gauge component. Similarly working out the boundary condition on U gives us

$$u_0^{-1} L(s_f)^{-1} L(0) u_0 R(0) R(s_f)^{-1}, \quad (4.50)$$

where as an intermediate step we used the fact above that P_0 commutes with the product $R(s_f) R^{-1}(0)$. Plugging (4.47) and (4.48) in (4.50) yields

$$e^{-2\Delta\alpha P_0} = u_0^{-1} M u_0 \bar{M}^{-1}, \quad (4.51)$$

Here M is the same matrix as the monodromy matrix M defined in (4.26) in section 3. \bar{M} is defined in an analogous way as the path-ordered integral over \bar{A} . Due to our restriction to scalar heavy operators (i.e. $\bar{h} = h$) the barred path-ordered integral gives

$$\bar{M} = \mathcal{P} \left\{ \exp \left(\oint \bar{a} \left(\bar{T}(\bar{z}) \right) ds \right) \right\} = \mathcal{P} \left\{ \exp \left(\oint a \left(T(\bar{z}) \right) ds \right) \right\} = M^{-1},$$

the physical reason for this being that from the perspective of the anti-holomorphic variable \bar{z} the contour is followed with the opposite orientation, hence

$$e^{-2\Delta\alpha P_0} = u_0^{-1} M u_0 M.$$

We can use (4.49) to simultaneously diagonalize the left- and right-hand side. Denoting the matrix that diagonalizes them by V ,

$$e^{-2\Delta\alpha P_0} = (u_0 V)^{-1} M (u_0 V) \bar{M}^{-1}.$$

As pointed out in [109], consistency between the left- and the right-hand side demands that $(u_0 V)^{-1} M (u_0 V)$ is a diagonal matrix. Therefore we can make the above expression cleaner by defining λ_M to be the diagonal matrix whose components are the eigenvalues of M

$$e^{-2\Delta\alpha P_0} = \lambda_M^2.$$

We can take the matrix logarithm on both sides, since all matrices involved are diagonal this reduces to the logarithms of the components

$$-\Delta\alpha P_0 = \log(\lambda_M) = \begin{pmatrix} \log(|\lambda|) & 0 \\ 0 & -\log(|\lambda|) \end{pmatrix}.$$

We know $\text{Tr}(P_0) = 0$ because it has to live in the Lie algebra of $SL(2, \mathbb{R})$. Then from the constraint $\text{Tr}(P_0^2) = \frac{1}{2}m^2$, the eigenvalues of P_0 are given by $\pm m/2$. Contracting both sides with the matrix

$$J_0 = \begin{pmatrix} \frac{1}{2} & 0 \\ 0 & -\frac{1}{2} \end{pmatrix}$$

gives us

$$-\frac{m}{2}\Delta\alpha = \log(|\lambda|).$$

Inserting the expression $\Delta\alpha = -L/m$ yields

$$\log(|\lambda|) = \frac{1}{2}L.$$

As mentioned before, we assume that this L is the proper length of the geodesic connecting the endpoints of the Wilson loop. Due to the topological nature of 3d gravity we can perform gauge transformations that correspond to continuously deforming the contour, the argument is that if there is a black hole in AdS_3 we can only continuously deform a contour to a minimum size measured by the holonomy. Hence L measures the proper size of the horizon of black hole in the center of AdS_3 . Making use of the Bekenstein-Hawking formule $S = A/4G$ and the Brown-Henneaux formula $c = \frac{3}{2G}$ finally gives us

$$\log(|\lambda|) = 2\pi^2 T_H.$$

This is the relationship between the eigenvalues of the monodromy matrix M and the temperature of the final state bulk black hole claimed in (4.31).

4.5 An example and numerical black holes with soft gravitational hair

In the preceding section it was established that the eigenvalues of a certain monodromy matrix govern the late Lorentzian time behavior of probe correlation functions. In this section we will first consider an example, which is the smooth limit considered in [84], the reason being that for this particular stress-energy tensor the monodromy matrix can be computed explicitly. In particular we will be able to see the transition from conical defect to black hole.

Secondly we perform a numerical analysis of the monodromy problem for various operator distributions and demonstrate that there can exist a deficiency between the initial energy injected in the bulk and the mass of the final black hole state. We interpret this deficiency as a fraction of the initial energy being frozen out in boundary gravitons, conserved charges associated with the asymptotic Brown-Henneaux Virasoro algebra of AdS_3 .

4.5.1 The continuous limit as an example

One particular state in which the monodromy matrix can be computed explicitly is the isotropically collapsing shell of null dust constructed in [84]. This smooth limit for the initial and final states was studied in [84], where the number of insertions is taken to infinity, which leads to a simpler expression of the stress tensor. It is an example where the thermalization of a Lorentzian correlator can be shown explicitly. It closely resembles an eternal black hole state. The state on which the correlator is evaluated is given by

$$|V\rangle = \lim_{n \rightarrow \infty} \frac{1}{\mathcal{N}} \prod_{k=1}^n O(e_k) |0\rangle, \quad e_k = (1 - \sigma) e^{2\pi i(k-1)/n}.$$

In the aforementioned paper it was shown that the stress-energy wave function for this particular state can be written as

$$T(z) = \frac{K}{z^2} \Theta(|z| - 1 + \sigma) \theta(1 - |z| + \sigma),$$

where K is a constant related to the CFT data through $K = \frac{H}{\sigma}$ and $\theta(z)$ denotes the heavyside function. It can easily be checked that this state has

no gravitational hair, the reason being that along the unit circle stress-energy tensor takes the form of the lowest energy element of either a $\mathcal{B}_0(b)$ or \mathcal{C}_ν Virasoro coadjoint orbit [104]. The stress tensor above is very similar to the one of an eternal black hole, the difference is the compact support of the above stress-energy tensor. For any cycle contained within the annulus the only visible pole would be the double pole located at $z = 0$, for this reason it is possible to explicitly solve the path-ordered integral in (4.26) in a straightforward manner. Inserting this stress-energy wave function into the flat connection (4.24) gives

$$a(z) = \begin{pmatrix} 0 & 1 \\ -\frac{6K}{cz^2} & 0 \end{pmatrix}.$$

The relevant information contained in the monodromy matrix are its eigenvalues. Hence we are only interested in its conjugacy class. We only need the connection up to an $\text{SL}(2, \mathbb{C})$ gauge transformation. There exists a theorem that states that there always exists a gauge transformation such that around a singular point z_0 of $A(z)$ the connection can be transformed to a new connection $a(z) \rightarrow (z - z_0)^{-1-R_0} a_0(z)$, where the matrix elements of $a_0(z)$ are all regular functions of z [88] [114]. The integer power R_0 is the Poincaré rank of the singular point, $R_0 = 0$ corresponds to a regular singular point. The connection transforms under a gauge transformation in the usual way

$$a(z) \rightarrow U a U^{-1} + \left(\frac{d}{dz} U \right) U^{-1},$$

a simple proposal for a gauge transformation that brings the connection to minimal form is the matrix that locally diagonalizes the connection $A(z)$, specifically

$$U(z) = \begin{pmatrix} -\frac{\sqrt{-\frac{3K}{2c}}}{z} & \frac{1}{2} \\ \frac{\sqrt{-\frac{3K}{2c}}}{z} & \frac{1}{2} \end{pmatrix},$$

this matrix is the inverse of the matrix of eigenvectors of $a(z)$. Under this transformation it can be found that the irregular part in z (and in fact all z -dependence) factors out of the connection. The resulting path-ordered integral can be resolved by means of the following identity [88]

$$M = P \left\{ e^{\oint dz \frac{1}{z} a_0(z)} \right\} = e^{2\pi i a_0(0)}.$$

The heuristic argument is that one can continuously deform the contour to a limiting circle around a pole, at which point the diagonalizing matrix becomes

exactly constant, subsequently rendering the path-ordered integral into a normal matrix integral. Unfortunately this particular approach does not generalize to multiple poles in a straight-forward manner, since one would need to consider integrating along paths connecting the poles. The eigenvalues of $2\pi i a_0(0)$ are given by

$$\{\lambda\} = i\pi \pm \pi \sqrt{\frac{24K}{c} - 1},$$

from which we can conclude that

$$\{\lambda\}_M = -e^{\pm \pi \sqrt{\frac{24K}{c} - 1}}.$$

In [84] it was established that $T_{BH} = \frac{1}{2\pi} \sqrt{24K/c - 1}$ therefore these eigenvalues are of the form derived in the previous sections. Which is exactly what was predicted above. One can observe both the the BTZ-mass threshold as well as the thermal behavior of the correlator at late time. This result is consistent with the statement made before that exact knowledge of the solutions of the Fuchs equation is over excessive for the purpose of finding the thermodynamic properties of the black hole at late time. Note that the analysis would have been identical for a state created by acting with a single primary operator at the origin on the vacuum.

4.5.2 Numerical results including soft gravitational hair

Solving the path-ordered integral in a general set-up is as mentioned in the previous section generically intractable. But since the path-ordered integral is the formal solution of an initial-value problem it is possible to draw some conclusions from numerical integration.

One potentially confusing aspect we will focus on is that there can be very large deviations between the initial energy injected into the system and the mass of the final black hole state. We denote by T'_H the temperature of a black hole in the hypothetical situation that all initial energy is converted into black hole rest mass. Using the Bekenstein-Hawking formula for a non-rotational black hole [115]

$$S = \frac{2}{3} \pi^2 c T'_H,$$

one can relate the temperature of the black hole to the Lorentzian energy $T_H = \frac{\sqrt{3}}{\pi} \sqrt{E_L/c}$, where the Lorentzian energy on the cylinder is given by

$$\frac{1}{2}E_L = \frac{1}{2\pi i} \left(-i \frac{\pi c}{12} + \oint dz z T(z) \right),$$

where the first term is the Casimir energy of the cylinder, which is also the minimal mass of the black hole [115]. The factor $1/2$ on the left-hand side is to emphasize that one has to add the identical holomorphic and anti-holomorphic contributions. Combining the above with the expression for the eigenvalues 4.31 one finds that these are given by

$$|\lambda'_{\pm}| = e^{\pm 2\sqrt{3}\pi \sqrt{\frac{1}{i\pi c} (\oint dz z T(z)) - \frac{1}{12}}},$$

in the case that all initial energy is converted into black hole mass at late time. The eigenvalues are pure phase, when the contour integral gives a value smaller than the minimal black hole mass, degenerate at the transition point ($\lambda = 1$), and real and greater than one in the black hole phase. This picture is misleading though as generally not all energy is converted to black hole mass. If sufficient energy is present to form a minimal black hole, it is not necessarily true that thermalization has to take over at late time [108]. The irregular part of the stress tensor expectation value is partially fixed by conformal invariance. Given a state in the semi-classical limit created by acting with n primary operators on the vacuum the stress-tensor is given by

$$T(z) = \sum_{j=0}^{n-1} \left(\frac{h_j}{(z - z_j)^2} + \frac{h_j}{(z - 1/\bar{z}_j)^2} + \frac{x_j}{z - z_j} + \frac{y_j}{z - 1/\bar{z}_j} \right) + \text{regular terms.} \quad (4.52)$$

where h_j are the scaling dimensions of the operators insertions and x_j and y_j are accessory parameters that generally depend on the dynamical data of the theory. To simplify the computations we will assume that the scaling dimensions of all operators are equal and real, so $h_j = h$. The accessory parameters satisfy

the following constraint equations to ensure that there is no pole at infinity

$$\begin{aligned}
2h + x_j z_j + \frac{\bar{y}_j}{z_j} &= 0 \\
\sum_{j=0}^{n-1} (x_j + y_j) &= 0 \\
\sum_{j=0}^{n-1} \text{Im}(x_j z_j + \frac{\bar{y}_j}{z_i}) &= 0.
\end{aligned}$$

As mentioned in a previous section, in [99] it was shown that these constraints imply the reflection symmetry $z^2 T(z) = \frac{1}{z^2} \bar{T}(1/z)$.

In the following section we will assume that the insertions are evenly distributed around the circle. Without loss of generality we take $|z| = 1 - \sigma$. In this case the $2n$ accessory parameters x_j and y_j can be expressed in terms of one free accessory parameter x as follows

$$\begin{aligned}
x_j &= e^{-\frac{j2\pi i}{n}} x \\
y_j &= -(2h + x(1 - \sigma))(1 - \sigma)e^{-\frac{j2\pi i}{n}}.
\end{aligned}$$

Colliding n clusters to form a black hole

There is interesting physics that can be studied when we move away from the smooth limit, which is analytically accessible. Therefore in this section we present a short numerical study of a set of such states. We will assume identical pairs of operators that are evenly distributed along the unit circle.

The free accessory parameter x is fixed by demanding a trivial monodromy around a mirror pair of insertions z_i and $1/\bar{z}_i$, depicted by the small red circle 4.5a. Given the reflection property of the Fuchs equation, the following two monodromy problems are equivalent; either you fix your accessory parameters such that the monodromy around a mirror pair is trivial or you fix your accessory parameters such that any cycle around a single regular singular point yields a monodromy that falls within $SU(1,1)$. Given the reflection property of $T(z)$ it was shown by [99] that there exists a basis of solutions with the property that their ratio satisfies the same reflection property. From this, combined with the conjugacy class of M being contained within $SU(1,1)$ it was shown

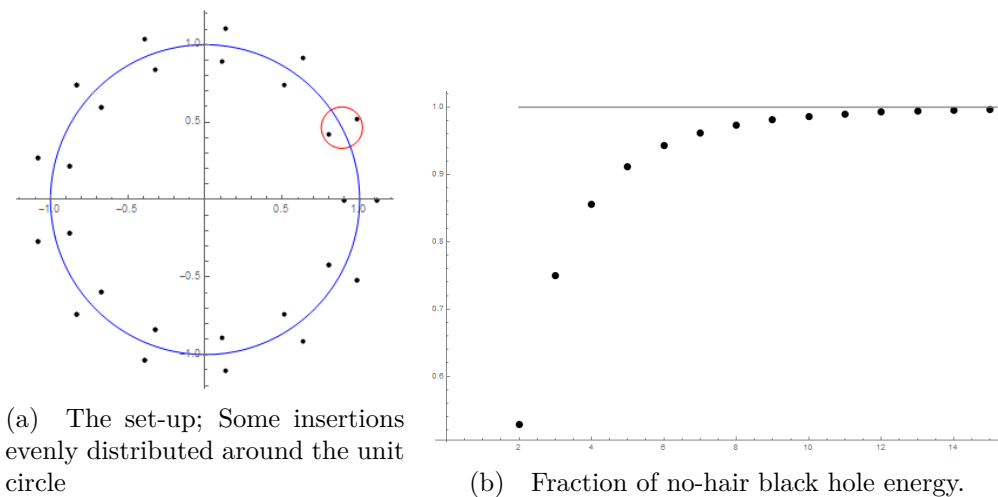


Figure 4.5: Colliding multiple conical defects.

that the monodromy of this pair of solutions around a mirror pair is trivial. Since the monodromy is a basis independent property this concluded the proof that the monodromy around a mirror pair is trivial. For an extensive proof of this statement we refer to [99]. This demand fully determines the irregular part of the stress tensor and hence it is a well-defined problem to compute the monodromy around the unit circle. Numerically integrating the connection field and determining its eigenvalue yields the mass of the black hole. In figure 4.5b one can see the fraction of energy stored in the black hole as a function of the number of regularly distributed insertions on a polygon, which was taken from two to fifteen. As the number of insertions increases the fraction goes to one, and it approaches the energy of the black hole that was created by a single primary acting at the origin. In this set-up the total energy $E \sim \frac{hn}{\sigma}$ that is injected was kept constant.

For two colliding conical defects about half the energy is stored in boundary gravitons. Note that as the number of conical defects increases the amount of deficient energy decays rapidly. For the regularly distributed conical defects the resulting black hole is expected to be at rest in the Fefferman-Graham gauge. Note that we obtain the expected result that as we increase the number of conical defects we converge to the situation of rotational symmetry discussed in [84].

Non spherically symmetric distributions

In figure 4.6a the set-up is displayed after relaxing the constraint of even distribution this will have the effect simulating oblique scattering. The first mirror pair is kept fixed at $\phi = 0$ and a second pair is placed at an angle ϕ , after which the eigenvalue is computed using the same procedure as described above. The eigenvalues were computed for angles varying from $\frac{\pi}{18}$ to π .

In 4.6b the mass of the late time black hole, divided by the energy of the initial state is plotted for a collision angle varying from $\frac{\pi}{18}$ to π . It is expected that these asymmetrical states lead to an oscillating black hole in the bulk, partially explaining the small fraction of energy in the black hole. At the level of the algebra there is no distinction between the energy stored in momentum or the energy stored in other conserved spacetime symmetry charges that we call boundary gravitons. For small collision angles $\phi < \frac{\pi}{6}$ the black hole threshold is not exceeded. This could be interpreted as two conical defects in stable orbits in the bulk, or a merger of two defects into one oscillating one.

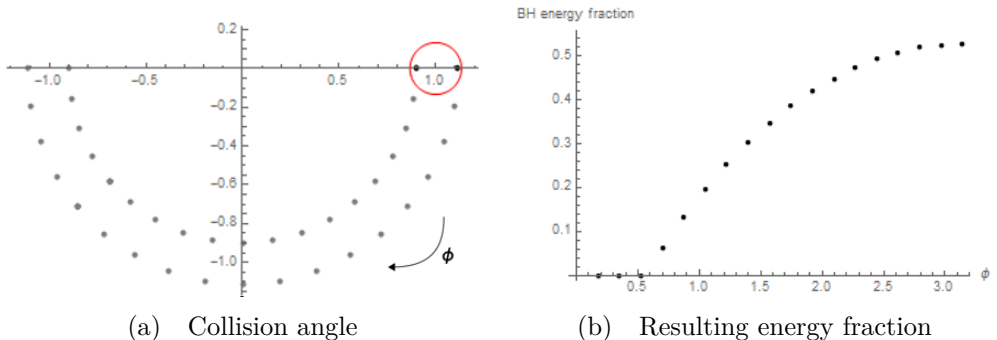


Figure 4.6: Colliding two conical defects under different angles.

4.6 Conclusion and discussion

In this chapter we considered probe correlation functions on an arbitrary “heavy state” in 2d conformal field theory. In particular we studied the conditions under which the late time behavior of the vacuum block contribution of these

correlators is indistinguishable from a thermal correlator. In the dual gravity picture this corresponds to the gravitational interaction of mass defects in AdS_3 which eventually, at a late Lorentzian time, collapses in a black hole spacetime, characterized by its Hawking temperature. In the CFT_2 picture this heavy state was created through insertions of a small number of heavy primary operators whose conformal dimensions scale with the central charge, c in the large c limit. The distribution of the operator on the radial plane was kept arbitrary.

For similar states created by a uniform distribution of a large ($n \rightarrow \infty$) number of operators, one can obtain systematic expansions of correlators of the form $\mathcal{A} = \langle V|Q(z_1)Q(z_2)|V \rangle$ as a power series in $\frac{1}{c}$ using monodromy methods for the dominant conformal block. The $O(1)$ contribution corresponds to the semi-classical limit which at late Lorentzian time yields thermal correlators. The same conformal blocks can also be obtained for background states created by finite number of heavy operators using “uniformization techniques”. Although this technique works in principle for any finite number of operator insertions, it becomes a daunting task to explicitly find the uniformization coordinates as the number of operators increases. On the other hand in order to obtain a thermal collapse state dual to a black hole, one needs at least four heavy operators to create the initial heavy state. This technical obstacle is related to the fact that in order to obtain the uniformization coordinates, one needs to solve a differential equation of Fuchsian class. For four or more insertions these equations do not possess known explicit analytic solutions (except for some very specific choices of parameters which do not fit our particular need).

The main statement of this chapter is that in order to extract the semi-classical thermal behavior of correlators at late Lorentzian time, one can actually bypass the requirement of solving the uniformization equation explicitly with non-trivial stress-energy function. We note that the thermal behavior at late time is entirely controlled by the eigenvalue of the monodromy matrix along a curve on the unit circle. In this work we show that we can extract this eigenvalue even without the need to compute the full monodromy matrix for the solutions of Fuchs equation. We present the explicit relation between this eigenvalue and the temperature of the final thermal state at late Lorentzian time. In the dual gravity picture this temperature corresponds to the Hawking temperature of the black hole formed through collisions among mass defects present in the bulk. This is the main result of this chapter.

We took two different routes to arrive at the aforementioned connection. The first proof relies on finding a conformal transformation that preserves the structure of the monodromy matrix while leading to a new Fuchs equation with a new stress energy function which can be solved analytically. For our Fuchsian system, we found that one can construct an element of the orientation preserving diffeomorphism, $\text{Diff}_0(S^1)$ on the circle such that the new Fuchs equation we get is associated with a uniform stress energy function. In this form the Fuchs equation can be easily solved. However, since the diffeomorphism, $\text{Diff}_0(S^1)$ preserves the structure of the monodromy matrix, we can actually read off the required eigenvalue by studying this much simpler equation. The second proof exploits the representation of the monodromy matrix in terms of a path ordered integral over a flat connection. Through the Chern-Simons formulation of pure gravity we relate this path ordered integral to the black hole surface area. Finally, upon using the Bekenstein-Hawking formula this finally yields the same expression for the eigenvalue.

However, having a Hawking temperature at the final state of the time evolution does not necessarily mean that one has a standard BTZ black hole at the end of the collapse process. In principle one can also have soft gravitational hair which can be interpreted as boundary gravitons. The bulk states associated with black holes dressed with gravitational hair correspond to points on the same Virasoro orbit. All these points are connected by large diffeomorphisms to a reference point identified with the bulk state describing the BTZ black hole. These are precisely the same diffeomorphisms we talked about in the first proof. The eigenvalue of the monodromy matrix is preserved on a particular Virasoro orbit. Following our identification of this eigenvalue with the temperature of the collapse state, this means all these bulk states related through diffeomorphisms must have the same temperature which in turn justifies the interpretation of these states as black holes states dressed with boundary gravitons. The way to distinguish between the BTZ black hole state and a state corresponding to black hole with gravitational hair is to compute the energy of the final configuration. The deficiency in the energy between the initial state and the predicted final black hole state without any gravitational hair is an indicator of the actual final state of the collapse process. In the work we set up a numerical program to demonstrate this phenomenon. We found that the energy stored in boundary gravitons can actually be sizable for states obtained by small number of heavy operator insertions. However, increasing the number of insertions seems to

restore rotational symmetry leading to a stationary black hole with little or vanishing hair. This is consistent to our theoretical understanding that the reference point on the Virasoro orbit is associated with a uniform stress energy function in the large c limit. We extended our numerical set up further to also include non-symmetric operator insertions which additionally allows oscillating black holes as the final states of time evolution.

In this work we primarily focused on understanding the thermalization process starting from an atypical initial state. This thermal behavior is observed for the semiclassical correlators, namely from its leading order, $O(1)$ contribution in the expansion in $\frac{1}{c}$. It will be interesting to understand the $\frac{1}{c}$ corrections to the correlator for which one would have to go beyond the vacuum block. These corrections are expected to modify the periodicity of Euclidean time order by order in $\frac{1}{c}$ while still maintaining the KMS condition. This expectation follows from the dual gravity picture where these $\frac{1}{c}$ corrections correspond to perturbation around the semiclassical large black hole solution. However, in [22] it was shown that this periodicity actually breaks down as a result of having another non-trivial monodromy which appears while going around the time circle. Although [22] argued that these new monodromies are unphysical and should go away with a resummation it will be interesting to understand this in our set up starting with an arbitrary initial state. It will also be worth investigating the role of boundary gravitons in the thermalization process in the next leading order of perturbative expansion. In particular, it will be interesting to understand the fate of the states corresponding to black holes with gravitational hair in higher order in $\frac{1}{c}$. Another important and perhaps the most interesting direction of study will be to understand the eventual breakdown of the perturbative $\frac{1}{c}$. This happens at the scrambling time [30, 33, 116] when the non-perturbative contributions $\sim e^{O(c)}$ become important. The associated timescale characterizes the onset of chaos [117–120]. Work in this direction is in progress and we hope to report on this soon.

5

Conclusions

Since the discovery of black hole radiation a lot of attention has been devoted to the process of black hole evaporation. Not only because it is an interesting problem by itself, black holes could give a hint to a theory of quantum gravity. In this thesis we set out to investigate the black hole interior and the process of black hole formation.

In chapter 3 we demonstrated that “mirror operators”, complicated operators that live near the boundary of AdS which, in a certain set up can describe physics behind a (black hole) horizon, are identified with simple local operators at a point in the interior of the black hole, are also present in empty AdS. These mirror operators are causally disconnected from the simple operators describing physics near the boundary. Large-scale non-locality is an essential feature of quantum-gravity. Such a loss of causality is an ingredient in proposals of black-hole complementarity. We showed that one can write the field at a point in the center of AdS purely in terms of a complicated polynomial of operators in a time band $T < \pi$, even though all of these operators are causally disconnected from the center of the AdS.

We can only make the distinction between simple and complicated operators, that is, light generalized free fields and complicated multi-trace operators in the large N limit. Here N is the parametric separation between the two. The simple operators form an approximate “algebra” in the time band, which we used to understand how locality arises within effective field theory. These operators, living in a time band of width $T < \pi$ obey a version of the Reeh-Schlieder theorem, which is the dual of the Reeh-Schlieder theorem for the bulk region that is causally connected to the time band. That is, all effective field theory excitations in AdS can be obtained by acting with operators within the

time band. When we only focus on the simple operators we see that locality emerges, whereas non-locality is hidden in complex polynomials.

In empty AdS, we can only examine non-locality on length scales that are the AdS radius. However in our set up we constructed a toy model of a black hole complementarity in AdS. We believe that the essentials of the ideas we presented above are applicable to flat-space black holes.

In chapter 4 we studied under which conditions we can form a black hole in the 3d bulk, from a CFT perspective. We did this by considering probe correlation functions on top of an arbitrary “heavy state” in the dual CFT_2 , and study what are the conditions under which the vacuum block contribution of these correlators appear thermal, in the late Lorentzian time limit. The heavy state was created by inserting a small number of heavy primary operators, with an arbitrary distribution on the radial plane. In the bulk this corresponds to masses being injected from the boundary of AdS_3 at arbitrary points, which gravitationally interact to eventually, in late Lorentzian time, collapse into a black hole. This black hole spacetime is characterized by its Hawking temperature.

For a finite number of heavy operator insertions it becomes hard to extract the leading order semi-classical behavior of the correlators. However we can absorb the heaviness of the operators in the background, so that the correlators in this new coordinate system can be expanded in a power series in $1/c$. To find this coordinate transformation is extremely complicated for multiple heavy insertions. However we showed that it can be bypassed. Instead of solving a second order differential equation of Fuchs’ class, we only need the eigenvalues of the monodromy matrix along a curve on the unit circle to find the late time behavior of the correlation function. We presented the relation between the eigenvalues and the temperature of the final state, at late Lorentzian time. This temperature corresponds to the Hawking temperature of the black hole formed by colliding masses in AdS.

The Hawking temperature of the final state does not necessarily mean that the final state is a standard BTZ black hole. There could be soft gravitational hair present, usually interpreted as boundary gravitons. The eigenvalue of the monodromy matrix corresponds to a particular black hole temperature. Large diffeomorphisms leave the temperature of the black hole unchanged, but change the amount of energy stored in boundary gravitons. We set up a numerical program to find the amount of energy stored in boundary gravitons by comparing

the temperature of the final state with the black hole temperature if all injected energy was converted to black hole mass. We found that a sizable amount of energy can be stored in these boundary gravitons, when the number of heavy operators inserted is small. Increasing the number of insertions leads to a stationary black hole with little or vanishing hair. Asymmetrical heavy operator insertions were considered that resulted in oscillating black holes in the bulk.

5.1 Outlook

It will also be worth investigating the role of boundary gravitons in the thermalization process in the next leading order of perturbative expansion. In particular, it will be interesting to understand the fate of the states corresponding to black holes with gravitational hair in higher order in $\frac{1}{c}$. Another important and perhaps the most interesting direction of study will be to understand the eventual breakdown of the perturbative $\frac{1}{c}$. This happens at the scrambling time [30, 33, 116] when the non-perturbative contributions $\sim e^{O(c)}$ become important. The associated timescale characterizes the onset of chaos [117–120]. Work in this direction is in progress and we hope to report on this soon.

We primarily focused on understanding the thermalization process starting from an atypical initial state. This thermal behavior is observed for the semi-classical correlators, namely from its leading order, $O(1)$ contribution in the expansion in $\frac{1}{c}$. It will be interesting to understand the $\frac{1}{c}$ corrections to the correlator for which one would have to go beyond the vacuum block. These corrections are expected to modify the periodicity of Euclidean time order by order in $\frac{1}{c}$ while still maintaining the KMS condition. This expectation follows from the dual gravity picture where these $\frac{1}{c}$ corrections correspond to perturbation around the semiclassical large black hole solution. However, in [22] it was shown that this periodicity actually breaks down as a result of having another non-trivial monodromy which appears while going around the time circle. Although [22] argued that these new monodromies are unphysical and should go away with a resummation it will be interesting to understand this in our set up starting with an arbitrary initial state.

These technical results are a big step for the researcher, but a small step for the scientific community on its way to a theory of quantum gravity.

6

Gluren achter de horizon

Algemene relativiteitstheorie beschrijft de gravitatie-interactie tussen deeltjes, oftewel zwaartekracht. Het is de meest nauwkeurige theorie die zwaartekracht beschrijft op dit moment. De Einstein-veldvergelijkingen beschrijven de kromming van ruimte en tijd door de aanwezigheid van energie en momentum van deeltjes en straling. Aan de andere kant hebben we kwantumveldentheorie, waarop het standaardmodel is gebaseerd. Kwantumveldentheorie beschrijft de andere drie krachten: de elektromagnetische kracht en de sterke en zwakke interacties. Het grote vraagstuk in theoretische natuurkunde is hoe we de vier krachten kunnen verenigen in een theorie van kwantumzwaartekracht. Omdat zwaartekracht de zwakste kracht is, bestuderen we het in een regime waarin het relatief sterk is, namelijk in de buurt van een zwart gat. Een zwart gat is een object waarvan de massa in een punt is geconcentreerd. De aantrekkingskracht in de buurt van het zwarte gat is zo sterk dat zelfs licht er niet aan kan ontsnappen. Het punt vanwaar licht net niet kan ontsnappen wordt de horizon genoemd. Dit betekent dat wanneer iets de horizon oversteekt het ontoegankelijk zal blijven voor een persoon die buiten het zwarte gat blijft.

Omdat berekeningen al snel erg complex worden, bestudeerden we het meest simpele zwarte gat: het schwarzschild-zwartegat. Dit zwarte gat wordt gekenmerkt door slechts één getal, namelijk de massa. De massa bepaalt waar de horizon ligt, en daarmee de grootte van het zwarte gat, en ook de temperatuur. Omdat de horizon volgens algemene relativiteit geen bijzondere plek in de ruimte is, wordt niets bijzonders waargenomen bij het doorkruisen van de horizon.

In 1973 stelde Bekenstein voor dat het oppervlak van een zwart gat is gerelateerd aan zijn entropie, en dat de oppervlaktezwaartekracht correspondeert met de temperatuur van het zwarte gat [2]. In 1974 ontdekte Hawking dat zwarte

gaten straling uitzenden, schijnbaar met het spectrum van een volmaakte zwarte straler [1]. Het enige kenmerk van de straler, dat af te leiden is uit de straling, is zijn temperatuur.

Het mechanisme van Hawkingstraling kan als volgt worden voorgesteld: in het vacuüm worden continu virtuele deeltjes en antideeltjes gecreëerd, die elkaar annihilieren als ze weer bij elkaar komen. Wanneer zo een paar gecreëerd wordt aan de horizon en één deeltje verdwijnt in het zwarte gat, wordt zijn partner een echt deeltje dat energie wegdraagt. Die energie wordt aan het zwarte gat onttrokken. Dit proces zorgt er uiteindelijk voor dat een zwart gat volledig verdampt.

Een resultaat van Hawking was dat de entropie gegeven wordt door het oppervlak van het zwarte gat te delen door viermaal Newtons constante. Dit lijkt tegenstrijdig met het voldoende zijn van slechts één getal om een zwart gat te karakteriseren. Want het aantal microstaten wordt verkregen door de entropie te exponentiëren. Voor een zwart gat met dezelfde massa als de zon komt dit neer op de exponent van 10^{77} , wat veel meer is dan 1. Er lijkt dus iets vreemds aan de hand te zijn als zwaartekracht met kwantummechanica gecombineerd wordt.

Het verbazingwekkende aan Hawkings resultaat is dat de straling thermisch lijkt, wat informatieverlies betekent. Er kan immers niet worden ontcijfert hoe, en door wat, het zwarte gat gevormd werd. Dit was een groot probleem onder theoretisch natuurkundigen. Naast accepteren dat informatie verloren ging bij het verdampen, waren er enkele alternatieven bedacht.

Een voorstel is dat de straling thermisch *lijkt*, maar in werkelijkheid draagt elk uitgestraald deeltje kleine correcties die, als we veel deeltjes samennemen, de informatie van het zwarte gat onthult. Als een analogie kunnen we denken aan het verbranden van een proefschrift. De fotonen die hierbij vrijkomen zullen thermisch lijken, maar wanneer elk foton en elk asdeeltje bestudeerd wordt dan is het in principe mogelijk om het volledige proefschrift inclusief inhoud te ontcijferen. Het grote verschil met zwarte gaten is het ontbreken van een horizon bij een proefschrift. De overeenkomst tussen het afmaken van een proefschrift en ontsnappen uit een zwart gat wordt overgelaten aan de inbeeldingskracht van de lezer. Wat gebeurt achter de horizon kan straling daarbuiten niet beïnvloeden volgens klassieke algemene relativiteit, terwijl een foton bij verbranding van een proefschrift vanaf het boekje vertrekt.

In dit proefschrift richten we ons op kleine correcties die, wanneer we een

heleboel deeltjes met kleine correcties samennemen, combineren om de straling puur maken. Page liet zien dat als we een subsysteem van een pure staat beschouwen, deze thermisch lijkt. Naarmate we het subsysteem dat we beschouwen vergroten, neemt de entropie af tot we uiteindelijk een pure staat overhouden. Als we de straling als subsysteem beschouwen dan lijkt dit de oplossing van het informatieprobleem.

Met de ontdekking van de AdS/CFT-correspondentie, die zegt dat een theorie met zwaartekracht in anti-De Sitterruimte equivalent is aan een hoekgetrouwe veldentheorie, werd de conclusie getrokken dat de verdamping unitair is; er gaat geen informatie verloren. Dit omdat de veldentheorie zich unitair manifesteert. De correspondentie vertelt niet hoe de informatie weggedragen wordt, maar het biedt wel nieuwe mogelijkheden tot het bestuderen van het probleem. De correspondentie overtuigde Hawking dat de straling puur is.

Vooralsnog hebben we het alleen gehad over hoe een zwart gat er van buitenaf uit ziet. Als we het interieur meenemen, wordt de informatieparadox subtieler. Wanneer we op dezelfde tijd het interieur en het exterieur van een oud zwart gat beschouwen dan zien we in het zwarte gat een object dat erin is gevallen, en alle informatie over dat object, wat ontcijferd kan worden uit de straling, op hetzelfde moment buiten het zwarte gat. Vanuit de kwantummechanica is dit niet toegestaan. Een manier om dit probleem te ondervangen is het opdelen van de operatoren op basis van hun energie. Laagenergetische operatoren commuteren als ze niet causaal verbonden zijn, en kunnen dus maximaal een verwaarloosbare invloed hebben op operatoren die de buitenkant van het zwarte gat beschrijven.

In een theorie van kwantumzwaartekracht bestaat er niet zoiets als lokaliteit bij benadering, omdat kwantumzwaartekracht niet lokaal is. Dit komt omdat de theorie invariant is onder coördinatentransformaties. Een commutator die niet lokaal lijkt in het ene coördinatenstelsel kan dat wel zijn in een ander. Daardoor kan de commutator niet vastgelegd worden.

Een theorie die werd voorgesteld door 't Hooft [10], en werd verfijnd door Susskind en anderen [11], wordt *complementariteit* genoemd. Het idee is dat een persoon ver bij het zwarte gat vandaan een heet membraan net buiten de horizon ziet. Dit noemen ze de uitgerekte horizon. Het membraan straalt thermische straling uit. Voor een persoon in vrije val verdwijnt het membraan, deze persoon ziet geen thermische straling en dus ook geen informatieverlies. Omdat de persoon in vrije val achter de horizon verdwijnt, en dus het verdwijnen

van het membraan niet naar buiten kan communiceren, is er geen discrepantie tussen beide beschrijvingen, omdat beide niet tegelijkertijd geverifieerd kunnen worden. Het voldoet aan de criteria van Bohr voor complementariteit [12]. Als een analogie kan aan het golf-deeltje dualiteit gedacht worden.

De informatieparadox werd recentelijk aangescherpt in [16, 17], waarin op twee manieren de fundamenteën van complementariteit aan de kaak werden gesteld.

Ten eerste bewees Mathur in [15] een argument dat kleine correcties niet kunnen combineren om de staat puur te maken.

Ten tweede beschouwen de auteurs een waarnemer die informatie uit de straling kan extraheren en die er vervolgens voor kiest om het zwarte gat in te duiken. Dit leidt tot een conflict met kwantummechanica. Om een pure staat van straling te garanderen, moet de vroege straling sterk verstrengeld zijn met de late straling. Maar om soepel de horizon te kunnen oversteken moet de vroege straling verstrengeld zijn met het interieur. Dit is niet compatibel met monogamie van verstrengeling. Het werd gesuggereerd dat de informatie uit de late straling ingebed is in dat van de vroege straling. Het probleem met dit voorstel is dat dit niet compatibel is met kwantummechanica. Stel dat we een kwantumbit het zwarte gat insturen, dan kan een waarnemer uit de vroege straling de kwantumstaat van de bit extraheren. Als de waarnemer vervolgens het zwarte gat induikt en daar de verstrengelde partner van die bit tegen komt, en de originele bit zelf, dan heeft de waarnemer dus toegang tot drie kwantumbeschrijvingen van dezelfde bit. In [30] werd vastgesteld dat een zwart gat informatie zo snel verdeelt over de beschikbare vrijheidsgraden dat het observeren van drie bits onmogelijk is. Het lijkt wel mogelijk om twee kwantumbeschrijvingen van de bit te krijgen. De oplossing van deze paradox volgens [17] is dat de bits niet verstrengeld zijn over de horizon. Dit heeft het onplezierige gevolg dat het oversteken van de horizon een nare ervaring wordt. De waarnemer in vrije val zal een muur van hoogenergetische deeltjes zien (dat is heet!).

Een mogelijke oplossing van de informatieparadox, ook wel de “firewallparadox” genoemd, werd voorgesteld door Papadodomas en Raju [18]. Zij hebben een meer exacte benadering van complementariteit. Dit is mogelijk door operatoren te classificeren als simpel en complex. Een waarnemer die alleen toegang heeft tot simpele operatoren kan alleen eenvoudige experimenten doen, hij zal een muur van hoogenergetische deeltjes aan de horizon zien. Een waarnemer die toegang heeft tot alle operatoren zal deze muur niet zien. De complexe op-

eratoren kunnen worden geconstrueerd uit simpele operatoren. De hoeveelheid operatoren in de hoekgetrouwe veldentheorie moet twee keer zo groot worden. Een eeuwig bestaand zwart gat heeft twee duale hoekgetrouwe theorieën die elk een universum beschrijven dat verbonden wordt door het zwarte gat. De operatoren die het ene universum beschrijven zijn als het ware het spiegelbeeld van het andere universum. Wanneer we alleen operatoren die het ene universum beschrijven in acht nemen, dan kan de horizon van het zwarte gat, vanuit dat universum, niet doorkruist worden zonder een muur van hoogenergetische deeltjes tegen te komen. Die muur bestaat niet als operatoren die beide universa beschrijven beschouwd worden bij het doorkruisen van de horizon. Een zwart gat in AdS heeft slechts één duale hoekgetrouwe veldentheorie, het is echter mogelijk om operatoren te creëren die de eigenschappen hebben van de andere, gespiegelde, veldentheorie. Dit zijn complexe operatoren, die ook wel spiegeloperatoren genoemd worden. Door de eigenschappen van deze operatoren verdwijnt de muur van hoogenergetische deeltjes ook in dit geval. Complementariteit lijkt een oplossing van de informatieparadox, consistent met de theorie van algemene relativiteit en met kwantummechanica.

In hoofdstuk 3 bestuderen we de vacuümstaat van AdS, en een band gebonden in tijd in de duale veldentheorie. Als deze band korter is dan de tijd die het kost voor licht om AdS te doorkruisen, wordt AdS op natuurlijke wijze verdeeld in twee regionen. Namelijk een causale diamant in het centrum van AdS die niet causaal verbonden is met de tijdstrip en het complement. We laten zien dat simpele operatoren en een klein product hiervan de annulus in AdS beschrijft. Complexe operatoren en ingewikkelde combinaties van simpele operatoren daarentegen beschrijven de causale diamant in het centrum. Beide sets van operatoren commuteren bij benadering met elkaar. Hiermee hebben we aangetoond dat zelfs in de vacuümstaat van AdS zoiets bestaat als simpele en complexe operatoren: het essentiële onderdeel van zwarte-gat-complementariteit.

In hoofdstuk 4 bestuderen we hoe een zwart gat gevormd wordt vanuit de duale hoekgetrouwe veldentheorie. In de veldentheorie wordt een zwartegatstaat in de bulk gekarakteriseerd door de Hawkingtemperatuur in de thermische staat. We beginnen door een zware staat te creëren dual aan de Vaidyageometrie in de bulk, waarbij de energieverdeling volledig willekeurig is gelaten. Vervolgens bestuderen we hoe een tweepuntcorrelatiefunctie zich gedraagt op late Lorentzische tijd. Het blijkt dat we een thermische functie overhouden, wat betekent dat in de bulk een zwart gat is gecreëerd. De temperatuur komt niet altijd overeen met de hoeveelheid energie die in de bulk geïnjecteerd werd, dit

is namelijk afhankelijk van de distributie van energie op de rand van AdS. Dit werd numeriek geverifieerd. Als de energiedistributie symmetrisch is, en zoveel mogelijk homogeen verdeeld, dan zal vrijwel alle energie omgezet worden in massa van het zwarte gat. Bij niet-symmetrische, of bij slechts enkele inserties van energie, is de temperatuur veel lager. Dit komt omdat een groot deel van de geïnjekteerde energie gaat zitten in oscillaties van het zwarte gat, en in gravitonen die aan de rand van AdS zijn ‘bevroren’.

7

Acknowledgments

I would like to thank my supervisors, my collaborators and the reading committee for enabling me to complete this thesis.

Ceyda and Ilse I would like to thank for taking on the burden of being my paranymphs, but more importantly for being such dear friends. Thanks to the people from my old department for “the good, the bad and the ugly” times. The colleagues and friends in the new department for being welcoming and fun. But also for being a pain in the ass about finishing the thesis, it would not be in this stage without you.

Thanking people for sharing coffee, food, stories and coffee seems to be customary. However, a wise man told me that serious theses have short acknowledgments, so to keep up appearances I would like to keep it short.

Last but not least I would like to thank my parents and brother for the support given and interest shown during my studies and PhD.

Appendices

A

Euclidean black hole temperature

In this appendix we shall derive the Hawking temperature by relating the partition function to the path integral. We start with

$$Z(\beta) = \sum_E e^{-\beta E}, \quad (\text{A.1})$$

with $\beta = 1/T$. The energy E_i is given by the eigenvalues of the Hamiltonian so that we can rewrite (A.1) to:

$$Z = \sum_i \langle i | e^{-\beta E_i} | i \rangle = \text{tr}[e^{-\beta H}], \quad (\text{A.2})$$

which can be related to a path integral

$$\langle f | e^{-iHt} | i \rangle = \int_{x(0)=x_i}^{x(t)=x_f} D[x] e^{iS[x]}. \quad (\text{A.3})$$

We can relate (A.3) to (A.2) if we take $t = -i\tau$, which is an analytic continuation to Euclidean time, and to ensure we are taking the trace we have to identify the final state with the initial state, which is effectively compactifying time, that is, $\tau \rightarrow \tau + \beta$. Whenever we have periodic Euclidean time in a statistical system, we can identify this periodicity with a temperature. For a general black hole solution we can derive the temperature starting from

$$ds^2 = -f(r)dt^2 + \frac{1}{f(r)}dr^2 + r^2 d\Omega_2^2, \quad (\text{A.4})$$

where $f(r)$ vanishes at the horizon $r = r_h$. Rotating to Euclidean time gives

$$ds^2 = f(r)d\tau^2 + \frac{1}{f(r)}dr^2 + r^2 d\Omega_2^2. \quad (\text{A.5})$$

We are interested in the region near the horizon, therefore we expand the metric near the horizon to obtain

$$ds^2 \approx f'(r_h)(r - r_h)d\tau^2 + \frac{1}{f'(r_h)(r - r_h)}dr^2 + r^2 d\Omega_2^2 \quad (\text{A.6})$$

We want to write this in the form $\rho^2 d\theta^2 + d\rho^2$ where we neglected the angular part. We henceforth require

$$d\rho^2 = \frac{1}{f'(r_h)(r - r_h)}dr^2. \quad (\text{A.7})$$

The metric now becomes

$$ds^2 \approx \frac{4}{f'(r_h)}(r - r_h)d(C\theta)^2 + d\rho^2, \quad (\text{A.8})$$

which we want to be equal to the τ component of (A.6), so we require $C = \frac{1}{2}f'(r_h)$. Since we demand periodicity $\tau = \tau + 2\pi$ to avoid a conical singularity we see that θ has a periodicity of $\beta = \frac{2\pi}{C} = \frac{4\pi}{f'(r_h)}$. Plugging in the Schwarzschild solution (2.1) where $f'(r_h) = \frac{1}{2GM}$ we obtain an inverse temperature

$$\beta = 8\pi GM, \quad (\text{A.9})$$

which matches with the earlier found result.

B The holographic bound

Using the fundamental thermodynamics relation between energy, temperature and entropy

$$\frac{\partial S}{\partial E} = \frac{1}{T} \Rightarrow \frac{\partial S}{\partial M} = 8\pi GM, \quad (\text{B.1})$$

we can find the Bekenstein-Hawking entropy of the black hole $S_{BH} = 4\pi GM^2 + \text{cst.}$ It is fair to assume that the entropy goes to zero when there is no mass present, hence we set the constant equal to zero. When we plug in the Schwarzschild radius $r_h = 2GM$ we find

$$S_B = \frac{4\pi r_H^2}{4G} = \frac{A}{4G}, \quad (\text{B.2})$$

remarkably the entropy of a black hole scales with its area.

This gave rise to the holographic principle [121, 122]. A later chapter we will devote to the AdS/CFT correspondence. Here we will quickly discuss some implications of combining a gravity theory with quantum field theory. When we have a ball with radius R , what would be the maximum entropy $S(R)$? We claim that in a theory with local degrees of freedom $S \propto R^3$ as $R \rightarrow \infty$, assuming there is a UV cutoff, l , the number of points in this volume goes as R^3/l^3 , with each point having k degrees of freedom. Hence the number of microstates is

$$N = k^{R^3/l^3}, \quad (\text{B.3})$$

the entropy being given by taking the logarithm of the above gives

$$S = \frac{\log k}{l^3} R^3. \quad (\text{B.4})$$

This is in contradiction with what we found before. We have three statements that cannot all be true:

- We have a theory of gravity ($S \sim R^2$)
- This theory has local degrees of freedom ($S \sim R^3$)
- The second law of thermodynamics holds $\delta S > 0$.

Since in a theory of gravity a large enough mass will eventually collapse into a black hole, whose entropy scales with the second power of the radius whereas we started with a ball whose entropy scaled with the volume, hence the entropy of the system decreases.

The proposed solution is that a theory of quantum gravity does not have local degrees of freedom, Quantum gravity is a holographic theory where the fundamental degrees of freedom live on the boundary of the spacetime.

C

A black hole formed by collapse

This appendix describes the physics in the bulk of the set-up that was considered in the previous chapter. We consider a thin, highly energetic and spherically symmetric lightlike shell that collapses into a black hole. The shell divides spacetime in two regions, before the shell is sent we have the AdS vacuum at zero temperature and after the shell we will have the BTZ geometry with corresponding temperature. The Vaidya geometry has been studied extensively, for example [82] studies two point functions across the shell using the geometric optics approximation and numerics. The geometric optics approximation has been used to study black holes formed by collapse by, amongst others [123,124] and in AdS₂ [125,126]. At the time of writing this manuscript work on this project is in progress.

C.1 Introduction

The AdS-Vaidya metric describes the formation of a black hole in AdS_3 by collapse. The metric written in the ingoing Eddington Finkelstein coordinate $v = t + r_*$, with r_* the tortoise coordinate defined in (2.2), is given by

$$ds^2 = -f(r, v)dv^2 + 2dvdr + r^2d\theta^2, \quad (C.1)$$

with

$$f(r, v) = 1 + \frac{r^2}{l^2} - \theta(v) \left(1 + r_h^2\right). \quad (C.2)$$

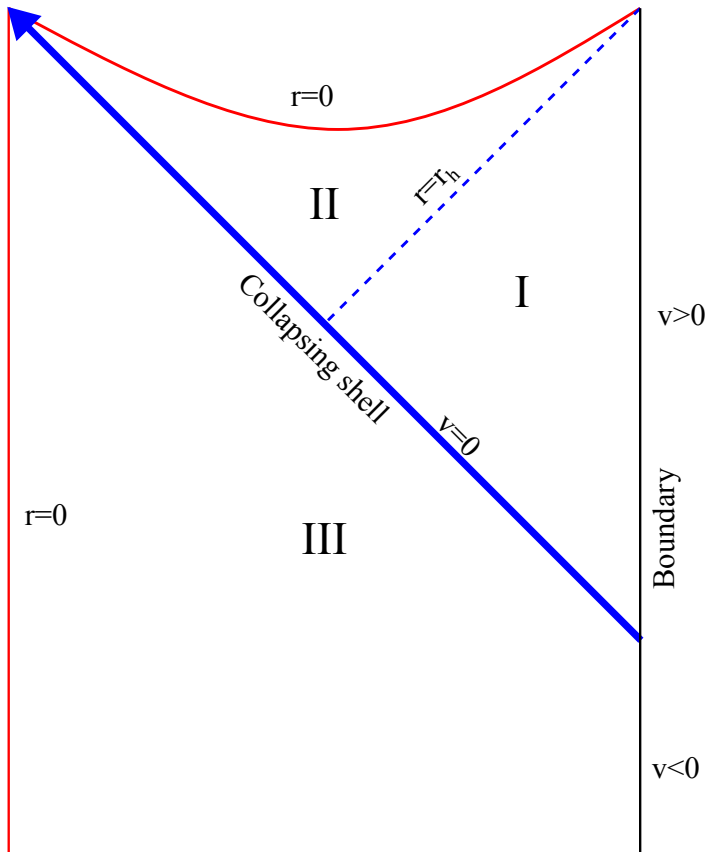


Figure C.1: Geometry of a collapsing shell in AdS. The solid line denotes in-falling matter while the dashed line denotes the formation of horizon.

Where $\theta(v)$ denotes the heavyside function. The metric before the shock at $v = 0$ is AdS_3 described by the metric (3.4) and after the shock it has the BTZ geometry

$$ds^2 = -\left(r^2 - r_h^2\right) dt^2 + \frac{dr^2}{r^2 - r_h^2} + r^2 d\theta^2, \quad (\text{C.3})$$

written in the standard (t, r, θ) -coordinates. The BTZ region can be subdivided into the black hole interior and exterior. We solve the Klein Gordon equation in each of the regions and match them. In total we have six conditions that need to be satisfied, namely

- Matching of ϕ^I and ϕ^{II}
- Matching of ϕ^I and ϕ^{III}
- Matching of ϕ^{II} and ϕ^{III}
- Normalizability of ϕ^I at the boundary $r \rightarrow \infty$
- Normalizability of ϕ^{III} at the boundary $r \rightarrow \infty$
- Regularity of ϕ^{III} at the center $r = 0$

C.1.1 Scalar field in AdS_3

Before the shell is injected, we have to solve the vacuum field equations. The spacetime metric is given by

$$ds^2 = -(r^2 + 1)dv^2 + 2dvdr + r^2 d\theta^2. \quad (\text{C.4})$$

We solve the Klein-Gordon equation using an ansatz of the form $\phi(v, r, \theta) = e^{-i\omega v + i l \theta} f(r)$. We obtain two linearly independent solutions for the radial function,

$$f_{\omega, l}^1(r) = c_1 r^l \left(r^2 + 1\right)^{\omega/2} e^{-i\omega \tan^{-1}(r)} {}_2F_1\left(\frac{1}{2}(l - \Delta + \omega + 2), \frac{1}{2}(l + \Delta + \omega); l + 1; -r^2\right), \quad (\text{C.5})$$

and

$$f_{\omega,l}^2(r) = c_2 r^{-l} (r^2 + 1)^{\omega/2} e^{-i\omega \tan^{-1}(r)} {}_2F_1\left(\frac{1}{2}(-l - \Delta + \omega + 2), \frac{1}{2}(-l + \Delta + \omega); 1 - l; -r^2\right). \quad (\text{C.6})$$

In general we have access to all v and we would impose regularity at the center and normalizability at the boundary to fix the constants c_i . However we need to be careful because the boundary region available for region I & III are bounded in v , hence when taking the Fourier transform we cannot integrate over all v .

C.1.2 Scalar field in BTZ

For $v > 0$ the geometry is that of the BTZ black hole, described by the metric

$$ds^2 = -(r^2 - r_h^2)dv^2 + 2dvdr + r^2 d\theta^2, \quad (\text{C.7})$$

with r_h denoting the position of the horizon. We solve the Klein Gordon equation with the ansatz $\phi = e^{-i\omega v + i n \theta} f(r)$, consequently we find two linearly independent solutions for the radial part,

$$f_{\omega l}^1(r) = c_1 r^{-2a} (r^2 - r_h^2)^{-b} e^{-2b \tanh^{-1}\left(\frac{r}{r_h}\right)} {}_2F_1\left(-a - b - \frac{\Delta}{2} + 1, \frac{1}{2}(\Delta - 2(a + b)); 1 - 2b; 1 - \frac{r^2}{r_h^2}\right) \quad (\text{C.8})$$

and

$$f_{\omega l}^2 = c_2 r^{-2a} \left(1 - \frac{r^2}{r_h^2}\right)^{2b} (r^2 - r_h^2)^{-b} e^{-2b \tanh^{-1}\left(\frac{r}{r_h}\right)} {}_2F_1\left(-a + b - \frac{\Delta}{2} + 1, -a + b + \frac{\Delta}{2}; 2b + 1; 1 - \frac{r^2}{r_h^2}\right), \quad (\text{C.9})$$

where $a = \frac{-in}{2r_h}$ $b = \frac{i\omega}{2r_h}$. Depending on whether we quantize the field inside or outside the black hole we will choose convenient boundary conditions to determine the constants. Again extra care has to be taken because of the boundedness of v .

C.1.3 Defining various modes

In AdS_3 the tortoise coordinate is given by

$$r_* = \arctan(r), \quad (C.10)$$

which ranges from zero to $\frac{\pi}{2}$. In the black hole region the tortoise coordinate is given by

$$r_* = \frac{1}{2r_h} \log \left(\frac{r - r_h}{r + r_h} \right) = -\frac{1}{r_h} \tanh^{-1}(r/r_h). \quad (C.11)$$

Clearly $r_* = 0$ is at the boundary of AdS and $r_* = -\infty$ is at the horizon. For every real ω and for every l , we define the following modes

1. **Normalizable mode:** $f_{\omega l}^N(r)$

This is normalized to behave like

$$f_{\omega l}^N(r) \sim 1 \times r^{-\Delta} \quad (C.12)$$

near the boundary. Once we specify this boundary condition there is no remaining ambiguity in the definition of this mode. An important result from the theory of differential equations (scattering theory) is that if we look at the function

$$f_{\omega l}^N(r) \quad (C.13)$$

for fixed l and fixed r and think of it as a function of ω , it is an analytic function in ω . Obviously, for real ω , the normalizable mode is real.

2. **Non-normalizable mode:** $\tilde{f}_{\omega l}(r)$ This is normalized to behave like

$$f_{\omega l}^{NN}(r) \sim 1 \times r^{d-\Delta}, \quad (C.14)$$

near the boundary. Unlike the normalizable mode, in this case the boundary condition does not uniquely fix the solution since we can always add to it some normalizable component. One can select the precise mode in such a way that the mode is analytic in ω , for fixed l, r .

3. **In/out going modes:** $f_{\omega l}^{\text{in/out}}(r)$ normalized to behave like

$$f_{\omega l}^{\text{in}}(r) \sim 1 \text{ and } f_{\omega l}^{\text{out}}(r) \sim 1 \times e^{2ir_*} \quad (C.15)$$

The ingoing mode is $e^{-i\omega v} = e^{-i\omega(t+r_*)}$ and the outgoing mode goes as $e^{-i\omega u} = e^{-i\omega(t-r_*)} = e^{-i\omega v + 2i\omega r_*}$.

$$e^{-i\omega t} f_{\omega l}^{\text{in/out}}(r) \sim 1 \times e^{-i\omega t \mp i\omega r_*} \quad (\text{C.16})$$

near the horizon. Hence for the above combination the complex conjugate of the ingoing mode gives the outgoing mode.

C.1.4 Mode expansions in various regions

Region I

The solutions we found can be rewritten in terms of normalizable and non normalizable solutions:

$$\phi^I(v, r, \theta) \int d\omega a_\omega e^{-i\omega v + i\theta} f_{\omega l}^N(r) + b_\omega e^{-i\omega v + i\theta} f_{\omega l}^{NN}(r) \quad (\text{C.17})$$

It was shown in [127] that when we use the boundary conditions as in the definition of $f_{\omega l}^{N/NN}(r)$ they are, for given r , entire functions of ω and l . Because the solution is valid only in the region where $v > 0$, we have to check that we do not count non normalizable modes in region III that become normalizable modes in I as non normalizable mode. To do that we first look at the near boundary expansion of the non normalizable mode:

$$\lim_{r \rightarrow \infty} \int_{\omega > 0} d\omega b_\omega e^{-i\omega v} f_{\omega l}^N(r) + \text{h.c.} = \int_{-\infty}^{\infty} d\omega b_\omega e^{-i\omega v} = K(v), \quad (\text{C.18})$$

which we demand to vanish for $v > 0$. We observe that when we close the contour of integration in the lower half plane (LHP), that is we take $\omega = -is$, b_ω should not have poles in the LHP and it should not grow exponentially. Another analytic property we can find by observing that the integral can be written as

$$\int_{-\infty}^0 dv K(v) e^{i\omega v} = b_\omega, \quad (\text{C.19})$$

since on \mathbb{R}_+ $K(v) = 0$. Using the Paley Wiener theorem which states that the Fourier transform of a holomorphic function that is supported on \mathbb{R}_- with ω analytic on the lower half plane is also a holomorphic function, and since $K(v)$ is holomorphic, so is b_ω .

When we take the non normalizable solution for a fixed radial depth inside the bulk we have

$$\int_{-\infty}^{\infty} d\omega b_{\omega} e^{-i\omega v} f_{\omega l}^{NN}(r) = 0, \quad (\text{C.20})$$

where $f_{\omega l}^{NN}(r)$ is a well behaved holomorphic function. This integral gives zero when we close the contour from below, since b_{ω} is a holomorphic function and so is $f_{\omega l}^{NN}(r)$, so their product is too.

They are normalized so that the coefficient of the NN mode is one, at infinity. The functions are

$$f_1(r) = \Omega \Gamma\left(-a-b+\frac{\Delta}{2}\right) \Gamma\left(-a+b+\frac{\Delta}{2}\right) e^{-2b \tanh^{-1}\left(\frac{r}{r_h}\right)} \Gamma(\Delta-1)^{-1} {}_2F_1\left(-a-b-\frac{\Delta}{2}+1, -a-b+\frac{\Delta}{2}; 1-2a; \frac{r^2}{r_h^2}\right) \quad (\text{C.21})$$

and

$$f_2(r) = \Omega \left(\frac{r^2}{r_h^2}\right)^{2a} \Gamma\left(a-b+\frac{\Delta}{2}\right) \Gamma\left(a+b+\frac{\Delta}{2}\right) e^{-2b \tanh^{-1}\left(\frac{r}{r_h}\right)} {}_2F_1\left(a-b-\frac{\Delta}{2}+1, a-b+\frac{\Delta}{2}; 2a+1; \frac{r^2}{r_h^2}\right), \quad (\text{C.22})$$

with $\Omega = \frac{\left(-\frac{1}{r_h^2}\right)^{1-\Delta} (r^2-r_h^2)^{-b}}{r^{2a}\Gamma(\Delta-1)}$. The behavior of these functions with varying conformal dimension was checked numerically. For large s and away from the horizon the functions are damped and well behaved. There are poles when $a = \frac{il}{2r_h} = \frac{i}{2} + in$, where n is an integer. From this we conclude that if there would be any contribution to the normalizable mode in region I from non normalizable modes in region III it would integrate out to give zero. We therefore can safely set the non normalizable mode to zero and remain with the normalizable mode that is given by

$$f_{\omega l}^N(r) = r_h^{-\Delta} \left(\frac{r^2}{r_h^2}\right)^a \left(\frac{r^2}{r_h^2} - 1\right)^{-a-\Delta/2} {}_2F_1\left(a-b+\Delta/2, a+b+\Delta/2, \Delta, \frac{r_h^2}{r_h^2-r^2}\right), \quad (\text{C.23})$$

where the factor $r_h^{-\Delta}$ comes from normalizing according to the definition of normalizable mode. The mode expansion is given by

$$\boxed{\phi^I(v, r, \theta) = \int_{\omega>0} d\omega \sum_{l=0}^{\infty} a_{\omega l} e^{-i\omega v + il\theta} f_{\omega l}^N(r) + \text{h.c.}} \quad (\text{C.24})$$

with $a = \frac{-il}{2r_h}$ and $b = \frac{i\omega}{2r_h}$

Region II

Behind the horizon we use the ingoing and outgoing basis of solutions with the appropriate normalization.

$$f_{\omega l}^{\text{in}}(r) = 4^b e^{-i\pi b} r^{-2a} r_h^{2(a+b)} (r^2 - r_h^2)^{-b} e^{-2b \tanh^{-1}\left(\frac{r}{r_h}\right)} {}_2F_1\left(-a-b-\frac{\Delta}{2}+1, \frac{1}{2}(\Delta-2(a+b)); 1-2b; 1-\frac{r^2}{r_h^2}\right),$$

and

$$f_{\omega l}^{\text{out}}(r) = 4^{-b} e^{i\pi b} r_h^{2(a+b)} r^{-2a} r_h^{-4b} (r^2 - r_h^2)^b e^{-2b \tanh^{-1}\left(\frac{r}{r_h}\right)} {}_2F_1\left(-a+b-\frac{\Delta}{2}+1, -a+b+\frac{\Delta}{2}; 2b+1; 1-\frac{r^2}{r_h^2}\right).$$

Hence the mode expansion goes as

$$\boxed{\phi^{II}(v, r, \theta) = \int_{\omega>0} d\omega \sum_{l=0}^{\infty} e^{-i\omega v + il\theta} (c_{\omega l} f_{\omega l}^{\text{in}}(r) + d_{\omega l} f_{\omega l}^{\text{out}}(r)) + \text{h.c.}} \quad (\text{C.25})$$

Region III

In this region we take a particular linear combination to expand in a N/NN basis. In this case we can repeat the Paley Wiener argument to demand that the NN solution vanishes. Hence on physical grounds we can say that the non normalizable mode is zero for all v . We concluded before that in regions I and II

no irregular modes are present, so we cannot kill irregular modes in the future that would be regular in III.

$$\phi^{III}(v, r, \theta) = e^{\frac{1}{2}i\pi(\Delta)} \int_{\omega>0} d\omega \left(g_{\omega} e^{-i\omega v} f_{\omega}^N(r) + h_{\omega} e^{-i\omega v} f_{\omega}^{NN}(r) \right) + \text{h.c.} \quad (\text{C.26})$$

We demand that in region III the non normalizable mode vanishes

$$\lim_{r \rightarrow \infty} \phi^{III}(v, r, \theta) = \int_{-\infty}^{\infty} d\omega h_{\omega} e^{-i\omega v} = 0 \quad \text{for } v < 0, \quad (\text{C.27})$$

where we used that $h_{\omega}^* = h_{-\omega}$. We observe that when we close the contour of integration in the upper half plane (UHP), that is we take $\omega = is$, h_{ω} should not have poles in the UHP and it should not grow too fast. Another analytic property we can find by observing that the integral can be written as

$$K(v) = \int_0^{\infty} d\omega h_{\omega} e^{-i\omega v} = 0 \quad \text{for } v < 0 \quad (\text{C.28})$$

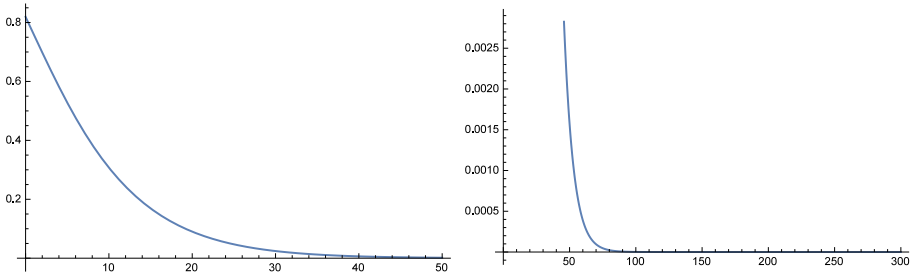
Using Paley Wiener

$$b_{\omega} = \int_0^{\infty} dv K(v) e^{i\omega v}, \quad (\text{C.29})$$

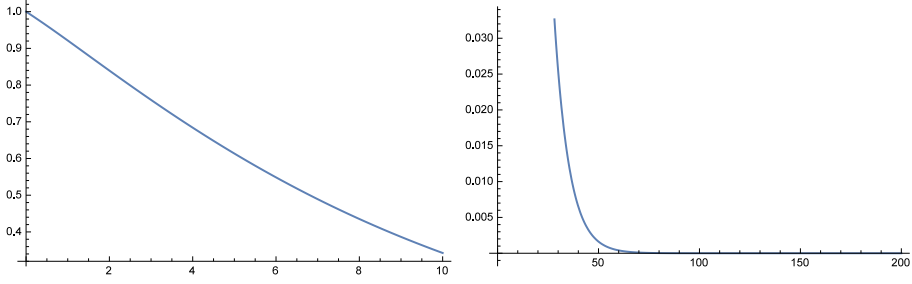
which states that when $K(v)$ is a square integrable function and is supported on \mathbb{R}_+ and ω analytic in the UHP we could conclude that h_{ω} is holomorphic in the UHP. Going deeper in the bulk, the solution is

$$\phi^{III}(v, r) = \int_{-\infty}^{\infty} d\omega h_{\omega} e^{-i\omega v} f_{\omega}^{NN}(r) = 0 \quad \text{for } v < 0 \quad (\text{C.30})$$

Using the same method as before we found that the NN mode is well behaved, for the first solution this looks like



and for the second



So we conclude that we can safely set the non normalizable mode to zero because it integrates out to give zero. The field expansion is hence given by

$$\phi^{III}(v, r, \theta) = e^{\frac{1}{2}i\pi(\Delta)} \int_{\omega>0} d\omega \sum_{l=0} g_{\omega l} e^{-i\omega v + il\theta} f_{\omega l}^N(r) + \text{h.c.} \quad (\text{C.31})$$

Where the normalizable radial function is given by

$$\begin{aligned} f_{\omega l}^N(r) = & \frac{\csc(\pi\Delta) \csc(\pi l) (\cos(\pi\omega) - \cos(\pi(\Delta + l))) \Gamma\left(\frac{1}{2}(-l - \omega - \Delta + 2)\right) \Gamma\left(\frac{1}{2}(-l + \omega - \Delta + 2)\right)}{2\Gamma(1 - \Delta)\Gamma(1 - l)\Gamma(l + 1)\Gamma\left(\frac{1}{2}(-l - \omega + \Delta)\right) \Gamma\left(\frac{1}{2}(-l + \omega + \Delta)\right)} \\ & (r^2 + 1)^{\omega/2} r^{\Delta-l} e^{\frac{1}{2}i\omega(\pi - 2 \tan^{-1}(r))} \left({}_2F_1\left(\frac{1}{2}(-l + \omega - \Delta + 2), \frac{1}{2}(-l + \omega + \Delta); 1 - l; -r^2\right) \right. \\ & \left. - r^{2l} \Gamma(1 - l) \Gamma\left(\frac{1}{2}(l - \omega + \Delta)\right) \Gamma\left(\frac{1}{2}(l + \omega + \Delta)\right) {}_2F_1\left(\frac{1}{2}(l + \omega - \Delta + 2), \frac{1}{2}(l + \omega + \Delta); l + 1; -r^2\right) \right) \end{aligned} \quad (\text{C.32})$$

C.1.5 Matching conditions

Across the horizon

Across the horizon we match the fields I and II.

Regions I and II

We take the field expansion in the exterior and expand it around r_h to find

$$\phi^I(v, r, \theta) = \int_{\omega>0} d\omega \sum_{l=0}^{\infty} a_{\omega l} e^{-i\omega v + il\theta} \left(e^{i\delta} + e^{-i\delta} e^{2i\omega r_*} \right) + \text{h.c.} \quad (\text{C.33})$$

Using Riemann Lebesgue we can neglect the part that rapidly oscillates since the tortoise coordinate goes to minus infinity near the horizon and thus we remain with

$$\phi^I(v, r, \theta) = \int_{\omega>0} d\omega \sum_{l=0}^{\infty} a_{\omega l} e^{-i\omega v + il\theta} e^{i\delta} + \text{h.c.} \quad (\text{C.34})$$

From the interior we know that the ingoing mode has a constant coefficient and the outgoing mode comes with a factor e^{2ir^*} which in a similar fashion vanishes, and thus the near horizon expansion becomes

$$\phi^{II}(v, r, \theta) = \int_{\omega>0} d\omega \sum_{l=0}^{\infty} c_{\omega l} e^{-i\omega v + il\theta} f_{\omega l}^{\text{in}}(r) + \text{h.c.} \quad (\text{C.35})$$

So we can match mode by mode to find

$$a_{\omega l} e^{i\delta} = c_{\omega l} \quad (\text{C.36})$$

Across the shock

Regions II and III

For $\phi^{II}(v, r)$ we use the ingoing and outgoing basis and for $\phi^{III}(v, r)$ we use the normalizable solution. For now we assume that in empty AdS we do not have a discrete mode expansion yet, since we only fulfilled one boundary condition. Inside the black hole we have two solutions since we have no boundary conditions to fulfil.

The matching condition

For the matching we only have to use the normalizable solution in region III but we remain with both solutions in region II. The matching condition is valid for $r < r_h 4$.

$$\begin{aligned} \lim_{v \rightarrow 0^-} \phi^{III}(v, r, \theta) &= \lim_{v \rightarrow 0^-} e^{\frac{1}{2}i\pi(\Delta+l)} \int_{\omega>0} d\omega \sum_{l=0}^{\infty} g_{\omega l} e^{-i\omega v + il\theta} f_{\omega, l}^N(r) + \text{h.c.} \\ &= \lim_{v \rightarrow 0^+} \int_{\omega>0} d\omega \sum_{l=0}^{\infty} e^{-i\omega v + il\theta} \left(c_{\omega l} f_{\omega l}^{\text{in}}(r) + d_{\omega l} f_{\omega l}^{\text{out}}(r) \right) + \text{h.c.} \\ &= \lim_{v \rightarrow 0^+} \phi^{II}(v, r, \theta) \end{aligned}$$

(C.37)

Regions I and III

For now we assume that in empty AdS we do not have a discrete mode expansion since we only fulfilled one boundary condition. For $\phi^I(v, r)$ consider the normalizable solution and for $\phi^{III}(v, r)$ also use the normalizable solution.

$$\phi^I(v, r, \theta) = \int_{\omega>0} d\omega \sum_{l=0}^{\infty} a_{\omega l} e^{-i\omega v + il\theta} f_{\omega l}^N(r) + \text{h.c.} \quad (\text{C.38})$$

After imposing the normalizability condition of the field at infinity we find **the matching condition**. Which is valid for $r > r_h$

$$\begin{aligned} \lim_{v \rightarrow 0^-} \phi^{III}(v, r, \theta) &= \lim_{v \rightarrow 0^-} e^{\frac{1}{2}i\pi(\Delta+l)} \int_{\omega>0} d\omega \sum_{l=0}^{\infty} g_{\omega l} e^{-i\omega v + il\theta} f_{\omega, l}^N(r) + \text{h.c.} \\ &= \lim_{v \rightarrow 0^+} \int_{\omega>0} d\omega \sum_{l=0}^{\infty} a_{\omega l} e^{-i\omega v + il\theta} f_{\omega l}^N(r) + \text{h.c.} = \lim_{v \rightarrow 0^+} \phi^I(v, r, \theta) \end{aligned}$$

(C.39)

It looks like we can match mode by mode, however the notation here is deceptive. The frequency ω is dual to the coordinate $v = t + r_*$, where the tortoise coordinate that was defined before is not the same for both regions.

D

Curriculum vitae

Jan-Willem Brijan • 26-12-1989 • +31651874981 • janwillem.bryan@gmail.com

D.1 Working experience

2018-present	Lecturer / project manager	University of Groningen
2014-2019	PhD in Physics	University of Groningen

As a lecturer I designed a course “Python for Physicists”, which is a first year course in the Physics program and I am working in the SOWISO team on e-learning. As a project manager I am, with a team, implementing learning analytics.

D.2 Education

2012-2014	Master Physics	University of Groningen
2008-2012	Bachelor Physics	University of Groningen

Bibliography

- [1] S. Hawking, “Particle Creation by Black Holes,” *Commun.Math.Phys.*, vol. 43, pp. 199–220, 1975.
- [2] J. D. Bekenstein, “Black holes and entropy,” *Phys. Rev.*, vol. D7, pp. 2333–2346, 1973.
- [3] A. Strominger and C. Vafa, “Microscopic Origin of the Bekenstein-Hawking Entropy,” *Phys. Lett.*, vol. B379, pp. 99–104, 1996.
- [4] Y. Aharonov, A. Casher, and S. Nussinov, “The Unitarity Puzzle and Planck Mass Stable Particles,” *Phys. Lett.*, vol. B191, p. 51, 1987.
- [5] D. N. Page, “Information in black hole radiation,” *Phys. Rev. Lett.*, vol. 71, pp. 3743–3746, 1993.
- [6] J. M. Maldacena, “The Large N limit of superconformal field theories and supergravity,” *Adv.Theor.Math.Phys.*, vol. 2, pp. 231–252, 1998.
- [7] E. Witten, “Anti-de Sitter space and holography,” *Adv. Theor. Math. Phys.*, vol. 2, pp. 253–291, 1998.
- [8] S. Gubser, I. R. Klebanov, and A. M. Polyakov, “Gauge theory correlators from noncritical string theory,” *Phys.Lett.*, vol. B428, pp. 105–114, 1998.
- [9] D. A. Lowe, J. Polchinski, L. Susskind, L. Thorlacius, and J. Uglum, “Black hole complementarity versus locality,” *Phys. Rev.*, vol. D52, pp. 6997–7010, 1995.
- [10] G. ’t Hooft, “On the Quantum Structure of a Black Hole,” *Nucl.Phys.*, vol. B256, p. 727, 1985.
- [11] L. Susskind, L. Thorlacius, and J. Uglum, “The Stretched horizon and black hole complementarity,” *Phys.Rev.*, vol. D48, pp. 3743–3761, 1993.

- [12] N. Bohr, “The Quantum Postulate and the Recent Development of Atomic Theory,” *Nature*, vol. 121, no. 3050, pp. 580–590, 1928.
- [13] S. D. Mathur, “A Proposal to resolve the black hole information paradox,” *Int. J. Mod. Phys.*, vol. D11, pp. 1537–1540, 2002.
- [14] K. Skenderis and M. Taylor, “The fuzzball proposal for black holes,” *Phys.Rept.*, vol. 467, pp. 117–171, 2008.
- [15] S. D. Mathur, “The Information paradox: A Pedagogical introduction,” *Class.Quant.Grav.*, vol. 26, p. 224001, 2009.
- [16] A. Almheiri, D. Marolf, J. Polchinski, and J. Sully, “Black Holes: Complementarity or Firewalls?,” *JHEP*, vol. 1302, p. 062, 2013.
- [17] A. Almheiri, D. Marolf, J. Polchinski, D. Stanford, and J. Sully, “An Apologia for Firewalls,” *JHEP*, vol. 1309, p. 018, 2013.
- [18] K. Papadodimas and S. Raju, “An Infalling Observer in AdS/CFT,” *JHEP*, vol. 1310, p. 212, 2013.
- [19] J. M. Maldacena, “Eternal black holes in anti-de Sitter,” *JHEP*, vol. 04, p. 021, 2003.
- [20] K. Papadodimas and S. Raju, “State-Dependent Bulk-Boundary Maps and Black Hole Complementarity,” *Phys.Rev.*, vol. D89, no. 8, p. 086010, 2014.
- [21] A. L. Fitzpatrick, J. Kaplan, and M. T. Walters, “Virasoro Conformal Blocks and Thermality from Classical Background Fields,” *JHEP*, vol. 11, p. 200, 2015.
- [22] A. L. Fitzpatrick and J. Kaplan, “Conformal Blocks Beyond the Semi-Classical Limit,” *JHEP*, vol. 05, p. 075, 2016.
- [23] N. Birrell and P. Davies, *Quantum fields in curved space*. Cambridge Univ Press, 1986.
- [24] D. N. Page, “Hawking radiation and black hole thermodynamics,” *New J. Phys.*, vol. 7, p. 203, 2005.

- [25] J. Polchinski, “The Black Hole Information Problem,” in *Proceedings, Theoretical Advanced Study Institute in Elementary Particle Physics: New Frontiers in Fields and Strings (TASI 2015): Boulder, CO, USA, June 1-26, 2015*, pp. 353–397, 2017.
- [26] Y. B. Zel’Dovich, “Amplification of Cylindrical Electromagnetic Waves Reflected from a Rotating Body,” *Soviet Journal of Experimental and Theoretical Physics*, vol. 35, p. 1085, 1972.
- [27] S. W. Hawking, “Information loss in black holes,” *Phys. Rev.*, vol. D72, p. 084013, 2005.
- [28] D. N. Page, “Average entropy of a subsystem,” *Phys.Rev.Lett.*, vol. 71, pp. 1291–1294, 1993.
- [29] D. Harlow, “Jerusalem Lectures on Black Holes and Quantum Information,” *Rev. Mod. Phys.*, vol. 88, p. 015002, 2016.
- [30] P. Hayden and J. Preskill, “Black holes as mirrors: Quantum information in random subsystems,” *JHEP*, vol. 09, p. 120, 2007.
- [31] G. ’t Hooft, “The black hole interpretation of string theory,” *Nucl.Phys.*, vol. B335, pp. 138–154, 1990.
- [32] L. Susskind and L. Thorlacius, “Gedanken experiments involving black holes,” *Phys.Rev.*, vol. D49, pp. 966–974, 1994.
- [33] Y. Sekino and L. Susskind, “Fast Scramblers,” *JHEP*, vol. 10, p. 065, 2008.
- [34] N. Lashkari, D. Stanford, M. Hastings, T. Osborne, and P. Hayden, “Towards the Fast Scrambling Conjecture,” *JHEP*, vol. 04, p. 022, 2013.
- [35] E. Lieb and M. Ruskai, “Proof of the strong subadditivity of quantum-mechanical entropy,” *J.Math.Phys.*, vol. 14, pp. 1938–1941, 1973.
- [36] G. ’t Hooft, “A Planar Diagram Theory for Strong Interactions,” *Nucl. Phys.*, vol. B72, p. 461, 1974. [,337(1973)].
- [37] Y. Nambu, “QCD and the String Model,” *Phys. Lett.*, vol. 80B, pp. 372–376, 1979.

- [38] J. Polchinski, “Dirichlet Branes and Ramond-Ramond charges,” *Phys. Rev. Lett.*, vol. 75, pp. 4724–4727, 1995.
- [39] G. T. Horowitz and A. Strominger, “Black strings and P-branes,” *Nucl. Phys.*, vol. B360, pp. 197–209, 1991.
- [40] V. E. Hubeny, “The AdS/CFT Correspondence,” *Class. Quant. Grav.*, vol. 32, no. 12, p. 124010, 2015.
- [41] V. E. Hubeny, “Black hole singularity in AdS / CFT,” in *Proceedings, 3rd International Symposium on Quantum theory and symmetries (QTS3): Cincinnati, USA, September 10-14, 2003*, pp. 524–530, 2004.
- [42] A. Hamilton, D. N. Kabat, G. Lifschytz, and D. A. Lowe, “Local bulk operators in AdS/CFT: A Holographic description of the black hole interior,” *Phys.Rev.*, vol. D75, p. 106001, 2007.
- [43] K. Papadodimas and S. Raju, “Comments on the Necessity and Implications of State-Dependence in the Black Hole Interior,” 2015.
- [44] R. Haag, *Local quantum physics: Fields, particles, algebras, 2nd ed.* Springer, 1992.
- [45] D. L. Jafferis, A. Lewkowycz, J. Maldacena, and S. J. Suh, “Relative entropy equals bulk relative entropy,” 2015.
- [46] D. Marolf and J. Polchinski, “Violations of the Born rule in cool state-dependent horizons,” *JHEP*, vol. 01, p. 008, 2016.
- [47] S. Banerjee, J.-W. Bryan, K. Papadodimas, and S. Raju, “A toy model of black hole complementarity,” *JHEP*, vol. 05, p. 004, 2016.
- [48] D. Marolf and J. Polchinski, “Gauge/Gravity Duality and the Black Hole Interior,” *Phys.Rev.Lett.*, vol. 111, p. 171301, 2013.
- [49] K. Papadodimas and S. Raju, “The Black Hole Interior in AdS/CFT and the Information Paradox,” *Phys.Rev.Lett.*, vol. 112, no. 5, p. 051301, 2014.
- [50] K. Papadodimas and S. Raju, “Local Operators in the Eternal Black Hole,” 2015.

- [51] V. Balasubramanian, B. D. Chowdhury, B. Czech, J. de Boer, and M. P. Heller, “Bulk curves from boundary data in holography,” *Phys. Rev.*, vol. D89, no. 8, p. 086004, 2014.
- [52] R. C. Myers, J. Rao, and S. Sugishita, “Holographic Holes in Higher Dimensions,” *JHEP*, vol. 06, p. 044, 2014.
- [53] M. Headrick, R. C. Myers, and J. Wien, “Holographic Holes and Differential Entropy,” *JHEP*, vol. 10, p. 149, 2014.
- [54] D. Marolf, “Holographic Thought Experiments,” *Phys. Rev.*, vol. D79, p. 024029, 2009.
- [55] D. Marolf, “Unitarity and Holography in Gravitational Physics,” *Phys.Rev.*, vol. D79, p. 044010, 2009.
- [56] E. Mintun, J. Polchinski, and V. Rosenhaus, “Bulk-Boundary Duality, Gauge Invariance, and Quantum Error Corrections,” *Phys. Rev. Lett.*, vol. 115, no. 15, p. 151601, 2015.
- [57] A. Almheiri, X. Dong, and D. Harlow, “Bulk Locality and Quantum Error Correction in AdS/CFT,” *JHEP*, vol. 04, p. 163, 2015.
- [58] S. B. Giddings, “Hilbert space structure in quantum gravity: an algebraic perspective,” *JHEP*, vol. 12, p. 099, 2015.
- [59] M. Headrick, V. E. Hubeny, A. Lawrence, and M. Rangamani, “Causality & holographic entanglement entropy,” *JHEP*, vol. 12, p. 162, 2014.
- [60] X. Dong, D. Harlow, and A. C. Wall, “Bulk Reconstruction in the Entanglement Wedge in AdS/CFT,” 2016.
- [61] B. Freivogel, R. A. Jefferson, and L. Kabir, “Precursors, Gauge Invariance, and Quantum Error Correction in AdS/CFT,” 2016.
- [62] I. A. Morrison, “Boundary-to-bulk maps for AdS causal wedges and the Reeh-Schlieder property in holography,” *JHEP*, vol. 1405, p. 053, 2014.
- [63] R. Bousso, B. Freivogel, S. Leichenauer, V. Rosenhaus, and C. Zukowski, “Null Geodesics, Local CFT Operators and AdS/CFT for Subregions,” 2012.

- [64] I. Heemskerk, J. Penedones, J. Polchinski, and J. Sully, “Holography from Conformal Field Theory,” *JHEP*, vol. 0910, p. 079, 2009.
- [65] A. Fitzpatrick, E. Katz, D. Poland, and D. Simmons-Duffin, “Effective Conformal Theory and the Flat-Space Limit of AdS,” *JHEP*, vol. 1107, p. 023, 2011.
- [66] S. El-Showk and K. Papadodimas, “Emergent Spacetime and Holographic CFTs,” 2011.
- [67] J. Polchinski, L. Susskind, and N. Toumbas, “Negative energy, superluminality and holography,” *Phys. Rev.*, vol. D60, p. 084006, 1999.
- [68] T. Banks, M. R. Douglas, G. T. Horowitz, and E. J. Martinec, “AdS dynamics from conformal field theory,” 1998.
- [69] I. Bena, “On the construction of local fields in the bulk of AdS(5) and other spaces,” *Phys.Rev.*, vol. D62, p. 066007, 2000.
- [70] A. Hamilton, D. N. Kabat, G. Lifschytz, and D. A. Lowe, “Holographic representation of local bulk operators,” *Phys.Rev.*, vol. D74, p. 066009, 2006.
- [71] A. Hamilton, D. N. Kabat, G. Lifschytz, and D. A. Lowe, “Local bulk operators in AdS/CFT: A Boundary view of horizons and locality,” *Phys.Rev.*, vol. D73, p. 086003, 2006.
- [72] A. Hamilton, D. N. Kabat, G. Lifschytz, and D. A. Lowe, “Local bulk operators in AdS/CFT and the fate of the BTZ singularity,” 2007.
- [73] L. Susskind and N. Toumbas, “Wilson loops as precursors,” *Phys. Rev.*, vol. D61, p. 044001, 2000.
- [74] S. B. Giddings and M. Lippert, “Precursors, black holes, and a locality bound,” *Phys.Rev.*, vol. D65, p. 024006, 2002.
- [75] D. L. Jafferis and S. J. Suh, “The Gravity Duals of Modular Hamiltonians,” 2014.
- [76] V. E. Hubeny, M. Rangamani, and T. Takayanagi, “A Covariant holographic entanglement entropy proposal,” *JHEP*, vol. 0707, p. 062, 2007.

- [77] S. Banerjee, J.-W. Brijan, and G. Vos, “On the universality of late-time correlators in semi-classical 2d CFTs,” *JHEP*, vol. 08, p. 047, 2018.
- [78] M. Banados, C. Teitelboim, and J. Zanelli, “The Black hole in three-dimensional space-time,” *Phys. Rev. Lett.*, vol. 69, pp. 1849–1851, 1992.
- [79] J. M. Maldacena, J. Michelson, and A. Strominger, “Anti-de Sitter fragmentation,” *JHEP*, vol. 02, p. 011, 1999.
- [80] J. Maldacena and D. Stanford, “Remarks on the Sachdev-Ye-Kitaev model,” *Phys. Rev.*, vol. D94, no. 10, p. 106002, 2016.
- [81] J. Maldacena, D. Stanford, and Z. Yang, “Conformal symmetry and its breaking in two dimensional Nearly Anti-de-Sitter space,” *PTEP*, vol. 2016, no. 12, p. 12C104, 2016.
- [82] V. Balasubramanian, A. Bernamonti, B. Craps, V. Keränen, E. Keski-Vakkuri, B. Müller, L. Thorlacius, and J. Vanhoof, “Thermalization of the spectral function in strongly coupled two dimensional conformal field theories,” *JHEP*, vol. 04, p. 069, 2013.
- [83] M. Srednicki, “The approach to thermal equilibrium in quantized chaotic systems,” *Journal of Physics A: Mathematical and General*, vol. 32, no. 7, p. 1163, 1999.
- [84] T. Anous, T. Hartman, A. Rovai, and J. Sonner, “Black Hole Collapse in the $1/c$ Expansion,” *JHEP*, vol. 07, p. 123, 2016.
- [85] B. Chen, J.-q. Wu, and J.-j. Zhang, “Holographic Description of 2D Conformal Block in Semi-classical Limit,” *JHEP*, vol. 10, p. 110, 2016.
- [86] B. Chen and J.-q. Wu, “Holographic Entanglement Entropy For a Large Class of States in 2D CFT,” *JHEP*, vol. 09, p. 015, 2016.
- [87] L. Hadasz and Z. Jaskolski, “Liouville theory and uniformization of four-punctured sphere,” *J. Math. Phys.*, vol. 47, p. 082304, 2006.
- [88] A. Castro, J. M. Lapan, A. Maloney, and M. J. Rodriguez, “Black Hole Scattering from Monodromy,” *Class. Quant. Grav.*, vol. 30, p. 165005, 2013.

- [89] S. Pasterski, A. Strominger, and A. Zhiboedov, “New Gravitational Memories,” *JHEP*, vol. 12, p. 053, 2016.
- [90] S. W. Hawking, M. J. Perry, and A. Strominger, “Soft Hair on Black Holes,” *Phys. Rev. Lett.*, vol. 116, no. 23, p. 231301, 2016.
- [91] S. W. Hawking, M. J. Perry, and A. Strominger, “Superrotation Charge and Supertranslation Hair on Black Holes,” *JHEP*, vol. 05, p. 161, 2017.
- [92] A. Strominger and A. Zhiboedov, “Gravitational Memory, BMS Supertranslations and Soft Theorems,” *JHEP*, vol. 01, p. 086, 2016.
- [93] T. Hartman, “Entanglement Entropy at Large Central Charge,” 2013.
- [94] T. Hartman, C. A. Keller, and B. Stoica, “Universal Spectrum of 2d Conformal Field Theory in the Large c Limit,” *JHEP*, vol. 09, p. 118, 2014.
- [95] K. Osterwalder and R. Schrader, “Axioms for Euclidean Green’s Functions. 2.,” *Commun. Math. Phys.*, vol. 42, p. 281, 1975.
- [96] M. Luscher and G. Mack, “Global Conformal Invariance in Quantum Field Theory,” *Commun. Math. Phys.*, vol. 41, pp. 203–234, 1975.
- [97] R. F. Streater and A. S. Wightman, *PCT, spin and statistics, and all that*. 1989.
- [98] D. A. Roberts and D. Stanford, “Two-dimensional conformal field theory and the butterfly effect,” *Phys. Rev. Lett.*, vol. 115, no. 13, p. 131603, 2015.
- [99] O. Hulík, T. Procházka, and J. Raeymaekers, “Multi-centered AdS_3 solutions from Virasoro conformal blocks,” *JHEP*, vol. 03, p. 129, 2017.
- [100] E. J. Martinec, “Conformal field theory, geometry, and entropy,” 1998.
- [101] E. Witten, “Coadjoint Orbits of the Virasoro Group,” *Commun. Math. Phys.*, vol. 114, p. 1, 1988.
- [102] M. Banados, “Three-dimensional quantum geometry and black holes,” 1998.

- [103] J. D. Brown and M. Henneaux, “Central Charges in the Canonical Realization of Asymptotic Symmetries: An Example from Three-Dimensional Gravity,” *Commun.Math.Phys.*, vol. 104, pp. 207–226, 1986.
- [104] J. Balog, L. Feher, and L. Palla, “Coadjoint orbits of the Virasoro algebra and the global Liouville equation,” *Int. J. Mod. Phys.*, vol. A13, pp. 315–362, 1998.
- [105] G. Compère, P. Mao, A. Seraj, and M. M. Sheikh-Jabbari, “Symplectic and Killing symmetries of AdS_3 gravity: holographic vs boundary gravitons,” *JHEP*, vol. 01, p. 080, 2016.
- [106] A. Garbarz and M. Leston, “Classification of Boundary Gravitons in AdS_3 Gravity,” *JHEP*, vol. 05, p. 141, 2014.
- [107] M. M. Sheikh-Jabbari and H. Yavartanoo, “On 3d bulk geometry of Virasoro coadjoint orbits: orbit invariant charges and Virasoro hair on locally AdS_3 geometries,” *Eur. Phys. J.*, vol. C76, no. 9, p. 493, 2016.
- [108] J. de Boer and D. Engelhardt, “Remarks on thermalization in 2D CFT,” *Phys. Rev.*, vol. D94, no. 12, p. 126019, 2016.
- [109] M. Ammon, A. Castro, and N. Iqbal, “Wilson Lines and Entanglement Entropy in Higher Spin Gravity,” *JHEP*, vol. 10, p. 110, 2013.
- [110] M. Ammon, M. Gutperle, P. Kraus, and E. Perlmutter, “Black holes in three dimensional higher spin gravity: A review,” *J. Phys.*, vol. A46, p. 214001, 2013.
- [111] A. L. Fitzpatrick, J. Kaplan, D. Li, and J. Wang, “Exact Virasoro Blocks from Wilson Lines and Background-Independent Operators,” *JHEP*, vol. 07, p. 092, 2017.
- [112] J. de Boer, A. Castro, E. Hijano, J. I. Jottar, and P. Kraus, “Higher spin entanglement and \mathcal{W}_N conformal blocks,” *JHEP*, vol. 07, p. 168, 2015.
- [113] E. Witten, “Topology-changing amplitudes in $2 + 1$ dimensional gravity,” *Nuclear Physics B*, vol. 323, pp. 113–140, Aug. 1989.
- [114] H. Röhl, “Holomorphic fiber bundles over riemann surfaces,” *Bull. Amer. Math. Soc.*, vol. 68, pp. 125–160, 05 1962.

- [115] O. Aharony, S. S. Gubser, J. M. Maldacena, H. Ooguri, and Y. Oz, “Large N field theories, string theory and gravity,” *Phys. Rept.*, vol. 323, pp. 183–386, 2000.
- [116] C. T. Asplund, A. Bernamonti, F. Galli, and T. Hartman, “Entanglement Scrambling in 2d Conformal Field Theory,” *JHEP*, vol. 09, p. 110, 2015.
- [117] S. H. Shenker and D. Stanford, “Black holes and the butterfly effect,” *JHEP*, vol. 03, p. 067, 2014.
- [118] J. Maldacena, S. H. Shenker, and D. Stanford, “A bound on chaos,” *JHEP*, vol. 08, p. 106, 2016.
- [119] P. Hosur, X.-L. Qi, D. A. Roberts, and B. Yoshida, “Chaos in quantum channels,” *JHEP*, vol. 02, p. 004, 2016.
- [120] P. Caputa, T. Numasawa, and A. Veliz-Orsorio, “Out-of-time-ordered correlators and purity in rational conformal field theories,” *PTEP*, vol. 2016, no. 11, p. 113B06, 2016.
- [121] G. ’t Hooft, “Dimensional reduction in quantum gravity,” *Conf. Proc.*, vol. C930308, pp. 284–296, 1993.
- [122] L. Susskind, “The World as a hologram,” *J. Math. Phys.*, vol. 36, pp. 6377–6396, 1995.
- [123] S. Sonogo, J. Almergren, and M. A. Abramowicz, “Optical geometry for gravitational collapse and Hawking radiation,” *Phys. Rev.*, vol. D62, p. 064010, 2000.
- [124] S. Hemming and E. Keski-Vakkuri, “Hawking radiation from AdS black holes,” *Phys. Rev.*, vol. D64, p. 044006, 2001.
- [125] D. A. Lowe and S. Roy, “Holographic description of asymptotically AdS(2) collapse geometries,” *Phys. Rev.*, vol. D78, p. 124017, 2008.
- [126] V. Keranen and P. Kleinert, “Non-equilibrium scalar two point functions in AdS/CFT,” *JHEP*, vol. 04, p. 119, 2015.
- [127] G. Festuccia and H. Liu, “Excursions beyond the horizon: Black hole singularities in Yang-Mills theories. I,” *JHEP*, vol. 0604, p. 044, 2006.